

Project	IEEE 802.20 Working Group on Mobile Broadband Wireless Access < http://ieee802.org/20/ >
Title	MBTDD Wideband Mode Performance Report 1
Date Submitted	2006-01-06
Source(s)	Jim Tomcik Qualcomm, Incorporated 5775 Morehouse Drive San Diego, CA, 92121 Voice: 858-658-3231 Fax: 858-658-2113 E-Mail: jtomcik@qualcomm.com
Re:	MBWA Call for Proposals
Abstract	This contribution (part of the MBTDD proposal package for 802.20), contains the MBTDD Wideband Mode Performance Report 1.
Purpose	For consideration of 802.20 in its efforts to adopt a TDD proposal for MBWA.
Notice	This document has been prepared to assist the IEEE 802.20 Working Group. It is offered as a basis for discussion and is not binding on the contributing individual(s) or organization(s). The material in this document is subject to change in form and content after further study. The contributor(s) reserve(s) the right to add, amend or withdraw material contained herein.
Release	The contributor grants a free, irrevocable license to the IEEE to incorporate material contained in this contribution, and any modifications thereof, in the creation of an IEEE Standards publication; to copyright in the IEEE's name any IEEE Standards publication even though it may include portions of this contribution; and at the IEEE's sole discretion to permit others to reproduce in whole or in part the resulting IEEE Standards publication. The contributor also acknowledges and accepts that this contribution may be made public by IEEE 802.20.
Patent Policy	The contributor is familiar with IEEE patent policy, as outlined in Section 6.3 of the IEEE-SA Standards Board Operations Manual < http://standards.ieee.org/guides/opman/sect6.html#6.3 > and in <i>Understanding Patent Issues During IEEE Standards Development</i> < http://standards.ieee.org/board/pat/guide.html >.

MBTDD Wideband Mode Performance Report 1

1 Simulation Calibrations

This document specifies the performance of the MBWA system proposed in [5] as required by the 802.20 System Requirements Document (SRD) [2]. The link level and system level simulations are carried out according to the methodology specified in the evaluation criteria document [1]. In this section, the link-to-system interface is described. Then the system simulation calibration results are presented in terms of deterministic location calibration and traffic model calibration. Finally we describe the generation of MIMO channel correlations for link and system level simulations. The rest of the document will be broken into sections to address each of the performance requirements in SRD.

1.1 Link – System Interface

An Effective SNR metric has been proposed to 802.20 working group as a link to system interface for MIMO system performance studies [6], [7]. In the proposed MBWA system, MMSE processing is employed for spatial processing of multiple antenna configurations. The effective SNR mapping is defined as follows: Let SNR_i denote the post MMSE processing SNR of the i 'th modulation symbol in a packet consisting of N modulation symbols (potentially over multiple HARQ transmissions). The effective SNR of the packet, denoted by SNR_{eff} is defined as

$$SNR_{eff} = C^{-1} \left(\frac{1}{N} \sum_{i=1}^N C(SNR_i) \right).$$

Here $C(\cdot)$ denotes the constrained capacity function corresponding to the modulation scheme being used. The link simulation generates FER results as a function of the effective SNR. The system-level simulation measures the effective SNR of the packet and indexes into the link level simulation. The link simulation can incorporate all the relevant imperfections, like channel estimation and interference power estimation. The effective SNR metric has been validated through simulations with different channel, interference models and antenna configurations.

1.1.1 Validation of Link to System Metric

The effective SNR metric has been validated through simulations with different channel, interference models and antenna configurations. Four channel models, i.e., AWGN, Ped B, Veh A and Veh B channels, have been simulated for MIMO single code word transmissions assuming perfect channel estimation. In Figure 1-1, the FER vs. effective C/I link curves are illustrated for 3 packet formats of spectral efficiency 0.5, 2 and 3 bps/Hz per MIMO layer. It is observed that all channel models have similar error performance for the same packet format. The maximum difference between the required effective C/I's corresponding to the same FER and rank over different channel modules are shown to be within 0.1 dB. The maximum difference between the required effective C/I's corresponding to the same

FER and different ranks are shown to be within 0.5 dB. The insensitivity of the effective C/I metric to channel models is a validation of the capacity based approach for link to system interface.

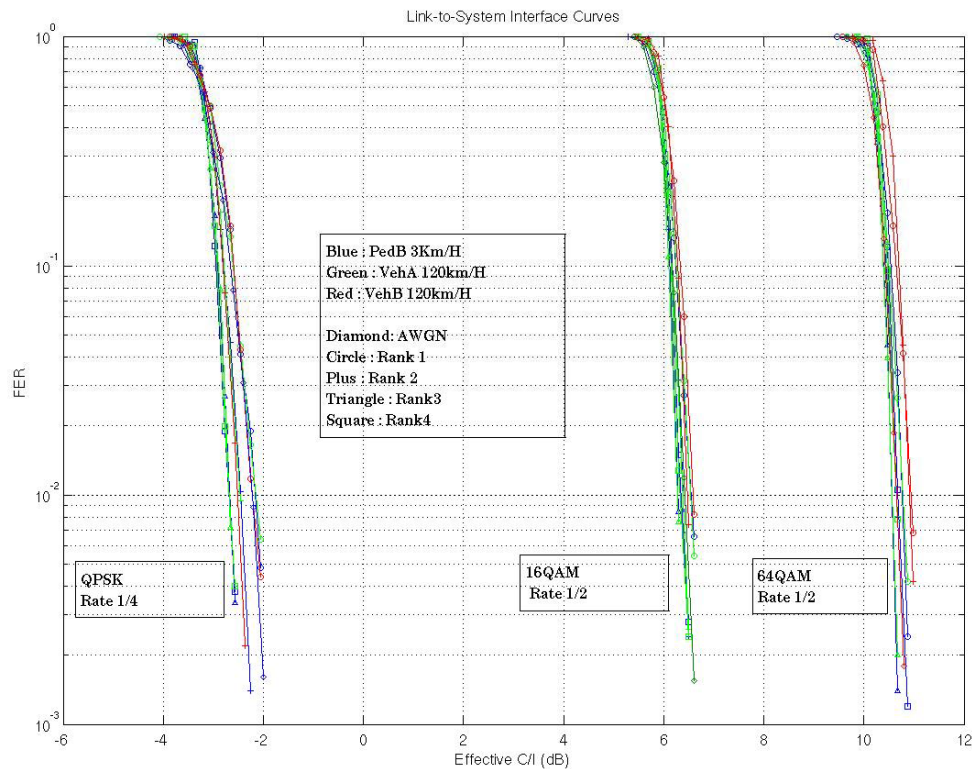


Figure 1-1 FER vs. effective SNR for different packet format, rank and channel models in a MIMO single codeword setup with 4 Tx and 4 Rx.

The FER vs. E_b/N_0 curves over AWGN channels are shown in Appendix C and Appendix D for FL and RL packet formats, respectively. Note that effective C/I and C/I are equivalent for AWGN channel. Since the link performances over different channels are insensitive to the channel model when the channel knowledge is available, only AWGN performance is shown. E_b/N_0 instead of C/I is used for performance comparison to further illustrate coding gain due to incremental redundancy HARQ.

When channel estimation algorithms are implemented in link level simulations, the loss due to channel estimation error is observed to be a backoff of the FER vs. effective C/I curves.

1.2 FER versus Average SINR

The FER versus average SINR performance for a set of packet formats are shown in Figure 1-2 **Error! Reference source not found.** to Figure 1-5 **Error! Reference source not found.** for Ped B 3 km/h, Veh A 120 km/h and Veh B 120 km/h, where simulations model actual channel estimation. The interference variation is modeled according to the FL interference observed in system level simulations. **Error! Reference source not found.**

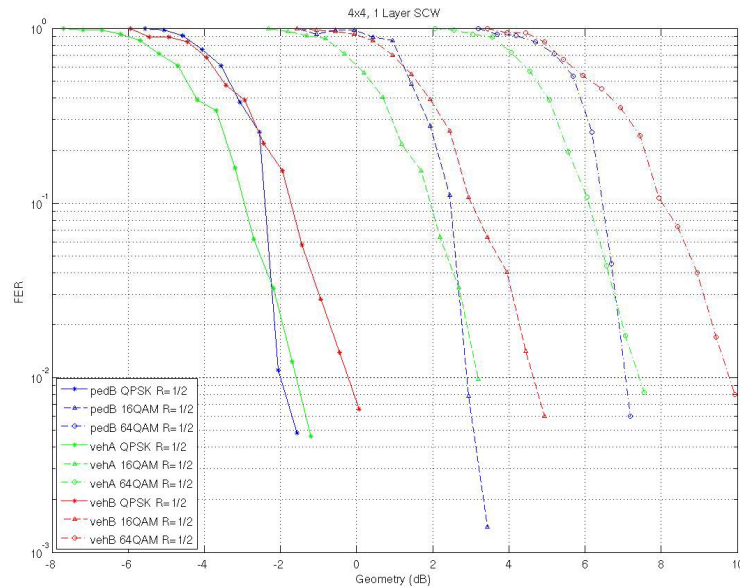


Figure 1-2 FER versus average SNR performance with channel estimation error for packet formats with spectral efficiency from 1 bps/Hz to 3 bps/Hz. MIMO configuration is 4 Tx 4 Rx with 1 layer transmission.

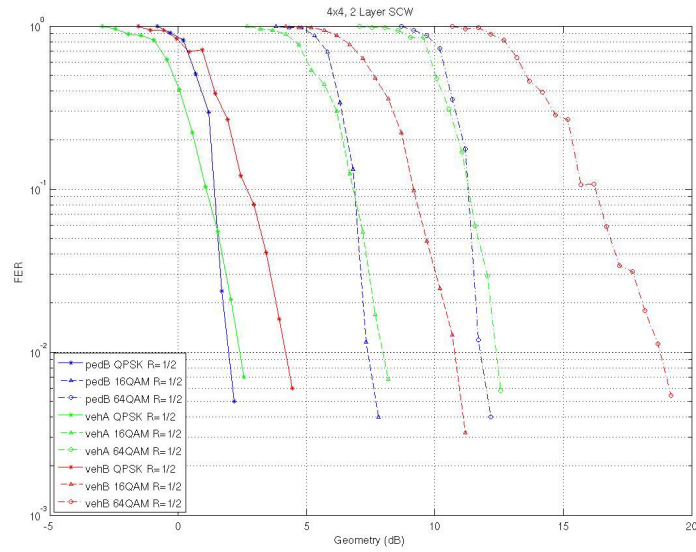


Figure 1-3 FER versus average SNR performance for packet formats with spectral efficiency from 1 bps/Hz to 3 bps/Hz. MIMO configuration is 4 Tx 4 Rx with 2 layers transmission.

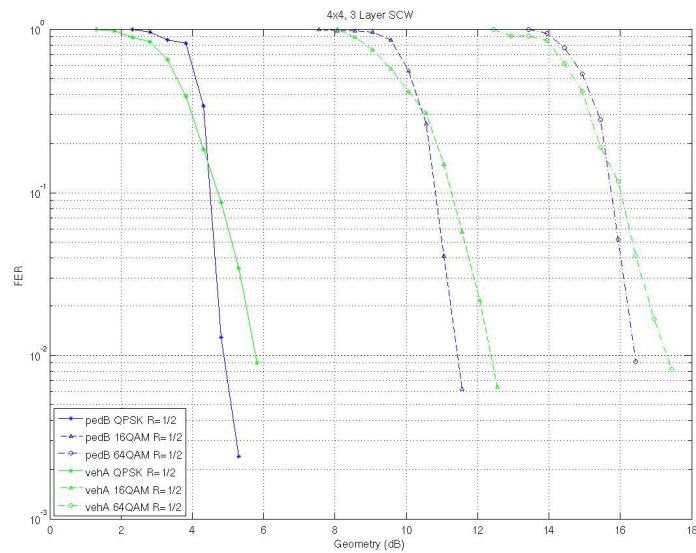


Figure 1-4 FER versus average SNR performance for packet formats with spectral efficiency from 1 bps/Hz to 3 bps/Hz. MIMO configuration is 4 Tx 4 Rx with 3 layers transmission

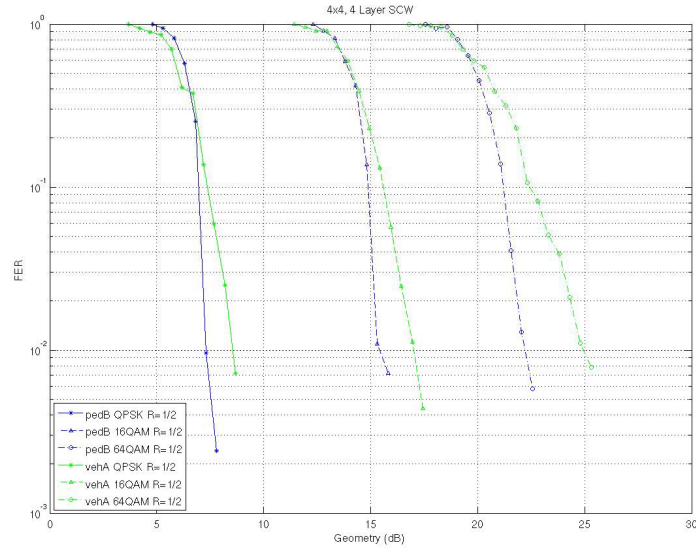


Figure 1-5 FER versus average SNR performance for packet formats with spectral efficiency from 1 bps/Hz to 3 bps/Hz. MIMO configuration is 4 Tx 4 Rx with 4 layers transmission

1.3 System Level Simulation

1.3.1 Location Calibration

Deterministic mobile locations, which are specified in the evaluation criteria document [1], are used in our system simulation calibration. In Appendix E, we append the achieved long term C/I per antenna for all mobiles that are specified in [1]. Each mobile's C/I is determined by the mobile location and a random shadowing realization between the mobile and all sectors in the system. In Figure 1-6, the CDF of the C/I values listed in Appendix E is compared with the C/I distribution obtained from other experiments. It is observed that the locations provided by the Evaluation Criteria is optimistic and results in up to 2.5 dB better C/I compared to C/I generated from 30 random drops of 570 users.

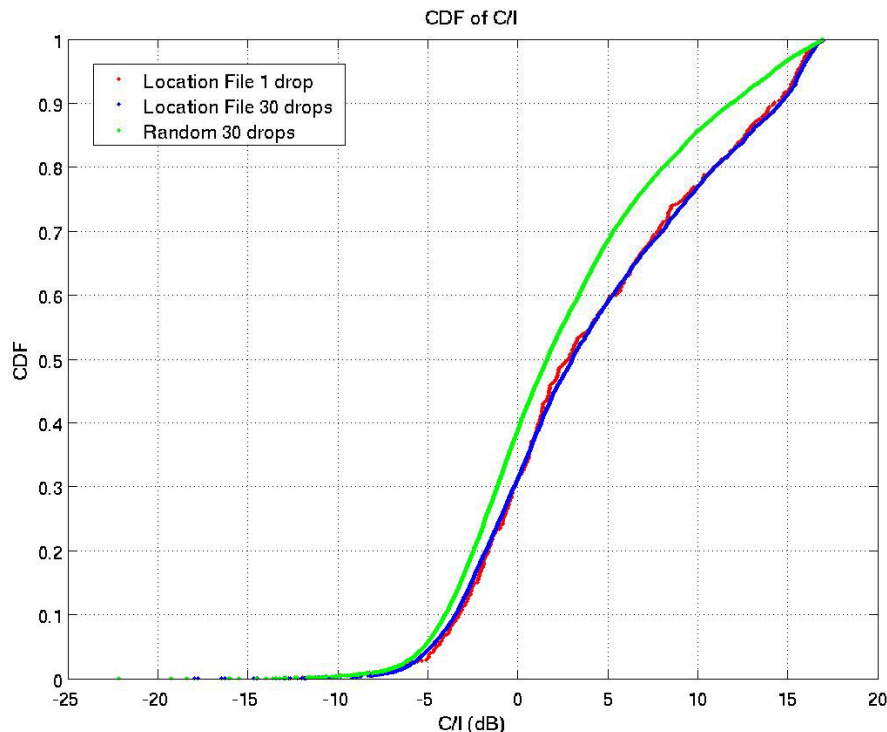


Figure 1-6 CDF of C/I distributions for fixed mobile locations and randomly generated mobile locations

1.3.2 Traffic Model Calibration

We implemented the HTTP, FTP, NRTV, and VOIP traffic models, and instrumented each model to log the completion of every significant event in the model. Data transfers were logged, as were delays (such as think time) introduced by the models, and object sizes.

A simulation topology was set up with 7 cells (21 sectors, 210 users) and wrap-around, and a PedB channel model. Although these parameters had no effect on the measured simulation results, we list them anyway to emphasize that verification was performed with a "real" simulation. The simulation time for HTTP, NRTV, and FTP was 80 minutes per run (3 runs total.). The simulation time for VOIP was 30 seconds with 700 users. In addition, all 4 models were run together in a 5th simulation, without

significantly different results. The simulation parameters specified by the 802.20 Evaluation Criteria document are depicted in Table 1-1. A post processing script analyzed the output logs from each simulation. The post-processing script extracted the mean, variance, and number of trials for all simulations. The difference between the expected mean (from the 802.20 spec) and the actual mean (from our simulation) is listed in the last column of this table, in the "Error %" column. As can be seen, the error is less than 2.2% for all simulation parameters.

Table 1-1 Traffic Model Parameter Verification

Traffic Model	Table/ Ref.	Variable	Params	Mean	Stddev	Measured Mean	Samples	Error %
HTTP Logfile = http_10_16_061935.txt, 80 minutes								
Main object size (bytes)	2	Truncated Lognormal	$\sigma = 1.37, \mu = 8.35$	10710	25032	10753.5	21391	0.4%
Embedded object size (bytes)	2	Truncated Lognormal	$\sigma = 2.36, \mu = 6.17$	7758	126168	7728.4	120135	0.4%
No. of embedded objects	2	Truncated Pareto - shifted by -2	$\alpha = 1.1, \kappa = 2$	5.64	-	5.62	21391	0.4%
Reading time	2	Exponential	$\lambda = 0.033$	30 sec	30 secs	29.758 (**)	21391	0.8%
Parsing time	2	Exponential	$\lambda = 7.69$	0.13 sec	0.13 sec	0.1302 (**)	21391	0.2%
FTP Logfile = ftp_10_21_102148.txt, 80 minutes								
File Size	3	Truncated Lognormal	$\sigma = 0.35, \mu = 14.45$	2.0 MB	0.722 MB	2043245	387	2.2%
Reading Time	3	Exponential	$\lambda = 0.00555$	180 sec	180 sec	181.2 (**)	387	0.7%
NRT Video Logfile = nrtv_10_17_121904.txt, 80 minutes								
Inter Arrival	4	Fixed		100 ms	0	100.1 ms(**)	12062	0.1%
Packets per frame	4	Fixed		8	0	8	12062	0%
Packet size (bytes)	4	Truncated Pareto	$\alpha = 1.2, \kappa = 20$	100	-	102.0	12062	2.0%
Inter arrival	4	Truncated Pareto	$\alpha = 1.2, \kappa = 2.5$	6 ms	-	5.933 ms(**)	12062	1.3%
VOIP Logfile = voice_10_17_121904.txt, 30 seconds								
Packet Size (bytes)	G.729	Fixed		10	0	10	2095785	0%
Packet Header (bytes)	§4.3.5	Fixed		4	0	4	2095785	0%
G.729A Period	G.729	Fixed		10 ms	0	10.00 ms	2095785	0%
Domestic Calls (%)	11	Fixed		80%	0	78..9%	700	1.4%
Backhaul Domestic	10, 11	Gamma shifted by +7.5	$\alpha=1, \beta=2.5$	10 ms	-	10.00 ms	2095785	0%
Backhaul International	10, 11	Gamma shifted by +107.5	$\alpha=1, \beta=2.5$	110 ms	-	110.0 ms	2095785	0%

(**) statistic has been adjusted to account for discrete time steps in simulation time.

In the following figures, we plot the CDF of statistics from the traffic model as mandated by the Evaluation Criteria.

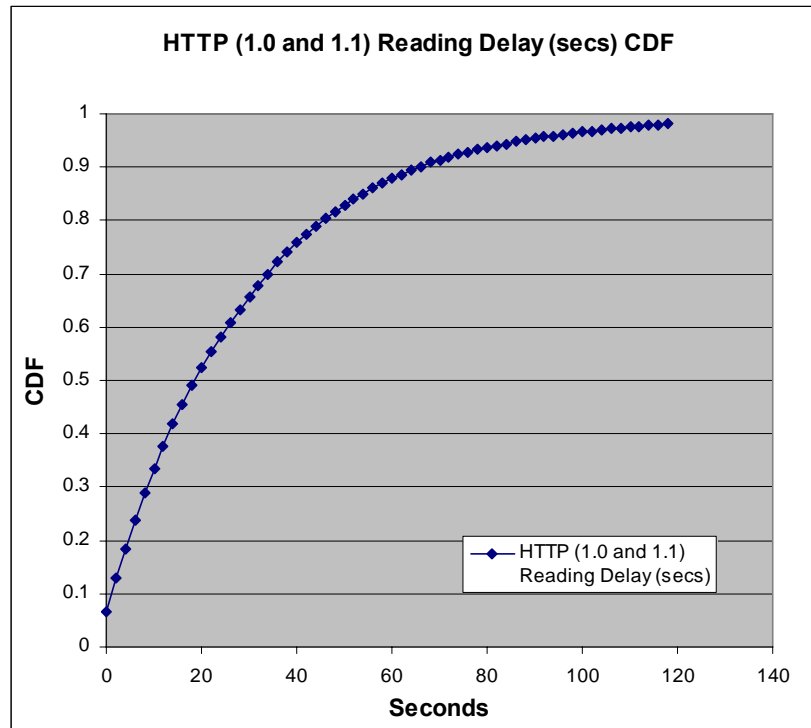


Figure 1-7 HTTP (1.0 and 1.1) reading delay CDF

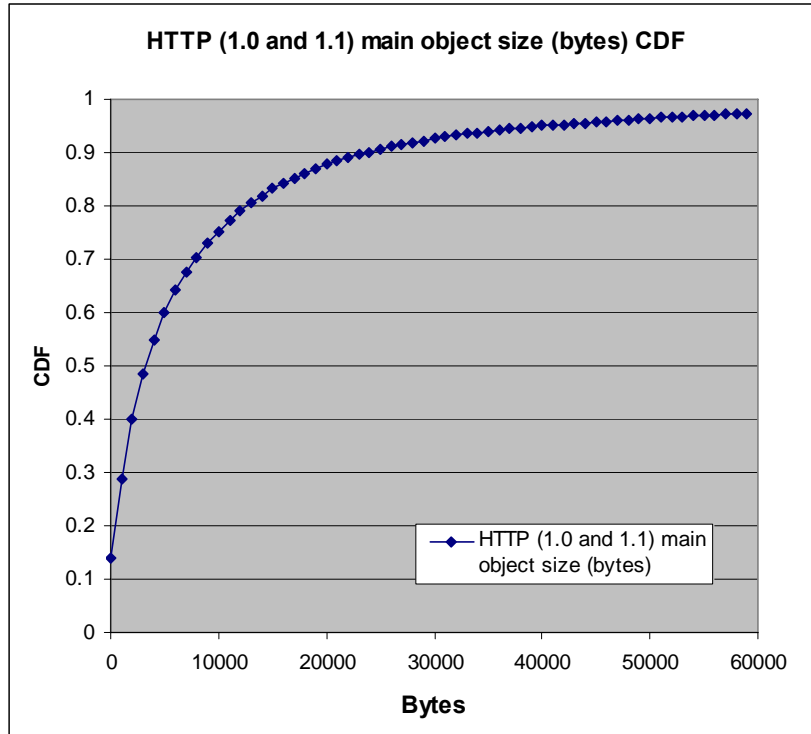


Figure 1-8 HTTP (1.0 and 1.1) main object size CDF

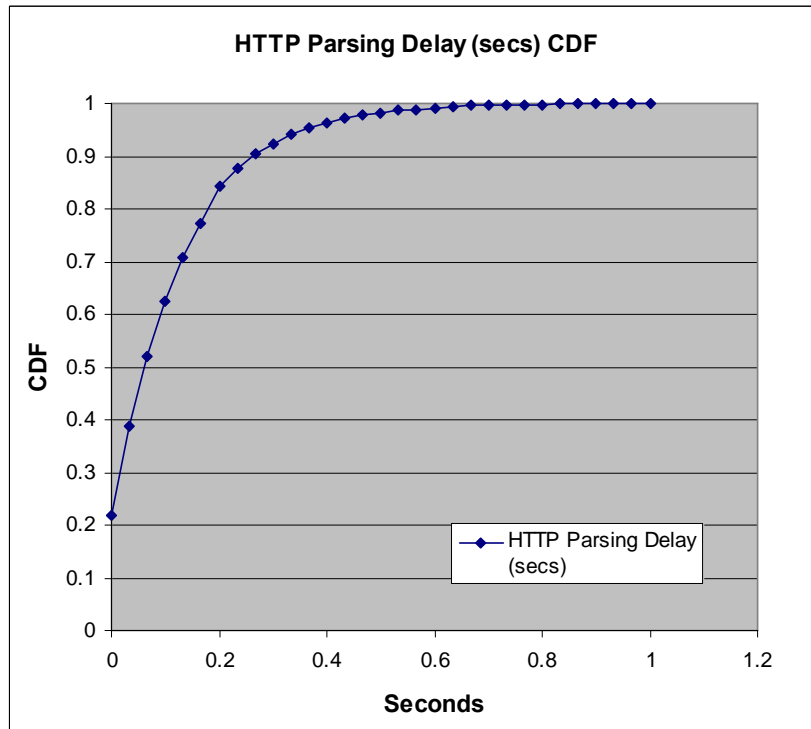


Figure 1-9 HTTP parsing delay CDF

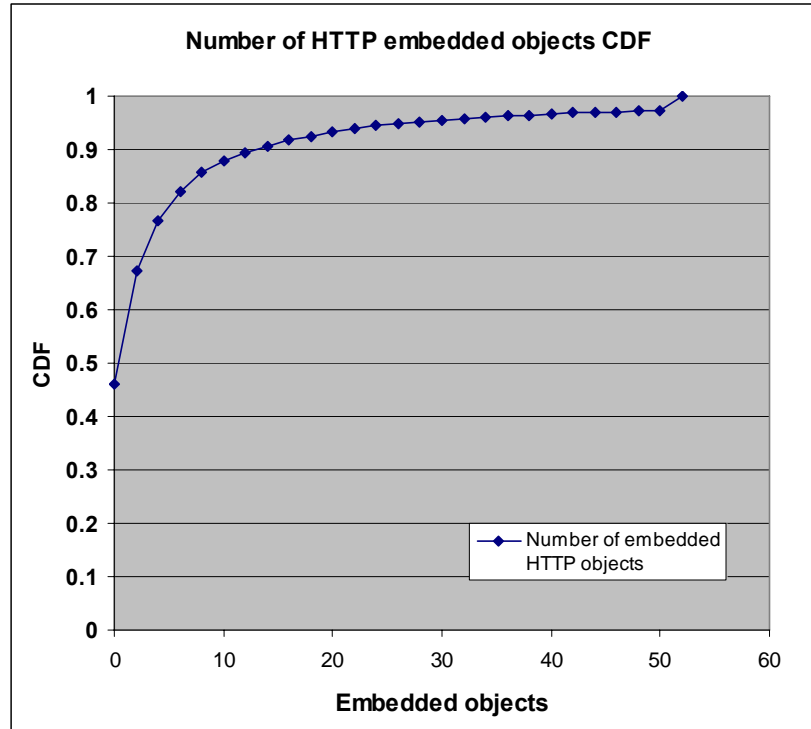


Figure 1-10 Number of HTTP embedded objects CDF

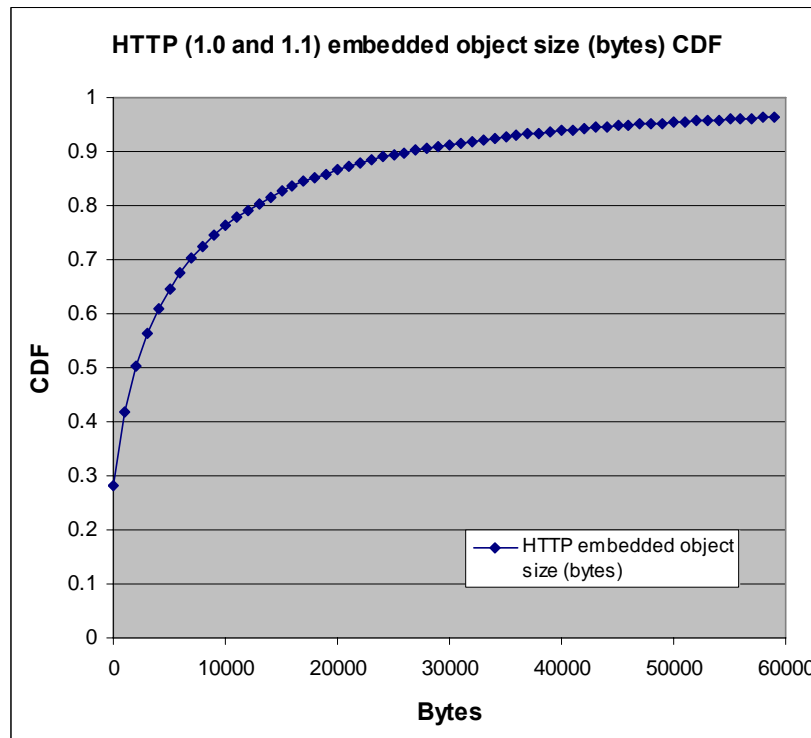


Figure 1-11 HTTP (1.0 and 1.1) embedded object size CDF

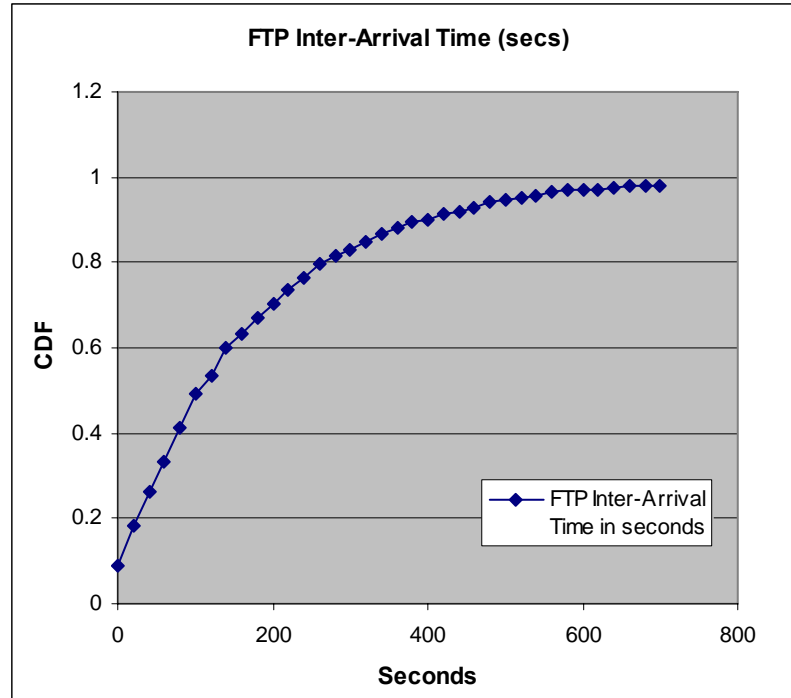


Figure 1-12 FTP inter-arrival time CDF

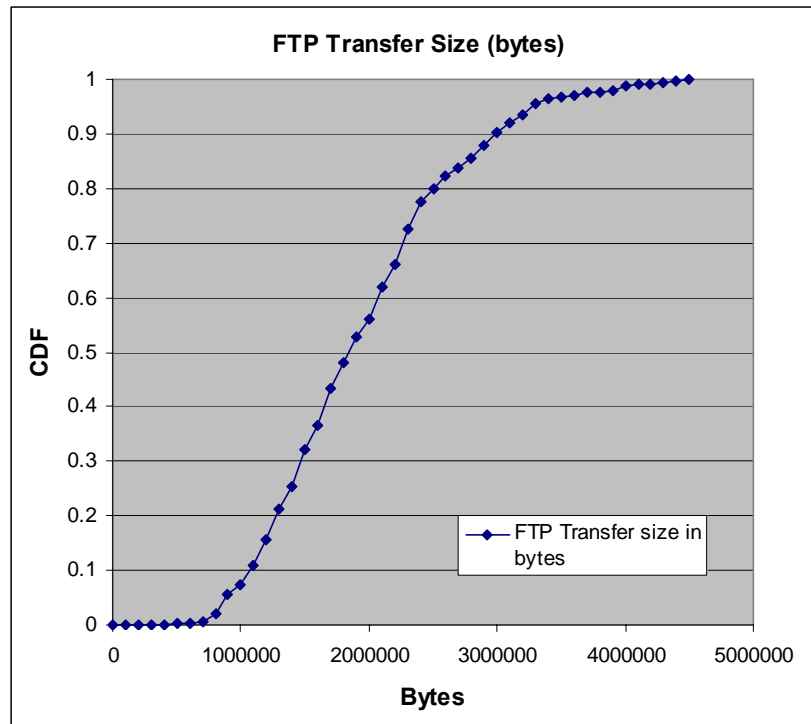


Figure 1-13 FTP transfer size CDF

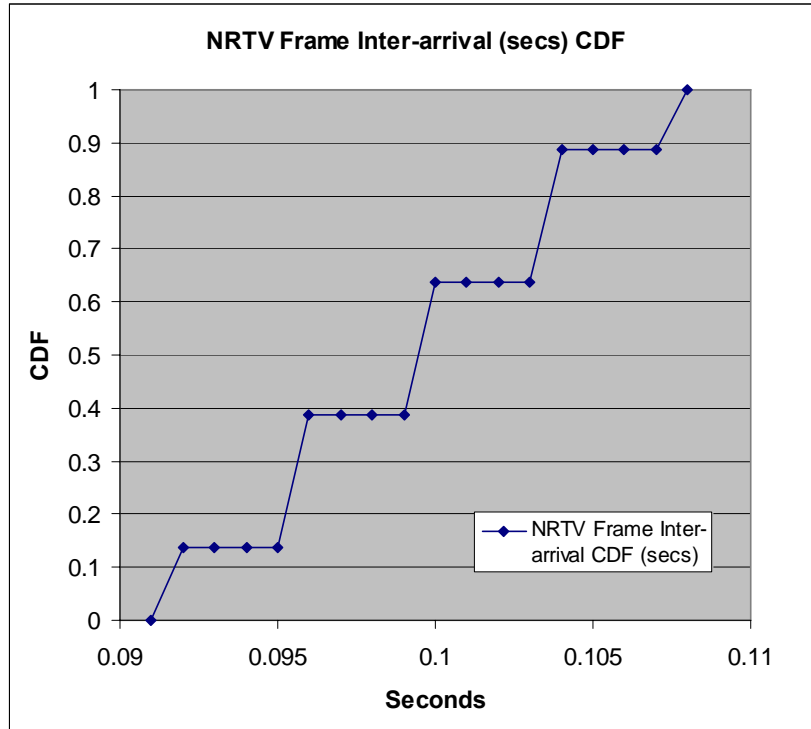


Figure 1-14 NRTV frame inter-arrival time CDF

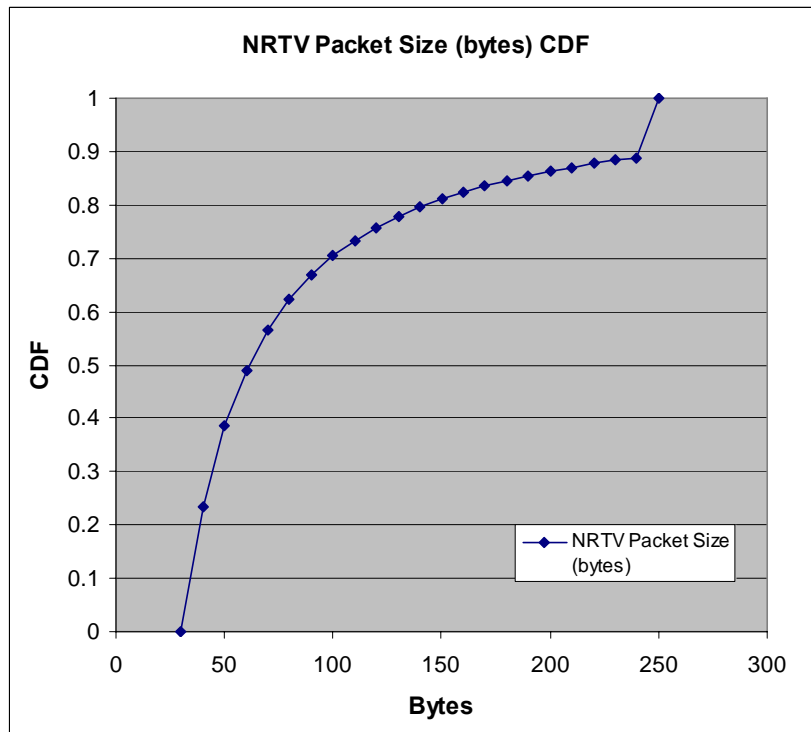


Figure 1-15 NRTV packet size CDF

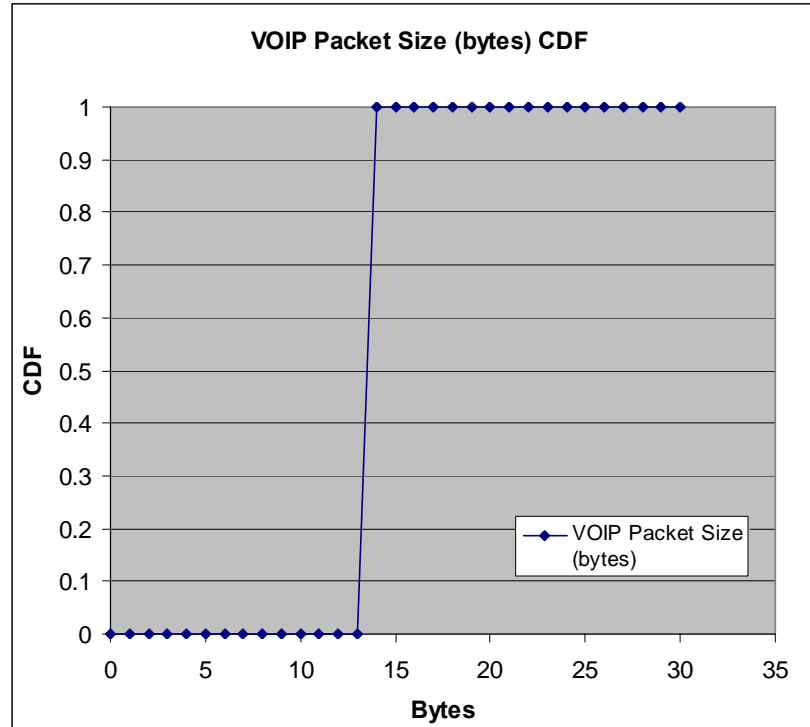


Figure 1-16 VoIP packet size CDF

1.3.3 Overhead Channel Modeling

Overhead channels are taken into account in the system simulation by taking a conservative estimate of fixed overhead. In a 10 MHz system, the forward link throughput is scaled down by 10% to model the F-SSCH overhead, which in reality takes 10% bandwidth overhead and less than 10% power overhead for all simulation scenarios in this report. This assumption is justified by the maximum assignment and acknowledgement activities for the simulated scenarios. The reverse link control channel transmitted on the CDMA control segment is assumed to take 4% overhead. As shown in Section 3.2.1, the CDMA control segment loading is very low for all the simulation scenarios in this report. The reverse link ACK/NAK channels are assumed to take 7% overhead.

1.3.3.1 Forward Link Overhead Channel Interference and Errors

For all the simulation scenarios in this report, the average PSD of F-SSCH is designed to be lower than or equal to data channel PSD. However, the interference from the F-SSCH to other sector data transmission on forward link is modeled conservatively by simulating 100% data transmissions in each sector.

F-SSCH assignment errors and acknowledgement errors have minimal impact on full buffer simulations since the error rate is designed to be 1% for the scenarios simulated in this report. Our simulations target a confidence interval of 90-95%, where 1% error events do not need to be modeled. Errors on bits transmitted on the FL for controlling RL transmission power are modeled at 10%. Errors on the OSICH are modeled with geometry based link curves.

1.3.3.2 Reverse Link Overhead Channel Interference and Error

For all the simulation scenarios in this report, the average PSD of reverse link ACK/NAK channel is designed to be lower than or equal to data channel PSD. However, the interference level from the ACK/NAK to other sector data transmission on reverse link is modeled conservatively by simulating 100% data transmissions in each sector. The reverse link CDMA control segments are orthogonal to data transmission, hence no interference need to be modeled.

Reverse link ACK to NAK and NAK to ACK error probabilities are designed to have minimal impact on packet errors, hence are not modeled for forward link full buffer simulations. R-CQICH erasure is modeled as 50% in forward link simulations. This assumption is validated by reverse link control channel power control simulations in Section 3.2.1, which demonstrate a tight R-CQICH erasure performance. REQ erasure is not modeled for full buffer simulations, since it only affects latency which is not evaluated for full buffer traffic.

1.4 MIMO Channel Modeling for Simulations

The channel spatial correlation matrices (transmit or receive) depend on three parameters: angle of arrival (AoA) and/or angle of departure (AoD), angle spread (AS), and the antenna spacing. The channel modeling document specifies several spatial channel models that use different combinations of these parameters. In addition the channel modeling document specifies that these channels are to be generated using the correlation matrix approach (see the channel modeling document for details). In our simulations, correlation matrices for link level simulation are generated using both SCM model and the analytical approach specified in [3]. Correlation matrices for system level simulations are generated using the SCM model.

1.4.1 MIMO Channels for Link Level Simulations

The channel models considered for link level simulations are suburban macro cell with 20 and 50 degree AoA at the BS and 67.5 degree AoA at the MS. The analytical correlation model specified in [1] assumes the same AoD/AoA for all paths and the angular spread follows Laplacian distribution. The correlation matrices used for link level simulation are listed in Appendix A. Also listed in Appendix A are the correlation matrices generated from SCM scattering model.

The robustness of the proposed system is tested for multi-path profiles and mobile speeds as checked in Table 1-2.

Table 1-2 Multipath profile and speed for link level simulations

	3 km/h	120 km/h	250 km/h
Case-II: Vehicular A		X	X
Case-III: Pedestrian B	X		
Case-IV: Vehicular B		X	X

1.4.2 MIMO Channels for System Level Simulations

In system simulations, transmitter correlation matrices are generated using the SCM suburban macro channel model in the following way:

1. All possible AoDs over the whole azimuth are quantized into 36 bins of 10° . All AoDs fall in one bin are mapped into one angle (mean angle of the corresponding bin)
2. For any give bin and antenna spacing, use the SCM model with the same parameters to generate a large number of channel realizations.
3. Use these channel realizations to estimate the corresponding correlation matrix.
4. Estimated correlation matrices are then stored in a look-up table that is indexed by the tuple: AoD and antenna spacing.

In a given drop, each user in that drop will have a specific AoD. This AoD will be mapped to one of the 36 quantized angles. For any user in that drop, his transmitter correlation matrix is selected based on his AoD and antenna spacing and then used to generate his corresponding channel using the correlation matrix approach.

Unlike the transmitter correlation matrices, the receiver correlation matrices are not clustered into AoA bins. Instead, one correlation matrix is computed for each SCM model and antenna configuration by averaging the receiver correlation of a large number of channel realizations from mobiles with arbitrary AoA. This assumption is justified by the fact that the mobile antenna array orientation and AoA could change significantly within the simulation time.

See Appendices A and B for a list of correlation matrices used.

2 PAR Requirement

In Table 2-1, we included the PAR values specified in the approved IEEE 802.20 PAR and the corresponding values of Proposed TDD MBWA system for 10 MHz deployment.

Table 2-1 Spectral Efficiency Requirements

Characteristic	Target Value	Proposal MBWA System
Mobility	Vehicular mobility classes up to 250 km/hr (as defined in ITU-R M.1034-1)	Satisfies requirement. Maximum Spectral Efficiency for VehA 250 km/h on FL and RL are around 7 bps/Hz and 2.5 bps/Hz, respectively.
Sustained spectral efficiency	> 1 b/s/Hz/cell	Satisfies requirement. > 2b/s/Hz/Sector on FL (pedestrian) > 1b/s/Hz/Sector on RL (pedestrian) Refer to Section 4.3
Peak user data rate (Forward link (FL))	> 1 Mbps*	Satisfies requirement. 63 Mbps Refer to Section 4.2
Peak user data rate (Reverse link (RL))	> 300 kbps*	Satisfies requirement. 15 Mbps Refer to Section 4.2
Peak aggregate data rate per cell (FL)	> 4 Mbps*	Satisfies requirement. 63 Mbps / Sector
Peak aggregate data rate per cell (RL)	> 800 kbps*	Satisfies requirement. 45 Mbps / Sector Achieved by multiplexing 3 users using quasi-orthogonal reverse link (QORL), where each of the user achieves 15 Mbps peak rate. Refer to Whitepaper
Airlink MAC frame RTT	< 10 ms	Satisfies requirement. Approximately 5.5 ms
Bandwidth	e.g., 1.25 MHz, 5 MHz	Support different bandwidths from 5MHz to 20MHz.
Cell Sizes	Appropriate for ubiquitous metropolitan area networks and capable of reusing existing infrastructure.	Satisfies requirement. Refer to link budget tables in Section 3.5.
Spectrum (Maximum operating frequency)	< 3.5 GHz	Satisfies requirement.

Characteristic	Target Value	Proposal MBWA System
Spectrum (Frequency Arrangements)	Supports FDD (Frequency Division Duplexing) and TDD (Time Division Duplexing) frequency arrangements	Satisfies requirement.
Spectrum Allocations	Licensed spectrum allocated to the mobile service	Satisfies requirement.
Security Support	AES (Advanced Encryption Standard)	Satisfies requirement. Refer to Section 5.6 of [5].

* Targets for 1.25 MHz channel bandwidth. This represents 2 x 1.25 MHz (paired) channels for FDD and a 2.5 MHz (unpaired) channel for TDD. For other bandwidths, the data rates may change.

3 PHY/RF Level Performance

3.1 Link Adaptation

The proposed system employs link adaptation on both forward link and reverse link. There are 15 packet formats for forward and reverse link transmissions as shown in Table 3-1 and Table 3-2. The FER vs. EbN0 curves over AWGN channels are shown in Appendix C and Appendix D for FL and RL packet formats, respectively.

Table 3-1 Forward link packet formats.

Packet Format Index	Spectral efficiency on 1 st transmission	Max number of transmissions	Modulation order for each transmission					
			1	2	3	4	5	6
0	0.2	6	2	2	2	2	2	2
1	0.5	6	2	2	2	2	2	2
2	1.0	6	2	2	2	2	2	2
3	1.5	6	3	2	2	2	2	2
4	2.0	6	4	3	3	3	3	3
5	2.5	6	6	4	4	4	4	4
6	3.0	6	6	4	4	4	4	4
7	4.0	6	6	6	4	4	4	4
8	5.0	6	6	6	4	4	4	4
9	6.0	6	6	6	4	4	4	4
10	7.0	6	6	6	4	4	4	4
11	8.0	6	6	6	6	4	4	4
12	9.0	6	6	6	6	4	4	4
13	10.0	6	6	6	6	6	4	4
14	11.0	6	6	6	6	6	4	4
15	NULL							

Table 3-2 Reverse link packet formats

Packet format index	Spectral efficiency on 1 st transmission	Max number of transmissions	Modulation order for each transmission					
			1	2	3	4	5	6
0	0.25	6	2	2	2	2	2	2
1	0.50	6	2	2	2	2	2	2
2	1.0	6	2	2	2	2	2	2
3	1.5	6	3	2	2	2	2	2
4	2.0	6	3	3	2	2	2	2
5	2.67	6	4	4	3	3	3	3
6	4.0	6	4	4	3	3	3	3
7	6.0	6	4	4	4	3	3	3
8	8.0	6	4	4	4	4	4	3
9	4.0	6	6	6	4	4	4	4
10	5.0	6	6	6	4	4	4	4
11	6.0	6	6	6	4	4	4	4
12	7.0	6	6	6	4	4	4	4
13	8.0	6	6	6	6	4	4	4
14	9.0	6	6	6	6	4	4	4

3.2 Power Control

3.2.1 Reverse Link Control Channel Power Control

The reverse link control channel power control is based on the R-CQICH channel erasures. The R-CQICH channel is part of the CDMA control segment which is TDM/FDM multiplexed with the traffic channels. Target error rate on the R-CQICH is 0.1%. By sending up commands when the R-CQICH channel is erased, and down commands otherwise, a R-CQICH erasure rate of 0.5 is targeted. The AT only responds to the up/down power control commands received from the RL serving sector, by increasing the R-CQICH channel PSD by .25 dB in response to an up command, and decreasing the R-CQICH channel PSD by .25 dB in response to a down command. In this section we present numerical results demonstrating the effectiveness of the proposed power control algorithm.

Figure 3-1 shows the trace of the R-CQICH erasure rate for one mobile. As we see, after the initial transient period, the erasure rate has converged to the target value of 50%.

Figure 3-2 shows the distribution of the resulting ratio of the total received PSD to the thermal noise PSD, also called RoT, for different numbers of receive antennas and mobiles per sector, obtained from system simulations for Pedestrian B channel at 3 Km/h. As we see in this figure, since the control channel power control algorithm is effectively controlling the control C/I value of each user, the resulting RoT value depends on the number of mobiles per sector. Furthermore, since the target C/I values are different for different numbers of receive antennas, the resulting RoT value also depends on the number of receive antennas.

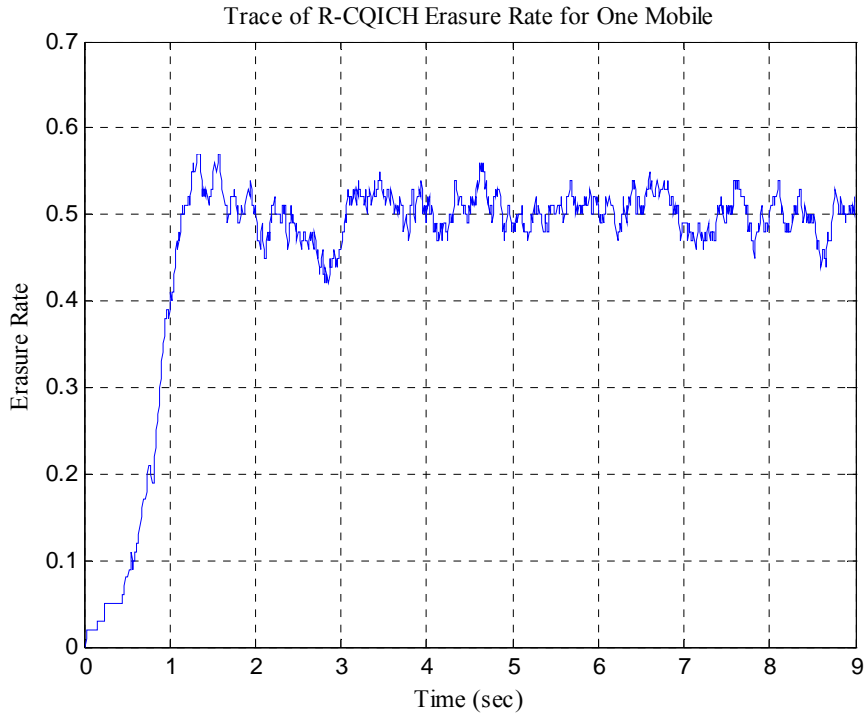


Figure 3-1 Trace of R-CQICH erasure rate for one mobile

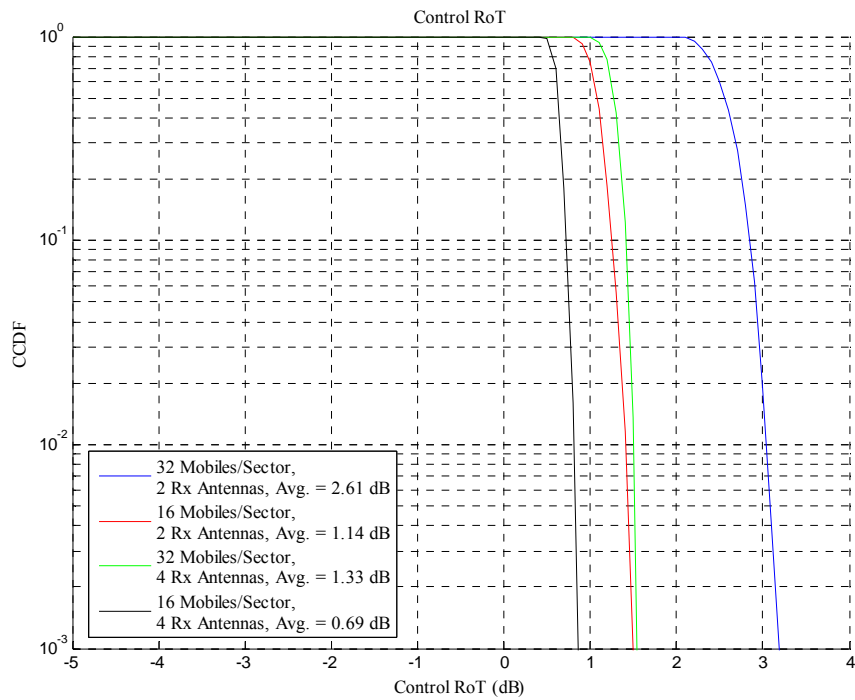


Figure 3-2 Control Channel RoT Distribution

3.2.2 Reverse Link Traffic Channel Power Control

The reverse link traffic channel power control is based on inter-sector interference control. Each sector broadcasts a three-level indication of the amount of interference it is receiving from the mobiles in the other sectors. The inter-sector interference indication is set based on a target value for the total interference and noise to thermal ratio (IoT). Each mobile monitors this indication from the neighboring sectors, and only responds to the indication broadcast from a non-serving sector that has the largest forward link channel gain to that mobile. Based on the value of this indication, the mobile increases or decreases the value of a parameter called delta, which is in turn used as an offset to set the traffic channel PSD with respect to the control channel (R-CQICH). A minimum and a maximum value (called delta_min and delta_max) are used to limit the range of the values for delta, and control the amount of ICI in high Doppler scenarios.

Figure 3-3 shows the distributions of IoT for 32 mobiles per sector and different cell radii and different IoT target values. The error rate on the inter-sector interference indications are modeled using the link-level performance curves. As we see, the target IoT is achieved on the average, with the 1% tail of the IoT distributions being only 1dB away from the target. The tight IoT tail distribution demonstrates the stability of the proposed power control design.

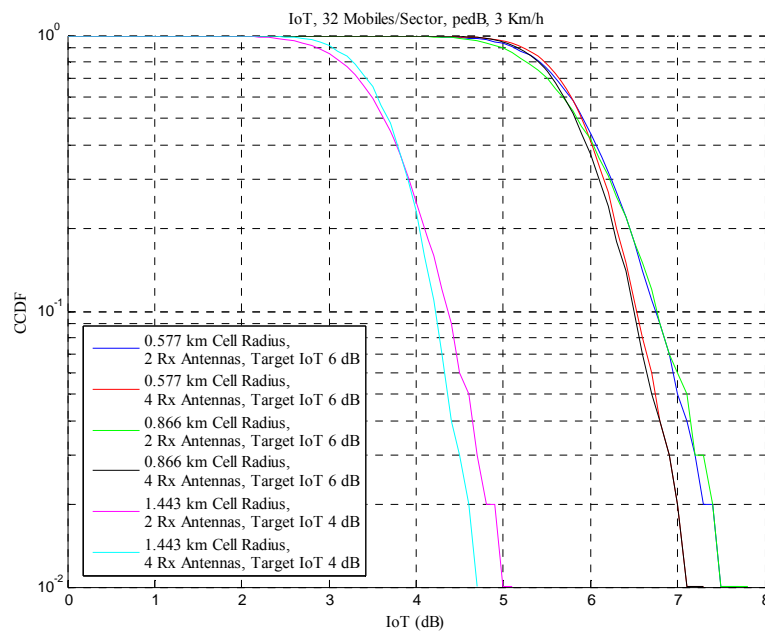


Figure 3-3 IoT Distribution

3.3 Mobility

To satisfy the requirement of “The AI shall support different rates of mobility from pedestrian (3 km/hr) to high vehicular speeds (250 km/hr).” in Section 4.1.4 of SRD, we demonstrate in the following sections robust performance under different channel speed and multipath profiles.

3.3.1 Forward Link Mobility Simulations

Link level simulations were carried out over different multipath profiles, Doppler spreads, and correlation models. The following simulations assume a 4x4 MIMO single codeword (SCW) design with MMSE receiver. Note that the spectral efficiency is obtained by running link simulations with adaptive rate and rank prediction, channel estimation, and HARQ with 6 maximum retransmissions. A large number of packets are simulated for each fixed geometry, i.e., long term average C/I per antenna. A certain packet format and the corresponding rank are selected based on the latest channel observations. If AT fails decoding, incremental redundancy subpackets will be transmitted until the packet decodes successfully or the maximum transmission is reached. The spectral efficiency computation takes into account the pilot overhead and residual packet errors. The interference variation is modeled according to the FL interference observed in system level simulations.**Error! Reference source not found.**

The analytical channel correlation models mandated in Section 3.7 of the channel model document [3] are used to generate the transmitter and receiver correlation matrices at the given AoD and AoA. It was observed that both the transmitter correlation and receiver correlation are very high (Appendix A). A suburban macro cell SCM model (AS 2 degree per path) is then used to calibrate the correlation matrix as stated in Section 1.4. The antenna correlation resulting from the SCM is observed to be significantly lower than the analytical model that assumes the same AoD for all paths with a Laplacian angular spread distribution (Appendix A).

The spectral efficiency curves based on the analytical correlation model are illustrated in Figure 3-4 and Figure 3-5, and the spectral efficiency curves based on the SCM model is illustrated in Figure 3-6. For all correlation models, it was observed that the spectral efficiency degrades gracefully as the mobility increases from 3 km/h to 250 km/h, where the highest spectral efficiency achieved at 250 km/h is greater than 7 bps/Hz. The MIMO throughput is observed to be notably higher with the SCM correlation model than the analytical correlation model. This is due to the high correlation of the analytical model which results in low rank channels, hence, lower spectral efficiency.

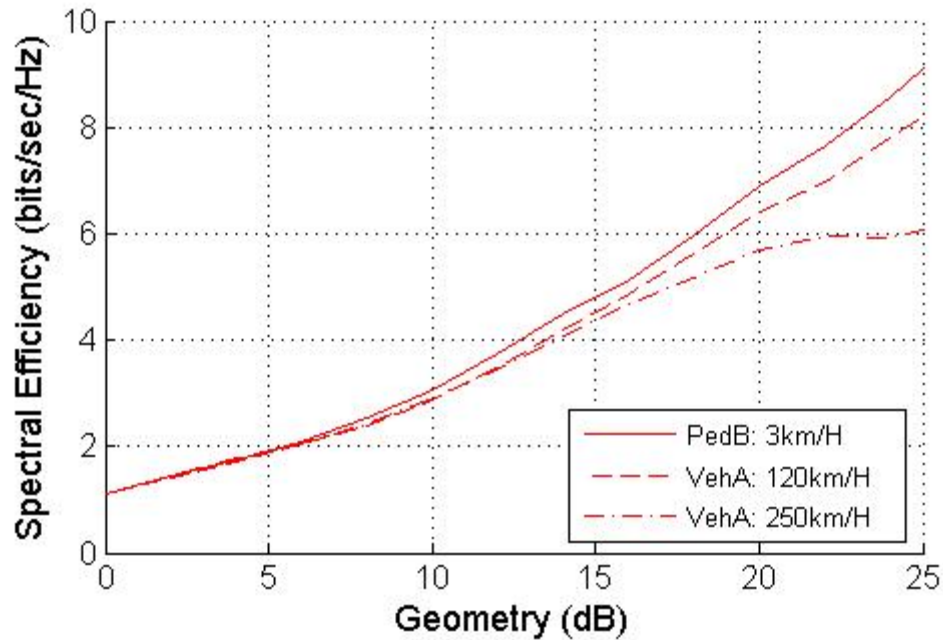


Figure 3-4 Spectral efficiency vs. SINR SCW-MIMO 4x4 with single path Laplacian correlation model. Base station AoD 50 degree, AS 2 degree; Mobile station AoD 67.5 degree, AS 35 degree.

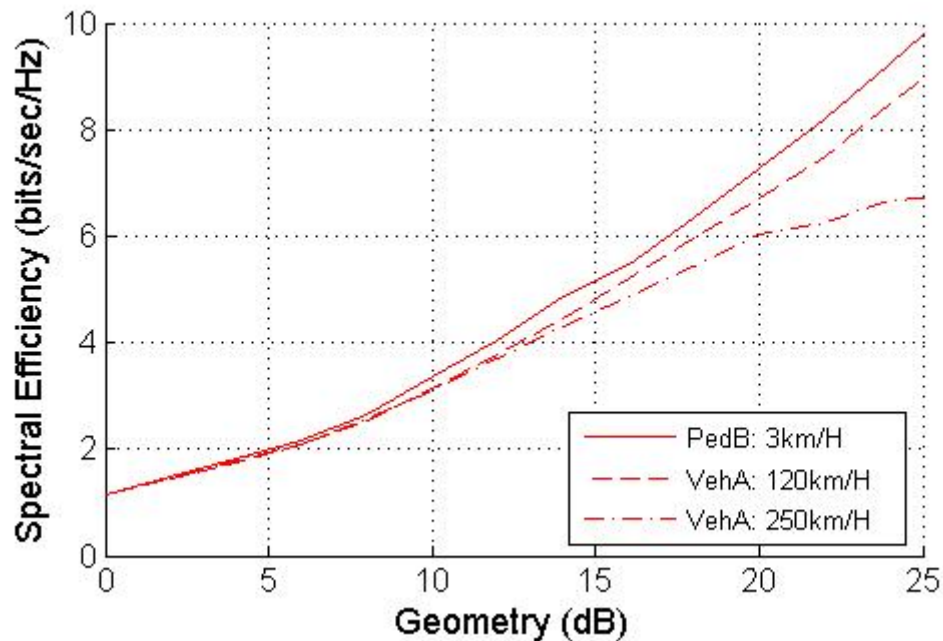


Figure 3-5 Spectral efficiency vs. SINR SCW-MIMO 4x4 with single path Laplacian correlation model. Base station AoD 20 degree, AS 5 degree; Mobile station AoD 67.5 degree, AS 35 degree.

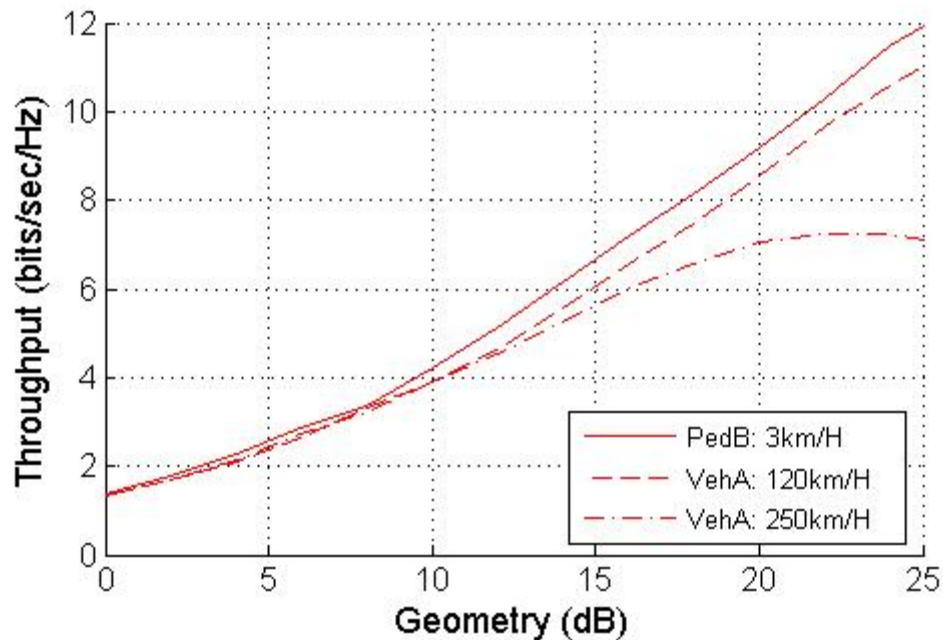


Figure 3-6 Spectral efficiency vs. SINR SCW-MIMO 4x4 with SCM suburban macro cell correlation model. Base station AoD 50 degree, AS 2 degree; Mobile station, AS 35 degree.

3.3.2 Reverse Link Mobility Simulations

Reverse link mobility sensitivity study results are presented in Figure 3-7 and Figure 3-8. RL packet formats of the desired spectral efficiencies are simulated over a range of SNR, so that an average SNR required to achieve 1% FER is obtained for each packet format. Each point in the plot is the spectral efficiency vs. the SNR for the simulated packet format, where pilot overhead is deducted from the final spectral efficiency. The interference is modeled as AWGN noise. Different curves corresponding to five different channel models. The two plots are for 2 and 4 receive antenna, respectively. Note that all link level spectral efficiency results take into account the pilot overheads.

As shown in the following figures, the link level performance degrades gracefully with mobility.

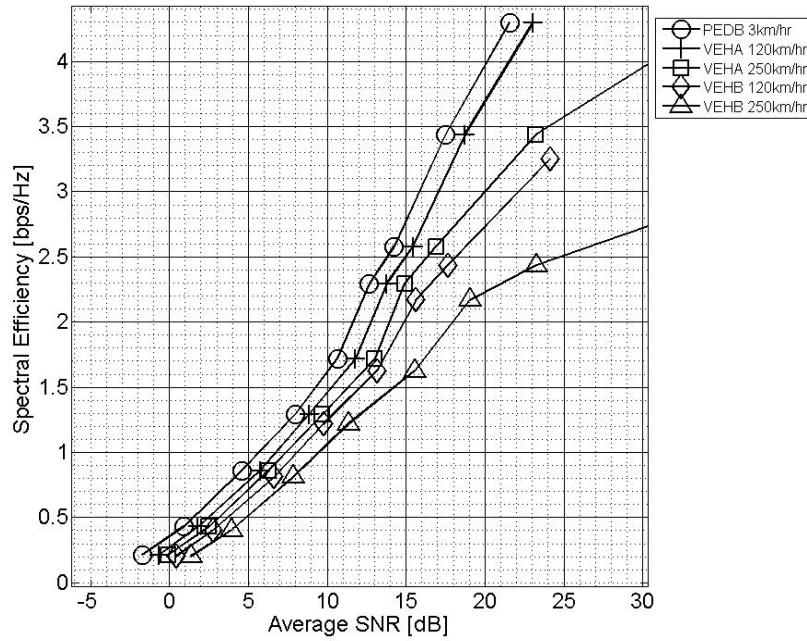


Figure 3-7 Spectral efficiency vs. SINR with dual Rx diversity at BS

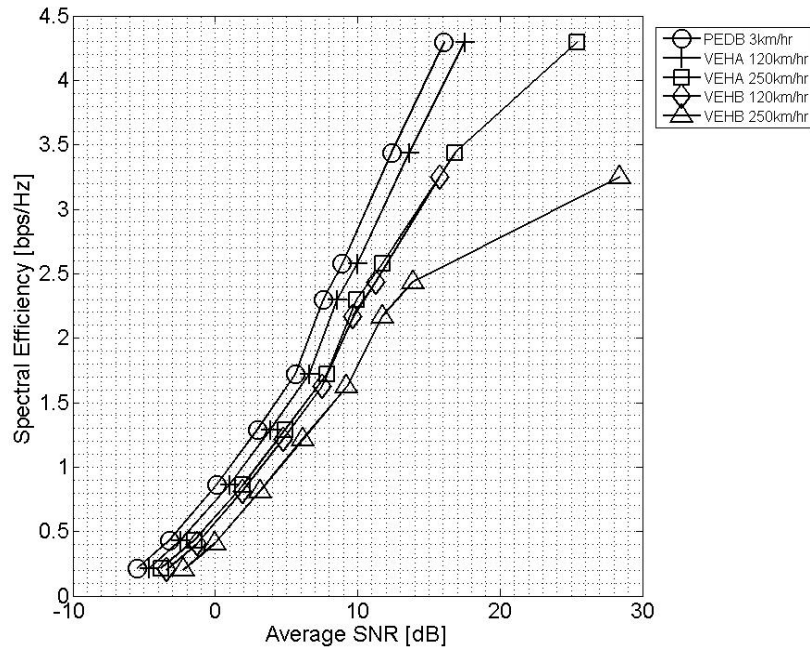


Figure 3-8 Spectral efficiency vs. SINR with 4 Rx diversity at BS

3.4 RF Specification Requirements

Figure 3-9 shows the transmit spectrum for the MBTDD downlink with 10MHz deployment. The spectrum was generated using 16 guard subcarriers at each edge of the band, and all the remaining 992 non-guard subcarriers were populated. The AM-AM and AM-PM characteristics of the power amplifier used to generate these spectra are shown in Figure 3-11 and Figure 3-12 respectively. These characteristics were measured from an implemented power amplifier. A zeroth order hold digital-to-analog convertor (DAC) was used, and the amplitude response of the low-pass filter used after the DAC is shown in Figure 3-13. An oversampling factor of 8 was used at the DAC input. The power-amplifier backoff used was 10.4 dB. A seventh order lowpass elliptic filter with a passband ripple of 0.15 dB and minimum stopband attenuation of 20 dB was implemented at the output of the power amplifier. The transition band of this filter is the band occupied by the guard subcarriers. The amplitude response of this filter is shown in Figure 3-10. The transmit spectrum meets the FCC emissions requirement.

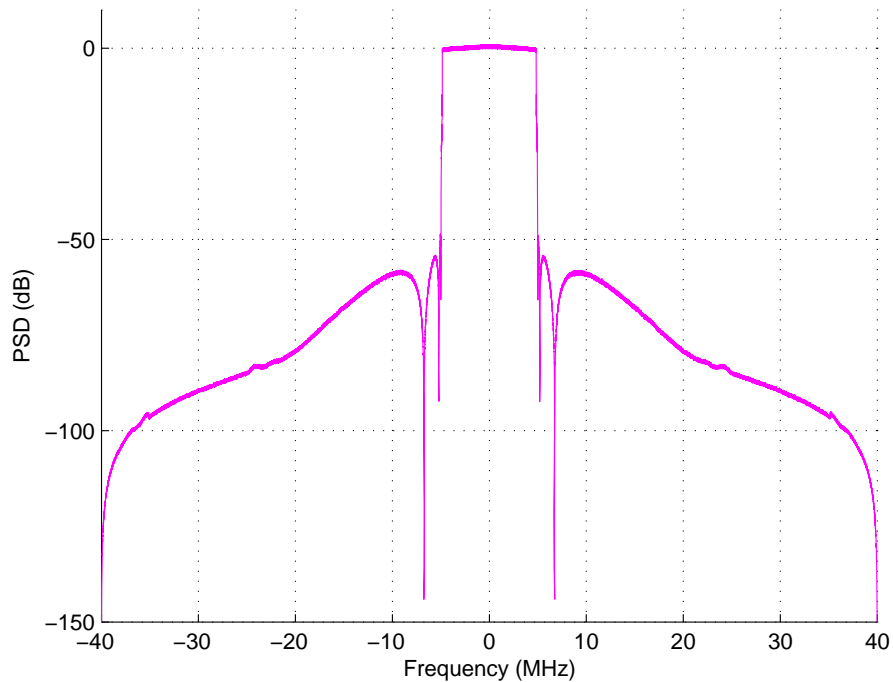


Figure 3-9 Forward link transmit spectrum

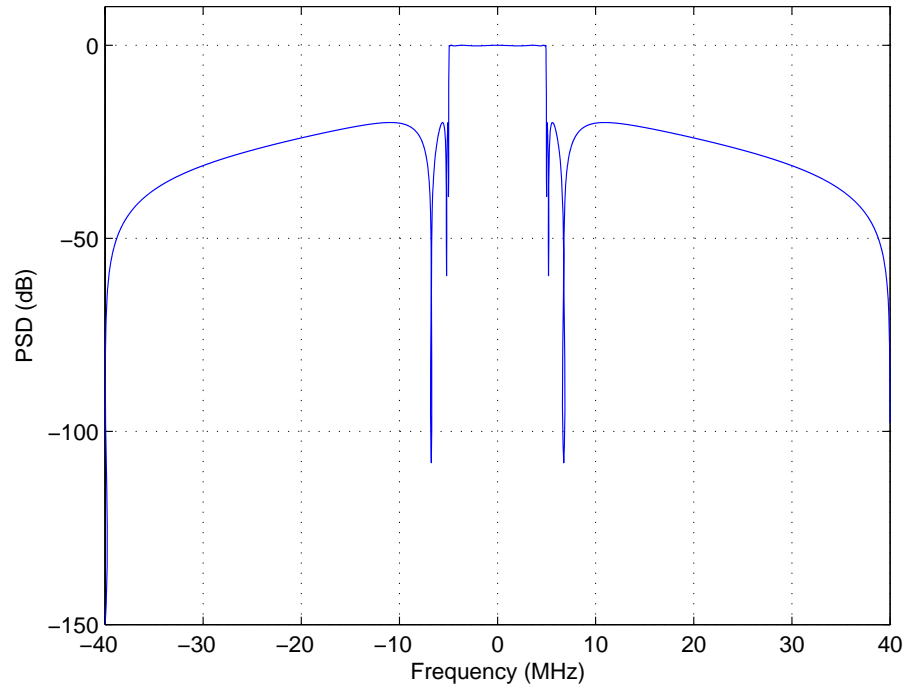


Figure 3-10 Amplitude response of downlink post-power amplifier elliptic filter

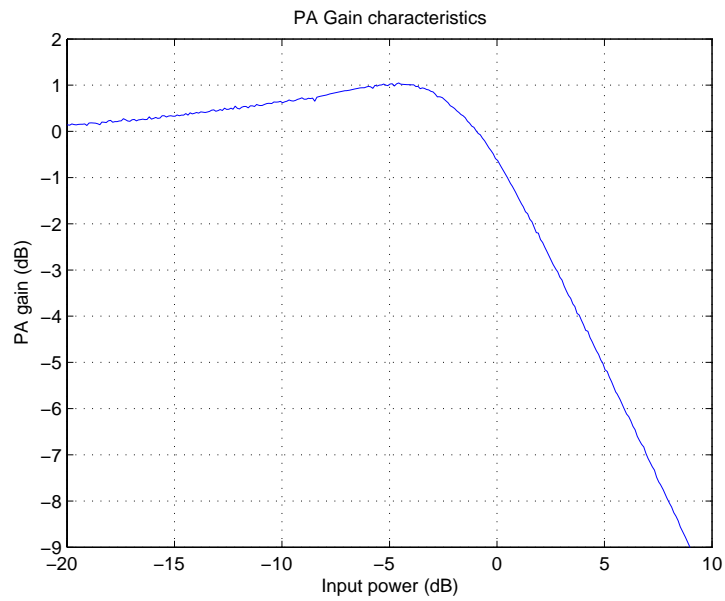


Figure 3-11 Power Amplifier AM-AM characteristic

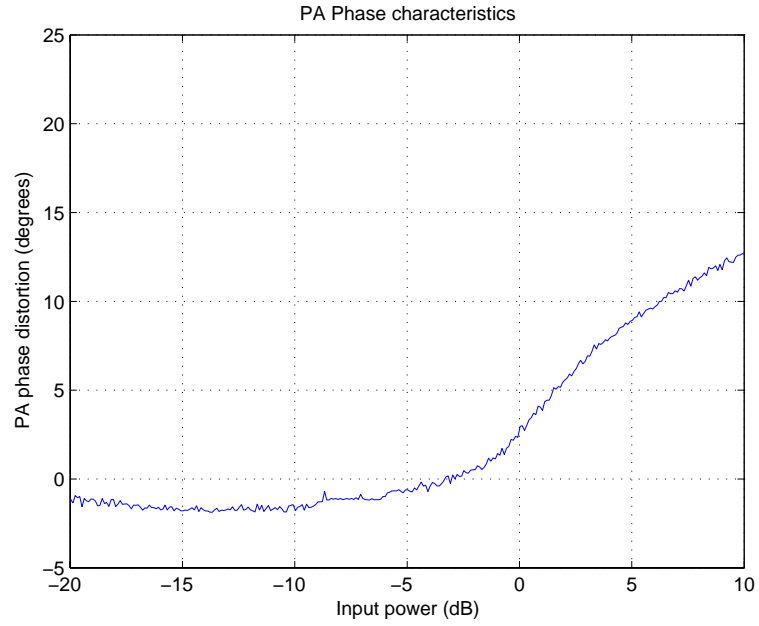


Figure 3-12 Power Amplifier AM-PM characteristic

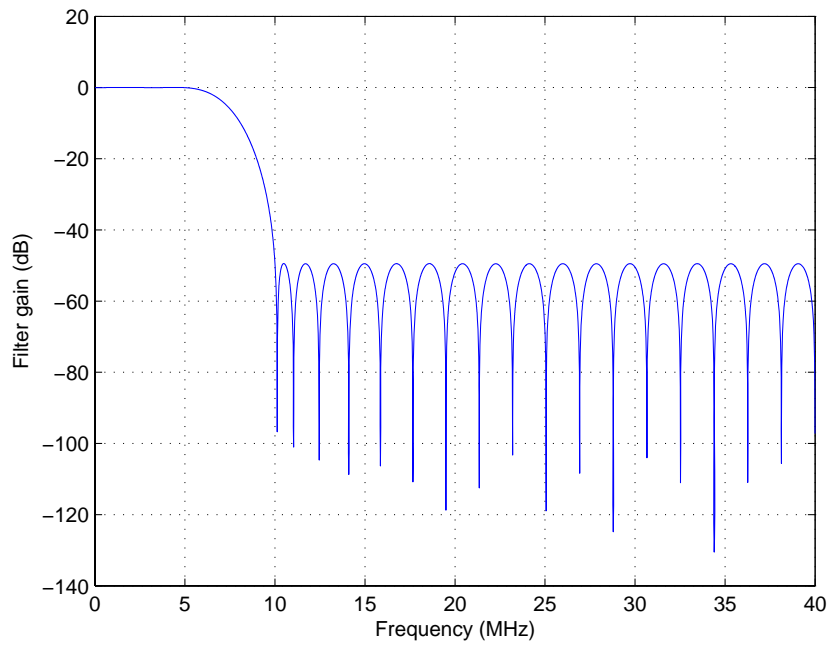


Figure 3-13 DAC low-pass filter amplitude response (8x oversampling)

Figure 3-14 shows the transmit spectrum for the MBTDD uplink with 10MHz deployment. The spectrum was generated using 16 guard subcarriers at each edge of the band, and of the remaining 992 subcarriers, the uplink user was allocated two independently hopping groups of 16 subcarriers each. The AM-AM and AM-PM characteristics of the power amplifier used to generate these spectra are shown in Figure 3-11 and Figure 3-12 respectively. These characteristics were measured from an implemented power amplifier. A zeroth order hold digital-to-analog convertor (DAC) was used, and the amplitude response of the low-pass filter used after the DAC is shown in Figure 3-13. An oversampling factor of 8 was used at the DAC input. The power-amplifier backoff used was 8.4 dB, and the FCC emissions criterion is met. No peak to average reduction techniques were used while generating these plots, hence the required backoff is conservative.

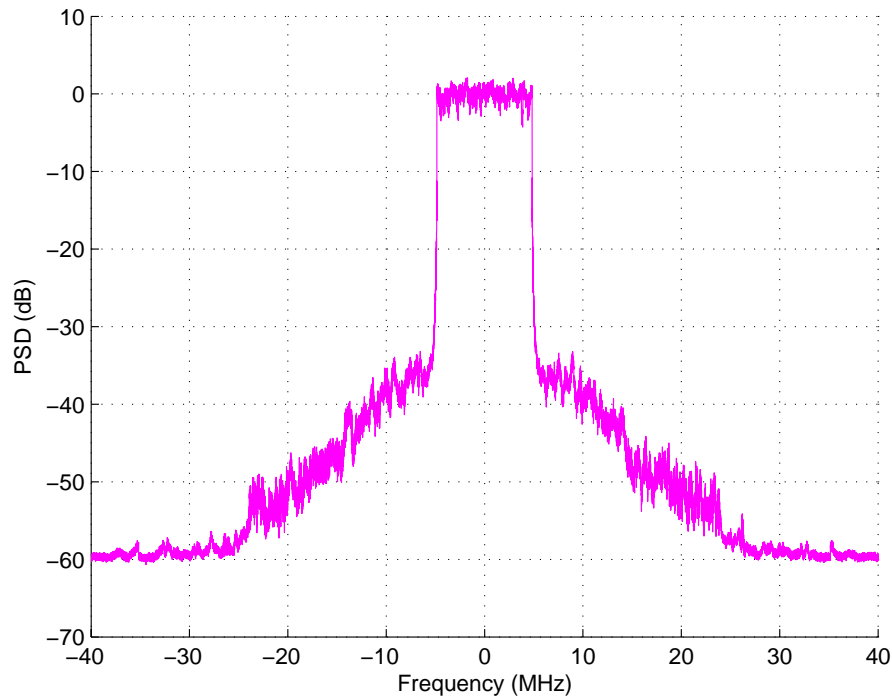


Figure 3-14 Reverse link transmit spectrum

Table 3-3 RF Specifications

#	RF Parameter	Base Value 1 MHz Channel	10 MHz Ch BW
1	Transmitter Power – BS	43 dBm/MHz	+53 dBm
2	Transmitter Power – MS	27 dBm	+27 dBm
3	Out of Band emission limits – BS and MS (emission measured in 1 MHz resolution bandwidth)	Attenuation of the transmit power P by: $43 + 10 \log(P)$ dB	-13 dBm
4*	ACLR - Attenuation of emissions into an adjacent channel (same Ch BW) – BS	---	60.2 dB

#	RF Parameter	Base Value 1 MHz Channel	10 MHz Ch BW
5*	ACLR - Attenuation of emissions into an adjacent channel (same Ch BW) – MS	---	37.7 dB
6	Receiver noise figure – BS	5 dB	5 dB
7	Receiver noise figure – MS	10 dB	10 dB
8	Receiver reference sensitivity (to be proposed by each technology)	Specify at FER of 1%	<i>value 3 (proposal specific)</i>
9*	Receiver Selectivity – BS	---	63 dB
10*	Receiver Selectivity – MS	---	33 dB
11[*]	Receiver Blocking – BS (level of same technology blocking signal at frequency offset of 2 times Channel BW)	---	-40 dBm
12[*]	Receiver Blocking – MS (level of same technology blocking signal at frequency offset of 2 times Channel BW)	---	-56 dBm

3.5 Link Budget

For reverse link, link budget was computed for 64Kbps edge rate, which was achieved using transmission on 32 tones each of bandwidth 9.6KHz, with scheduling on all interlaces. A maximum of 6 HARQ attempts was allowed, with EbNo and spectral efficiency chosen such that the packet error rate was less than 1% after the 6th attempt and the desired data rate was achieved. The raw BER corresponding to this packet error rate is less than 0.1%. For forward link, the same method was applied to compute the link budget. The resulting link budget applies to edge rate of 64Kbps assuming 32 tones and to 1.984Mbps assuming all the available 992 tones are used. Note that we are only considering the TDD mode with equal duty-cycle for forward and reverse links.

Table 3-4 Link budget assumptions

id/ ii	Item	Forward link	Reverse link
	Test environment	Suburban/urban macro-cell, micro-cell,	Suburban/urban macro-cell, micro-cell,
	Operating frequency	1.9GHz	1.9GHz
	Test service		
	Multipath channel class	Cases I-IV	Cases I-IV
Ii/i d	(a0) Average transmitter power per traffic channel (when transmitting)	52.79 dBm (no power control, so average and maximum power is same)	27dBm (no power control, so average and maximum power is same)

id/ ii	Item	Forward link	Reverse link
id	(a1) Maximum transmitter power per traffic channel (when transmitting)	52.79 dBm (Find power per tone based on 43dBm/MHz, multiply by total 992 tones in 10MHz design)	27dBm
id	(a2) Maximum total transmitter power (when transmitting)	43 dBm/MHz	27dBm
ii	(b) Cable, connector, and combiner losses (enumerate sources)	3 dB	0 dB
	Body Losses	0 dB	3 dB
ii	(c) Transmitter antenna gain	17 dBi	0 dBi
id	(d1) Transmitter e.i.r.p. per traffic channel = (a1 – b + c)	66.79 dBm	27 dBm
id	(d2) Total transmitter e.i.r.p. = (a2 – b + c)	57 dBm (per MHz)	27 dBm
	Penetration Loss (Ref: 3GPP2)	10 dB or 20 dB depending on indoor/outdoor	10 dB or 20 dB depending on indoor/outdoor
Ii	(e) Receiver antenna gain	0 dBi	17 dBi
Ii	(f) Cable and connector losses	0 dB	3 dB
	Body Losses	3 dB	0 dB
Ii	(g) Receiver noise figure	10 dB	5 dB
Ii	(h) Thermal noise density (H) (linear units)	-174 dBm/Hz 3.98×10^{-18} mW/Hz	-174 dBm/Hz 3.98×10^{-18} mW/Hz
Id	(i) Receiver interference density (NOTE 1) (I) (linear units)	-infinity dBm/Hz 0 mW/Hz Isolated cell, thermal-limited	-infinity dBm/Hz 0 mW/Hz Isolated cell, thermal-limited
id	(j) Total effective noise plus interference density = $10 \log (10^{((g + h)/10)} + I)$	-174+10= -164 dBm/Hz	-174+5= -169 dBm/Hz
ii	(k) Information rate ($10 \log (R_b)$)	62.98 dB (Hz) (1.984 Mbps)	48 dB (Hz) (64 Kbps)
id	(l) Required $E_b/(N_0 + I_0)$	$E_s N_0 + 10 \log(992 * 9600) - (k)$ (user bandwidth=992 tones, each 9.6KHz.). See tables below for $E_s N_0$	$E_s N_0 + 10 \log(32 * 9600) - (k)$ (user bandwidth=32 tones, each 9.6KHz.). See tables below for $E_s N_0$
id	(m) Receiver sensitivity = (j + k + l)	(based on $E_s N_0$ tables below. Eg. for $E_s N_0$ of -2.2dB, value is -96.4 dBm)	(based on $E_s N_0$ tables below. Eg. for $E_s N_0$ of -2.2dB, value is -116.3 dBm)

id/ ii	Item	Forward link	Reverse link
id	(n) Hand-off gain	0dB	0dB (fast cell-switching handoff)
id	(o) Explicit diversity gain	0dB (included in Eb/(No+Io))	0dB (included in Eb/(No+Io))
id	(o') Other gain	0dB Early-termination gain not accounted for	0dB Early-termination gain not accounted for
id	(p) Log-normal fade margin	6.9 dB	6.9 dB
Id	(q) Maximum path loss $= \{d1 - m + (e - f) + o + n + o' - p\}$	See table below	See table below
id	(r) Maximum range	See table below (used suburban Macro, pathloss in dB= $31.5+35\log(\text{range})$)	See table below (used suburban Macro, pathloss in dB= $31.5+35\log(\text{range})$)

Table 3-5 Reverse link link budget for 2 Rx 64 Kbps (10dB penetration loss)

CHANNEL	EsNo per antenna (dB) (for item I in link-budget template)	Maximum pathloss in dB (item q in link-budget template)	Maximum range in metres (item r in link-budget template)
I (ped-A)	-0.9	136.1	974
II (veh-A)	-2.4	137.6	1075
III (ped-B)	-2.2	137.4	1061
IV (veh-B)	-1.7	136.9	1027

Table 3-6 Reverse link link budget for 4 Rx 64 Kbps (10dB penetration loss)

CHANNEL	EsNo per antenna (dB) (for item I in link-budget template)	Maximum pathloss in dB (item q in link-budget template)	Maximum range in metres (item r in link-budget template)
I (ped-A)	-4.5	139.7	1238
II (veh-A)	-5.6	140.8	1327
III (ped-B)	-5.8	141.0	1345
IV (veh-B)	-4.6	139.8	1243

Table 3-7 Forward link link budget for 2 Rx, 1.984 Mbps (10dB penetration loss)

CHANNEL	EsNo per antenna (dB) (for item l in link-budget template)	Maximum pathloss in dB (item q in link-budget template)	Maximum range in metres (item r in link-budget template)
I (ped-A)	-0.9	145	1749
II (veh-A)	-2.4	146.5	1931
III (ped-B)	-2.2	146.3	1906
IV (veh-B)	-1.7	145.8	1844

Table 3-8 Reverse link link budget for 2 Rx 64 Kbps (20dB penetration loss)

CHANNEL	EsNo per antenna (dB) (for item l in link-budget template)	Maximum pathloss in dB (item q in link-budget template)	Maximum range in metres (item r in link-budget template)
I (ped-A)	-0.9	126.1	504
II (veh-A)	-2.4	127.6	557
III (ped-B)	-2.2	127.4	550
IV (veh-B)	-1.7	126.9	532

Table 3-9 Reverse link link budget for 4 Rx 64 Kbps (20dB penetration loss)

CHANNEL	EsNo per antenna (dB) (for item l in link-budget template)	Maximum pathloss in dB (item q in link-budget template)	Maximum range in metres (item r in link-budget template)
I (ped-A)	-4.5	129.7	639
II (veh-A)	-5.6	130.8	687
III (ped-B)	-5.8	131.0	696
IV (veh-B)	-4.6	129.8	644

Table 3-10 Forward link link budget for 2 Rx, 1.984 Mbps (20dB penetration loss)

CHANNEL	EsNo per antenna (dB) (for item l in link-budget template)	Maximum pathloss in dB (item q in link-budget template)	Maximum range in metres (item r in link-budget template)
I (ped-A)	-0.9	135	906
II (veh-A)	-2.4	136.5	1000
III (ped-B)	-2.2	136.3	987
IV (veh-B)	-1.7	135.8	955

4 System Level Performance

4.1 Simulation Assumptions

We simulated system full buffer throughput for a 10 MHz TDD system. The suburban macro cell channel model with PedB, VehB and VehA multipath profiles are simulated. The simulation assumptions are listed in Table 4-1 and Table 4-2.

Table 4-1 System Simulation Parameters (I)

	FL Evaluation	RL Evaluation
Network Topology	Hexagonal Grid, 19 cells with wrap around.	Hexagonal Grid, 19 cells with wrap around.
TDD Mode	1:1 (FL:RL)	1:1 (FL:RL)
Site-to-Site distance	1km, 2.5km	1km, 2.5km
Sectorization	3 sectors/cell	3 sectors/cell
Horizontal Antenna Pattern	70 deg@3dB bandwidth, 20dB maximum attenuation.	70 deg@3dB bandwidth, 20dB maximum attenuation.
Vertical Antenna Pattern	None	None
Propagation model.	Suburban macro $31.5 + 35\log_{10}(d \text{ in m})\text{dB}$	Suburban macro $31.5 + 35\log_{10}(d \text{ in m}) \text{ dB}$
BTS Minimum Separation	35m	35m
BTS Ant Height	32m (macro)	32m(macro)
AT Ant Height	1.5m	1.5m
Carrier Frequency	1.9GHz	1.9GHz
Bandwidth	10MHz	10MHz
Admission Control	None	None
Log-normal Shadowing	10dB	10dB
Site-to-site shadow correlation coefficient	0.5	0.5
Thermal Noise Density	-174dBm/Hz	-174dBm/Hz
Noise Figure	10dB	5dB
Max Transmit Power	43dBm/MHz	27dBm
Peak base-station antenna gain with cable loss	17dBi-3dB = 14dBi	17dBi-3dB=14dBi
Penetration Loss	10dB(Veh)	10dB(Veh)
MS Antenna Gain	0dBi	0dBi
Body Losses	3dB	3dB
Maximum C/I achievable per antenna	30dB	30dB

		FL Evaluation	RL Evaluation
BTS Antennas		1, 4 transmitter antennas	2, 4 receiver antennas
AT Antennas		2, 4 receiver antennas	1 transmitter antenna
ITU Channels		Suburban macro, pedB@3km/h, VehA,VehB@120km/h	Suburban macro, pedB@3km/h, VehA,VehB@120km/h
AT	Ant. Spacing	0.5λ	0.5λ
	Correlation	SCM suburban macro	SCM suburban macro
BTS	Ant. Spacing	10λ	10λ
	Correlation	SCM suburban macro	SCM suburban macro
Fairness		DV fairness (0.1, 0.1), (0.5, 0.5) normalized throughput line.	DV fairness (0.1, 0.1), (0.5, 0.5) normalized throughput line.
Traffic		Full Buffer	Full Buffer
Receiver Combining		MMSE	MMSE

Table 4-2 System Simulation Parameters (II)

Transmission Bandwidth	10MHz
Subcarrier Spacing	9.6kHz
Sampling Frequency	9.8304MHz
FFT Size	1024
Guard Carriers	32
Cyclic Prefix Length	6.51 μ s
Windowing Duration	3.26 μ s
OFDM Symbol Duration	113 μ s
Number of OFDM Symbols Per Frame	8

4.2 Peak Data Rates

The user peak data rate is computed according to the following formula:

$$R = r(B - B_{Guard})T_{Link} (1 - O_{ctrl})(1 - O_{pilot})(1 - O_{CPandWGI}),$$

where

- R denotes the peak data rate,
- r denotes the maximum spectral efficiency before counting the pilot overhead,
- B denotes the total bandwidth,
- B_{Guard} denotes the guard bandwidth,

- T_{Link} denotes the fraction of time for the desired link.
- O_{ctrl} denotes the control overhead as a fraction of the usable bandwidth,
- O_{pilot} denotes the pilot overhead,
- $O_{\text{CP/WGI}}$ denotes the cyclic prefix and windowing guard time.

For the 10 MHz simulations, the guard band is set to 32 subcarriers per 1024 subcarriers on both FL and RL. For a TDD system with 1:1 partitioning, the fraction of time for FL and RL are the same, 48%, where the preamble overhead is 4%. The control overhead is assumed to be 10% on FL and 11% on RL. The pilot overhead for block hopping is 14% for non-MIMO transmissions and 19% for rank 4 MIMO transmissions. The cyclic prefix and windowing overhead is 8.5%.

The forward link peak rate for 10 MHz bandwidth with 9.8 Mcps sampling rate is 63 Mbps for a user that uses the highest FL packet format of 5.5 bps/Hz and transmits on 4 layers. The reverse link peak rate for 10 MHz bandwidth with 9.8 Mcps sampling rate is 15 Mbps for a user that uses the highest RL packet format of 5 bps/Hz.

Table 4-3 Forward link and reverse link peak rate

Parameter	Bandwidth 10 MHz	
	Forward link	Reverse link
Required Peak User Data Rate	18 Mbps	9 Mbps
MBWA TDD Proposal	63 Mbps	15 Mbps

4.3 System Spectral Efficiency (bps/Hz/sector)

The spectral efficiency values of the proposed MBWA system are listed in Table 4-4 together with the requirement in SRD. The simulations assume 10 MHz block assignment. Note that the spectral efficiencies are computed based on the aggregated data rates listed in Table 4-5 and Table 4-7 for 1 km BS to BS distance. SCM based correlation model is used for all system simulations.

Table 4-4 Spectral Efficiency

Parameter	Spectral Efficiency Requirements			
	Downlink		Uplink	
	PedB 3 km/hr	VehA 120 km/hr	PedB 3 km/hr	VehA 120 km/hr
Required Spectral Efficiency (b/s/Hz/sector)	2.0	1.5	1.0	0.75
MBWA TDD Spectral efficiency (b/s/Hz/sector)	2.11	1.85	1.27	1.15

4.4 Aggregate Data Rates –Forward link and Reverse link

The aggregated data rates and corresponding system spectral efficiency for a 10 MHz block assignment for FL and RL simulations are shown in Table 4-5, Table 4-6, Table 4-7, and Table 4-8. The fairness of all simulations are shown in Figure 4-1 to Figure 4-5. It is observed that all simulations meet the fairness requirements in the Evaluation Criteria [1].

Table 4-5 FL sector throughput

Sector Throughput (Kbps)		1x2	1x4	4x4
1km BS to BS	pedB 3km/h	5775	7409	10544
	vehA 120km/h	5366	6801	9262
	vehB 120km/h	3096	4613	6599
2.5km BS to BS	pedB 3km/h	5659	7152	9119
	vehA 120km/h	5048	6765	7784
	vehB 120km/h	2944	4300	5354

Table 4-6 FL system spectral efficiency

Spectral Efficiency (b/s/Hz/sector)		1x2	1x4	4x4
1km BS to BS	pedB 3km/h	1.16	1.48	2.11
	vehA 120km/h	1.07	1.36	1.85
	vehB 120km/h	0.62	0.92	1.32
2.5km BS to BS	pedB 3km/h	1.13	1.43	1.82
	vehA 120km/h	1.01	1.35	1.56
	vehB 120km/h	0.59	0.86	1.07

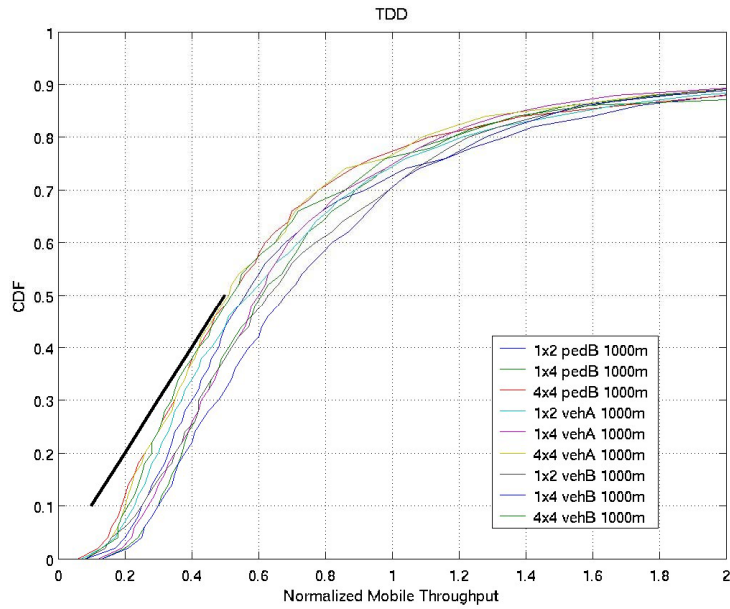


Figure 4-1 Fairness, FL, 4x4, pedB,vehA,vehB, 1000m site to site

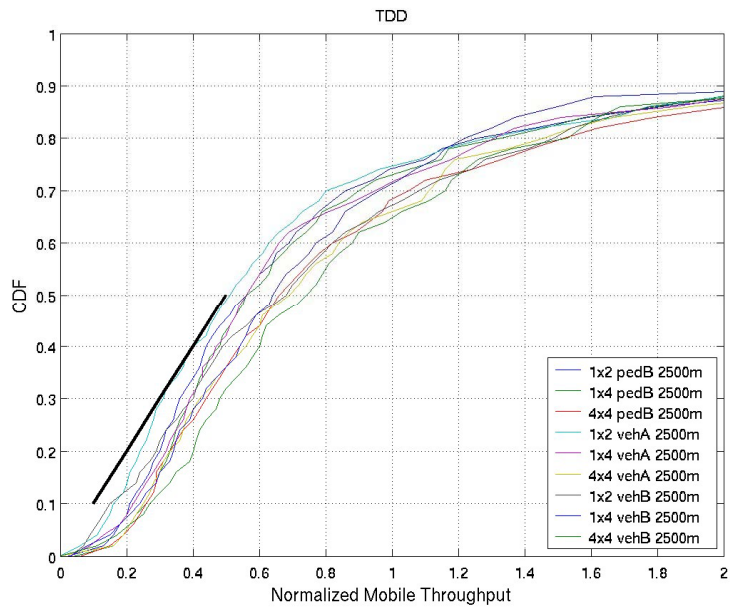


Figure 4-2 Fairness, FL, pedB,vehA,vehB, 2500m site to site

Note that RL simulations only use packet formats 0 to 8, hence the throughput results are conservative

Table 4-7 RL Sector Throughput

Sector Throughput (Kbps)		1x2	1x4
1km BS to BS	pedB 3km/h	3938	6341
	vehA 120km/h	3387	5746
	vehB 120km/h	2788	4926
2.5km BS to BS 16 users/sector	pedB 3km/h	3140	4900
	vehA 120km/h	2516	4341
	vehB 120km/h	2656	3881
2.5km BS to BS 32 users/sector	pedB 3km/h	2324	3591
	vehA 120km/h	2196	3460
	vehB 120km/h	1773	2574

Table 4-8 RL system spectral efficiency

Spectral Efficiency (b/s/Hz/sector)		1x2	1x4
1km BS to BS	pedB 3km/h	0.79	1.27
	vehA 120km/h	0.68	1.15
	vehB 120km/h	0.56	0.99
2.5km BS to BS 16 users/sector	pedB 3km/h	0.63	0.98
	vehA 120km/h	0.5	0.87
	vehB 120km/h	0.53	0.78
2.5km BS to BS 32 users/sector	pedB 3km/h	0.46	0.72
	vehA 120km/h	0.44	0.69
	vehB 120km/h	0.35	0.51

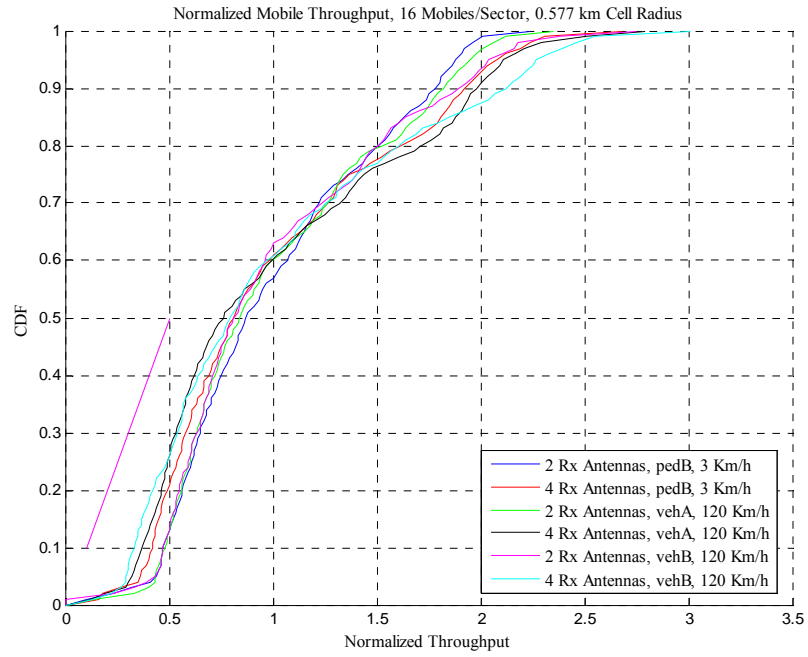


Figure 4-3 Fairness, RL, 1000m Site-to-Site Distance

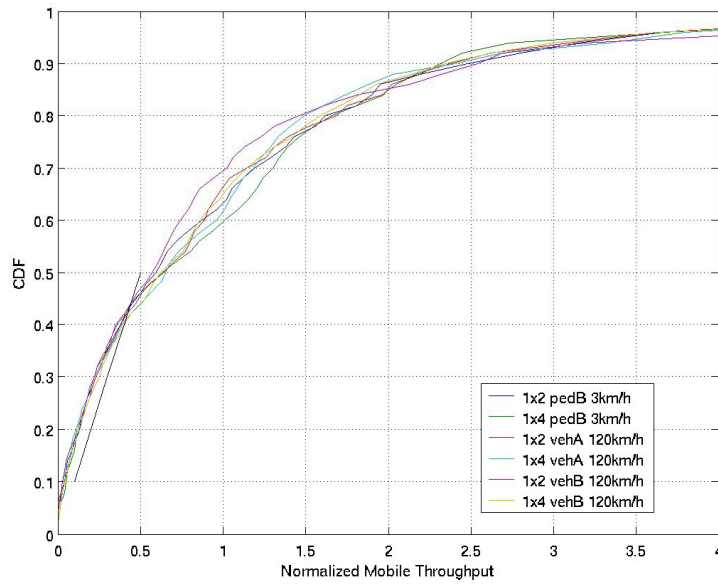


Figure 4-4 Fairness, RL, 2500m Site-to-Site Distance, 16 users per sector

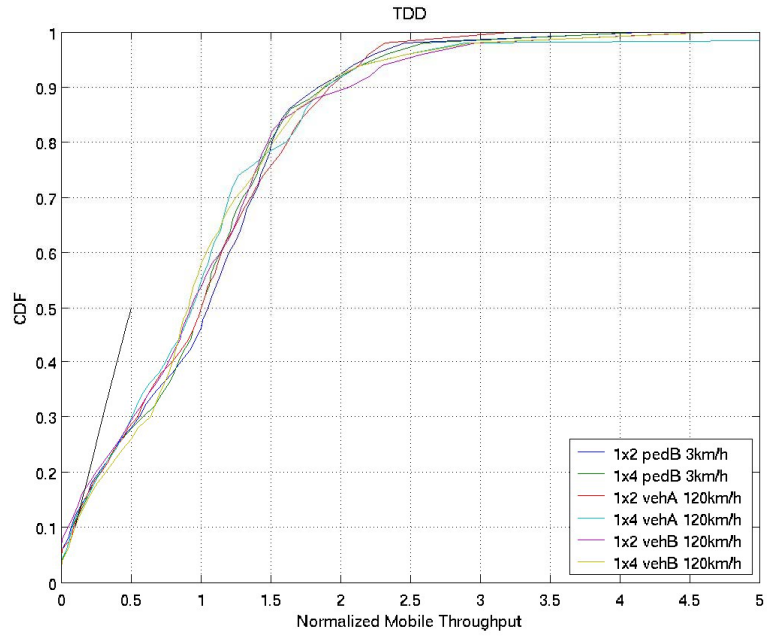


Figure 4-5 Fairness, RL, 2500m Site-toSite Distance, 32 users per sector

4.5 Throughput Coverage Tradeoff

4.5.1 Forward Link

4.5.1.1 802.20 Fairness Scheduling

In this section we present throughput and coverage trade off for forward link with an 802.20 fairness scheduler which meets the fairness criteria specified in the Evaluation Criteria. Figure 4-6 shows the CDF of mobile throughput for a 4x4 system in a suburban macro cell deployment with a site-to-site distance of 1000m with 8 users per sector. Table 4-9 and Table 4-10 show the sector throughput and spectral efficiency, and edge user throughput values as a function of the site-to-site distance and number of users per sector. Figure 4-7 shows the edge user throughput against system load (users per sector) vs. site-to-site distance as tabulated in Table 4-10. Figure 4-8 shows the edge user throughput vs. sector throughput and site-to-site distance as tabulated in Table 4-9 and Table 4-10. Figure 4-9 shows the system spectral efficiency vs. site-to-site distance for edge user throughputs as tabulated in Table 4-9 and Table 4-10.

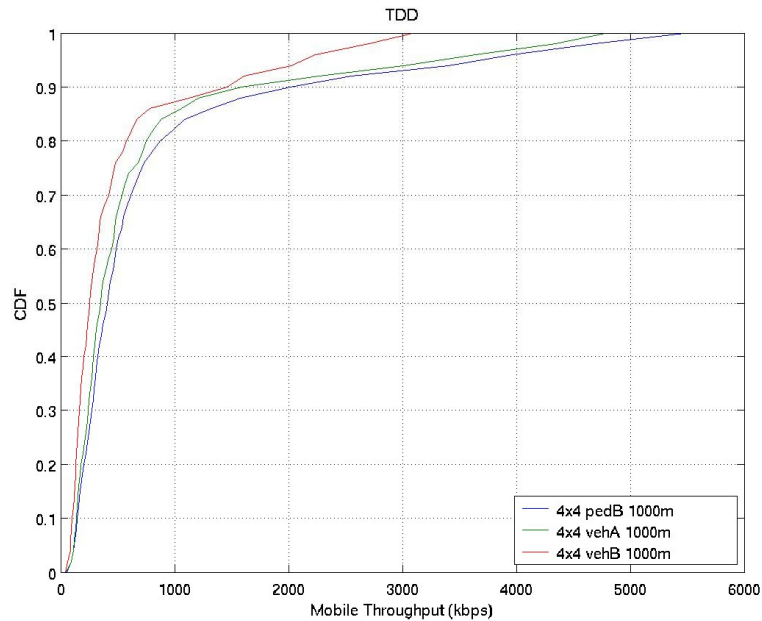


Figure 4-6 CDF of user throughput (1000m, 16 users/sector) for a 4x4 MIMO system with 802.20 fairness

Table 4-9 Sector throughput and spectral efficiency vs. site-to-site distance and the number of users for a 4x4 MIMO system with 802.20 fairness, pedB 3km/h

Sector Throughput (Kbps) and Spectral Efficiency (b/s/Hz/sector)	16 users/sector	32 users/sector
1km BS to BS	10544 kbps (2.11 b/s/Hz)	11199 kbps (2.24 b/s/Hz)
2.5km BS to BS	9119 kbps (1.83 b/s/Hz)	9126 kbps (1.83 b/s/Hz)

Table 4-10 Edge user throughput vs. site-to-site distance and the number of users for 4x4 MIMO system with 802.20 fairness, pedB 3km/h

Edge Throughput (Kbps)	16 users/sector	32 users/sector
1km BS to BS	177	94
2.5km BS to BS	159	81

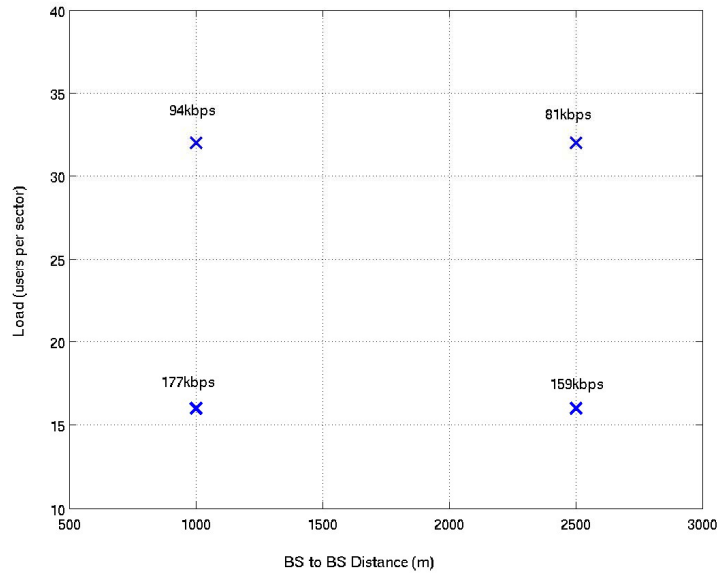


Figure 4-7 Edge user throughput against system load (users per sector) and site-to-site distance for a 4x4 MIMO system with 802.20 fairness, pedB 3km/h

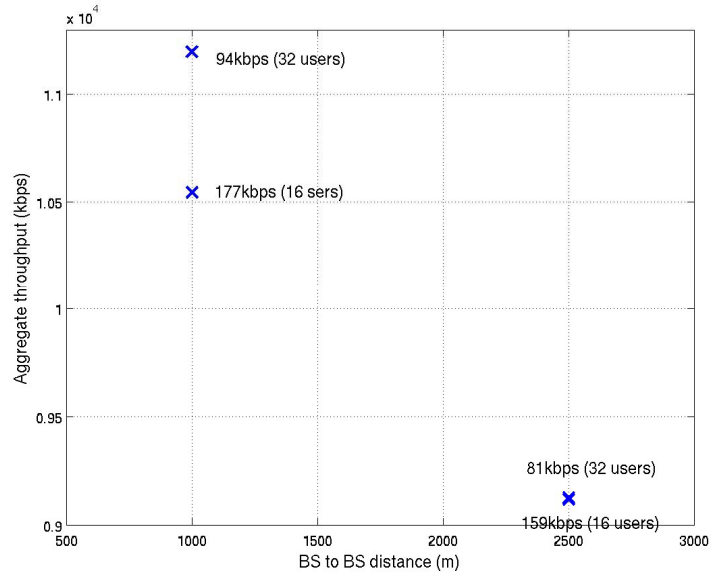


Figure 4-8 Edge user throughput vs. sector throughput and site-to-site distance for a 4x4 MIMO system with 802.20 fairness, pedB 3km/h

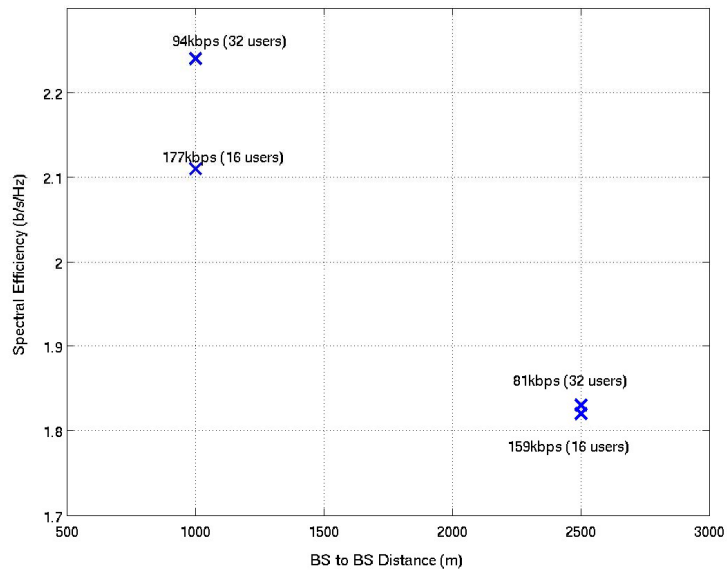


Figure 4-9 Edge user throughput against spectral efficiency vs. site-to-site distance for a 4x4 MIMO system with 802.20 fairness scheduling, pedB 3km/h

4.5.1.2 Equal Grade of Service Scheduling

In this section we present throughput and coverage trade off for forward link with an EGoS scheduler. Figure 4-10 shows the CDF of mobile throughput for a 4x4 system in a suburban macro cell deployment with a site-to-site distance of 1000m with 8 users per sector. Table 4-11 and Table 4-12 show the sector throughput and spectral efficiency, and edge user throughput values as a function of the site-to-site distance and number of users per sector. Figure 4-11 shows the edge user throughput against system load (users per sector) vs. site-to-site distance as tabulated in Table 4-12. Figure 4-12 shows the edge user throughput vs. sector throughput and site-to-site distance as tabulated in Table 4-11 and Table 4-12. Figure 4-13 shows the system spectral efficiency vs. site-to-site distance for edge user throughputs as tabulated in Table 4-11 and Table 4-12.

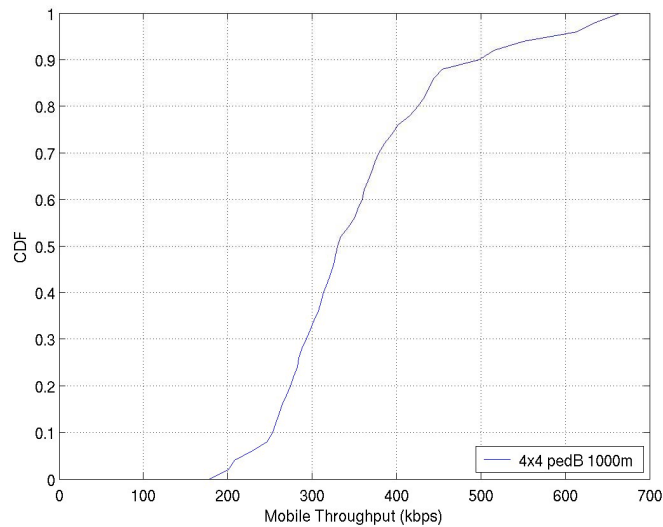


Figure 4-10 CDF of mobile throughput (1000m, 16 users/sector) for a 4x4 MIMO system with EGoS fairness

Table 4-11 Sector throughput and spectral efficiency vs. site-to-site distance and the number of users for a 4x4 MIMO system with EGoS fairness, pedB 3km/h

Sector Throughput (Kbps) and Spectral Efficiency (b/s/Hz/sector)	16 users/sector	32 users/sector
1km BS to BS	5650 kbps (1.13 b/s/Hz)	5603 kbps (1.12 b/s/Hz)
2.5km BS to BS	4583 kbps (0.92 b/s/Hz)	4514 kbps (0.9 b/s/Hz)

Table 4-12 Edge user throughput vs. site-to-site distance and the number of users for a 4x4 MIMO system with EGoS fairness, pedB 3km/h

Edge Throughput (Kbps)	16 users/sector	32 users/sector
1km BS to BS	274	155
2.5km BS to BS	197	111

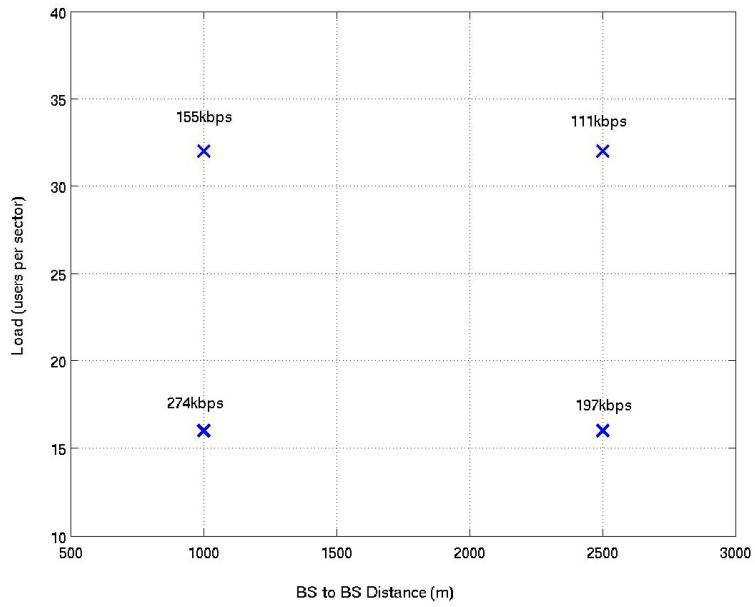


Figure 4-11 Edge user throughput against users per sectors vs. base station separation for a 4x4 MIMO system with 802.20 fairness scheduling, pedB 3km/h

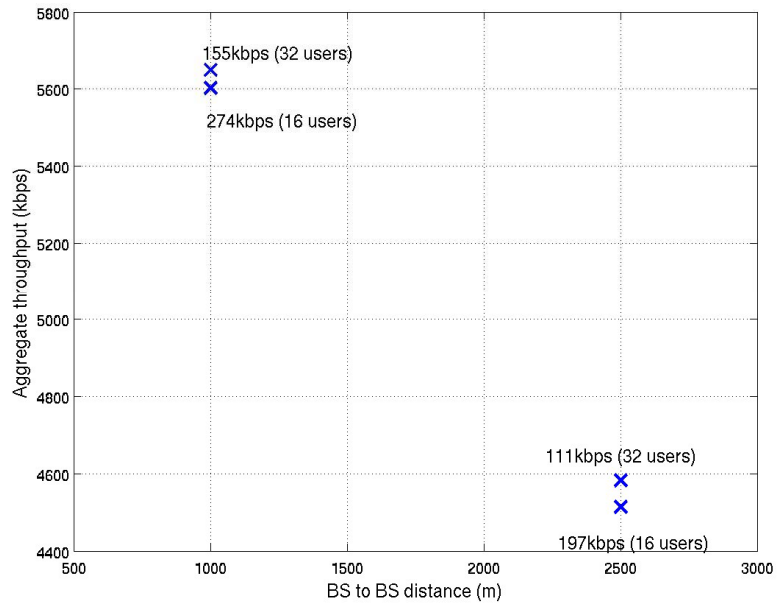


Figure 4-12 Edge user throughput vs. sector throughput and site-to-site distance for a 4x4 MIMO system with EGoS fairness

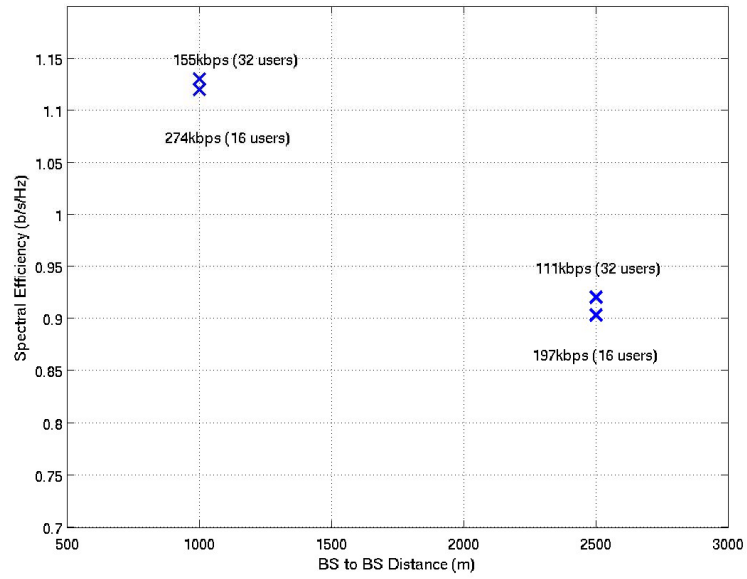


Figure 4-13 Edge user throughput against spectral efficiency vs. site-to-site distance for a 4x4 MIMO system with 802.20 fairness scheduling, pedB 3km/h

4.5.2 Reverse Link

In this section we present throughput and coverage trade off for reverse link with an EGoS scheduler. Figure 4-14 shows the CDF of mobile throughput for 1x2 and 1x4 systems in a suburban macro cell deployment with a site-to-site distance of 1000m with 8 users per sector. Table 4-13 and Table 4-14 show the sector throughput and spectral efficiency, and edge user throughput values as a function of the site-to-site distance and number of users per sector. Figure 4-15 shows the edge user throughput against system load (users per sector) vs. site-to-site distance as tabulated in Table 4-14. Figure 4-16 shows the edge user throughput vs. sector throughput and site-to-site distance as tabulated in Table 4-13 and Table 4-14. Figure 4-17 shows the system spectral efficiency vs. site-to-site distance for edge user throughputs as tabulated in Table 4-13 and Table 4-14.

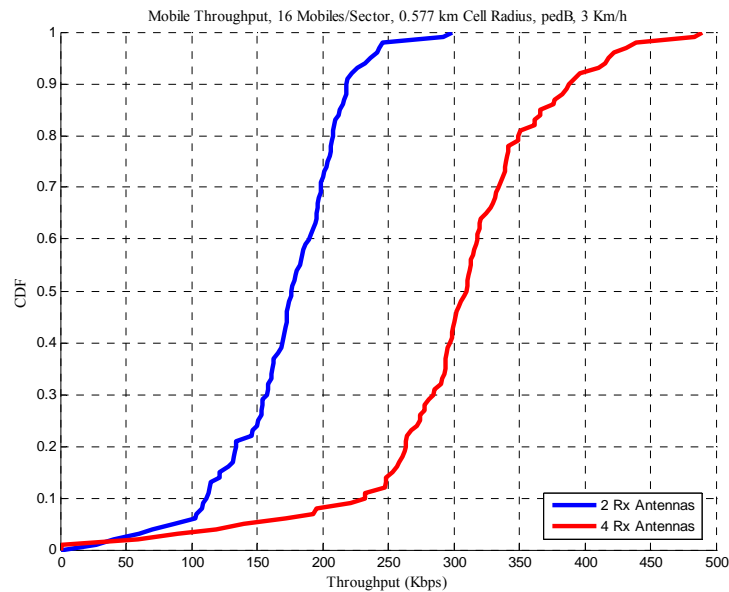


Figure 4-14 User throughput CDF for 1000m site-to-site distance and 16 users/sector, with EGoS fairness

Table 4-13 Sector throughput and spectral efficiency vs. site-to-site distance and number of users with four receive antennas and EGoS fairness, pedB 3km/h

Sector Throughput (Kbps) and Spectral Efficiency (b/s/Hz/sector)	16 users/sector	32 users/sector
1km BS to BS	4836 kbps (0.97 b/s/Hz)	4699 kbps (0.94 b/s/Hz)
2.5km BS to BS	4499 kbps (0.9 b/s/Hz)	4290 kbps (0.86 b/s/Hz)

Table 4-14 Edge user throughput vs. site-to-site distance and number of users with four receive antennas and EGoS fairness

Edge Throughput (Kbps)	16 users/sector	32 users/sector
1km BS to BS	266	135
2.5km BS to BS	53	50

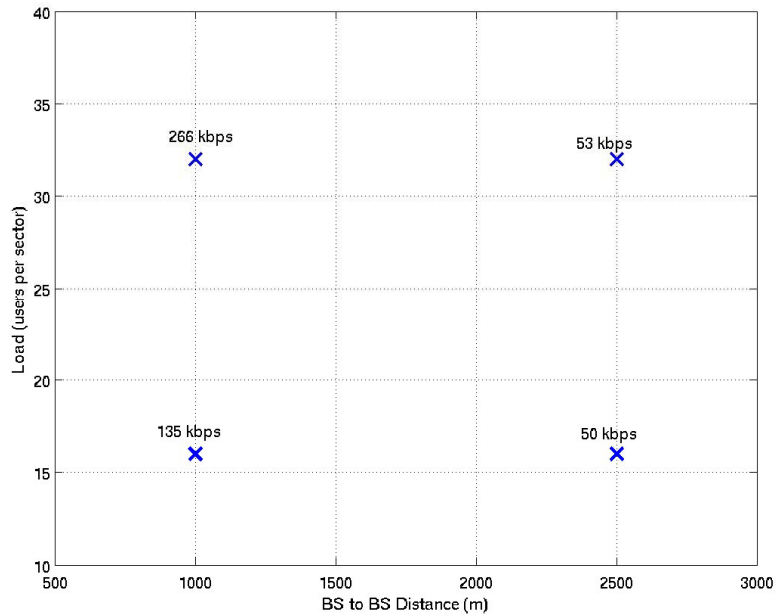


Figure 4-15 Edge user throughput against system load (users per sector) and site-to-site distance with four receive antennas and EGoS fairness, pedB 3km/h

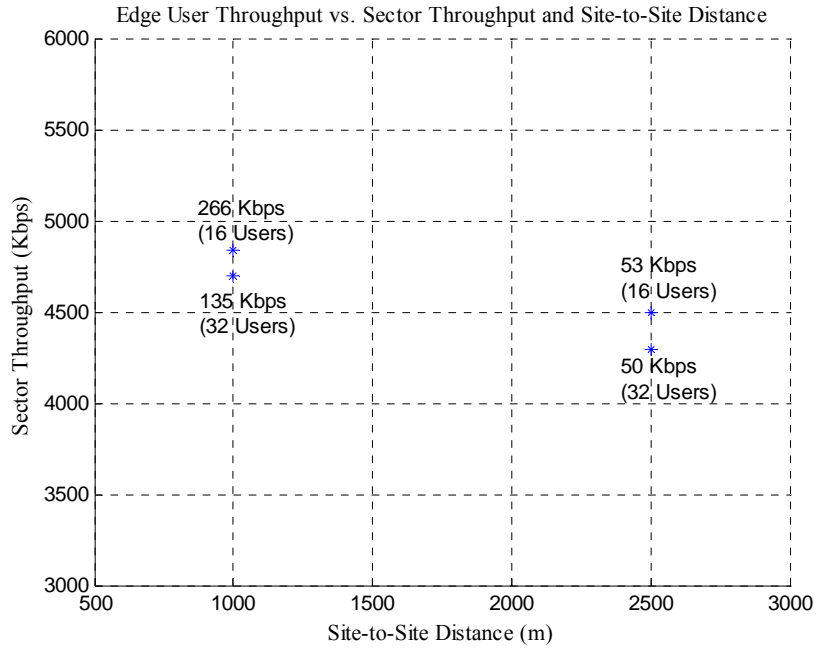


Figure 4-16 Edge user throughput vs. sector throughput and site-to-site distance with four receive antennas and EGoS fairness, pedB 3km/h

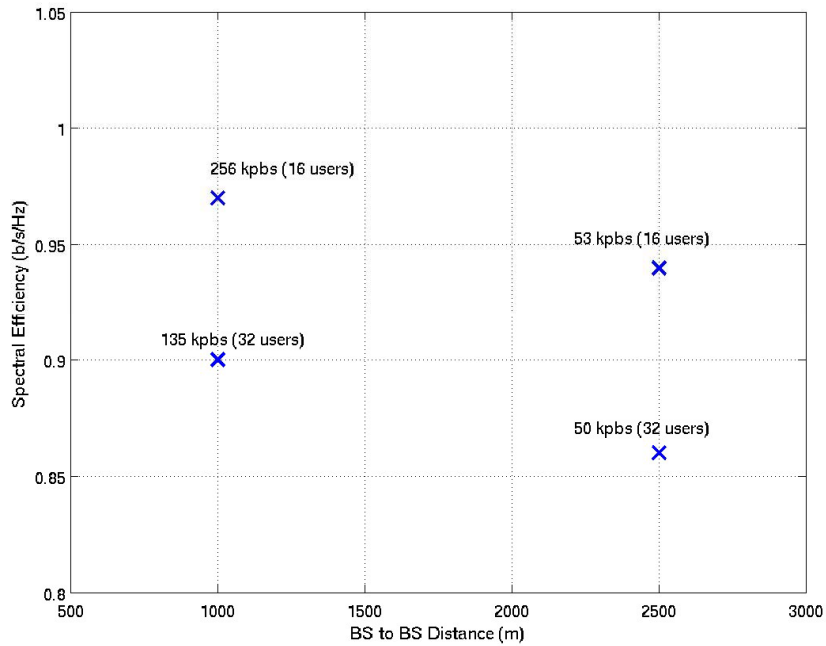


Figure 4-17 Edge user throughput against spectral efficiency vs. site-to-site distance with four receive antennas and EGoS fairness, pedB 3km/h

5 References

- [1] IEEE 802.20 – The approved version of the Evaluation Criteria Document (ECD), 802.20-PD-09.
- [2] IEEE 802.20 – The approved System Requirements Document (SRD),802.20-PD-06r1.
- [3] IEEE 802.20 – The adopted Channel Models Document, 802.20-PD-08.
- [4] IEEE P802.11 – Task Group N - Selection Procedure, 802.11-03/665r8.
- [5] IEEE C802.20-06/04 “MBFDD and MBTDD: Proposed Draft Air Interface Specification”.
- [6] IEEE C802.20-04-67 “Link-System Interface Simulation Methodologies”
- [7] IEEE C802.20-05-03r1 “Mapping SISO and MIMO Channel Performance”

Appendix A Correlation Matrices for Link Level Simulations

The correlation matrices at the BS are listed in Table 5-1 for a linear array of 4 antennas with 10λ spacing. The first 2×2 sub-matrix of each matrix is also the correlation matrix for a linear array of 2 antennas. The matrices corresponding to two different spatial correlation models namely, the Laplacian model and the SCM model are shown in the table below.

Table 5-1 Correlation matrices for BS at 50 and 20 degree AoD for 4 antennas

Laplacian Model				
Antenna Spacing $10 \times \text{Wavelength}$, AoA=20, AS=5	1	-0.061884+0.032678i	0.010079-0.015489i	-0.00059694+0.0082371i
	-0.061884-0.032678i	1	-0.061884+0.032678i	0.010079-0.015489i
	0.010079+0.015489i	-0.061884-0.032678i	1	-0.061884+0.032678i
	-0.00059694-0.0082371i	0.010079+0.015489i	-0.061884-0.032678i	1
Antenna Spacing $10 \times \text{Wavelength}$, AoA=50, AS=2	1	-0.26151-0.42845i	-0.091214+0.17899i	0.099976-0.009446i
	-0.26151+0.42845i	1	-0.26151-0.42845i	-0.091214+0.17899i
	-0.091214-0.17899i	-0.26151+0.42845i	1	-0.26151-0.42845i
	0.099976+0.009446i	-0.091214-0.17899i	-0.26151+0.42845i	1
SCM Model				
Antenna Spacing $10 \times \text{Wavelength}$, AoA=50, AS=2	1	0.011345+0.0047899i	0.0043835+0.0052649i	-0.0047587+0.0017224i
	0.011345-0.0047899i	0.99999	0.0076282+0.0065688i	0.0013711+0.0059998i
	0.0043835-0.0052649i	0.0076282-0.0065688i	0.99999	0.011046+0.0040806i
	-0.0047587-0.0017224i	0.0013711-0.0059998i	0.011046-0.0040806i	0.99999

The correlation matrices at the MS are listed in Table 5-2 for a linear array of 4 antennas with 0.5λ spacing. The first 2×2 sub-matrix of each matrix is also the correlation matrix for a linear array of 2 antennas.

Table 5-2 Correlation matrices for MS at 67.5 degree AoA for 4 antennas

Laplacian Model				
Antenna Spacing $0.5 \times \text{Wavelength}$, AoA=67.5, AS=35	1	-0.71515+0.32409i	0.52663-0.35021i	-0.41482+0.33932i
	-0.71515-0.32409i	1	-0.71515+0.32409i	0.52663-0.35021i
	0.52663+0.35021i	-0.71515-0.32409i	1	-0.71515+0.32409i
	-0.41482-0.33932i	0.52663+0.35021i	-0.71515-0.32409i	1
SCM Model				
Antenna Spacing $0.5 \times \text{Wavelength}$, AoA=67.5, AS=35	1	-0.32045+0.018231i	0.22542-0.0082376i	-0.18756+0.0060785i
	-0.32045-0.018231i	1	-0.32038+0.018776i	0.22616-0.0084026i
	0.22542+0.0082376i	-0.32038-0.018776i	0.99999	-0.31983+0.019627i
	-0.18756-0.0060785i	0.22616+0.0084026i	-0.31983-0.019627i	1

Table 5-5 Antenna Spacing 10 λ, Angular Spread 2 degrees, Laplacian Model

Angle of Arrival/Departure	Angular Spread 2, Antenna Spacing 10xWavelength					Angular Spread 2, Antenna Spacing 10 x Wavelength			
	0.29361	0.09414	0.29361	0.09414		0.29361	0.09414	0.29361	0.09414
0	0.29361	0.09414	0.29361	0.09414	180	0.29361+2.0237e-15i	0.09414+1.6958e-15i	0.043947-3.9274e-15i	0.29361+2.0237e-15i
10	0.29361	0.09414	0.29361	0.09414	190	0.29361+2.0237e-15i	0.09414+1.6958e-15i	0.043947-3.9274e-15i	0.29361+2.0237e-15i
20	0.29361	0.09414	0.29361	0.09414	200	0.29361+2.0237e-15i	0.09414+1.6958e-15i	0.043947-3.9274e-15i	0.29361+2.0237e-15i
30	0.29361	0.09414	0.29361	0.09414	210	0.29361+2.0237e-15i	0.09414+1.6958e-15i	0.043947-3.9274e-15i	0.29361+2.0237e-15i
40	0.29361	0.09414	0.29361	0.09414	220	0.29361+2.0237e-15i	0.09414+1.6958e-15i	0.043947-3.9274e-15i	0.29361+2.0237e-15i
50	0.29361	0.09414	0.29361	0.09414	230	0.29361+2.0237e-15i	0.09414+1.6958e-15i	0.043947-3.9274e-15i	0.29361+2.0237e-15i
60	0.29361	0.09414	0.29361	0.09414	240	0.29361+2.0237e-15i	0.09414+1.6958e-15i	0.043947-3.9274e-15i	0.29361+2.0237e-15i
70	0.29361	0.09414	0.29361	0.09414	250	0.29361+2.0237e-15i	0.09414+1.6958e-15i	0.043947-3.9274e-15i	0.29361+2.0237e-15i
80	0.29361	0.09414	0.29361	0.09414	260	0.29361+2.0237e-15i	0.09414+1.6958e-15i	0.043947-3.9274e-15i	0.29361+2.0237e-15i
90	0.29361	0.09414	0.29361	0.09414	270	0.29361+2.0237e-15i	0.09414+1.6958e-15i	0.043947-3.9274e-15i	0.29361+2.0237e-15i
100	0.29361	0.09414	0.29361	0.09414	280	0.29361+2.0237e-15i	0.09414+1.6958e-15i	0.043947-3.9274e-15i	0.29361+2.0237e-15i
110	0.29361	0.09414	0.29361	0.09414	290	0.29361+2.0237e-15i	0.09414+1.6958e-15i	0.043947-3.9274e-15i	0.29361+2.0237e-15i
120	0.29361	0.09414	0.29361	0.09414	300	0.29361+2.0237e-15i	0.09414+1.6958e-15i	0.043947-3.9274e-15i	0.29361+2.0237e-15i
130	0.29361	0.09414	0.29361	0.09414	310	0.29361+2.0237e-15i	0.09414+1.6958e-15i	0.043947-3.9274e-15i	0.29361+2.0237e-15i
140	0.29361	0.09414	0.29361	0.09414	320	0.29361+2.0237e-15i	0.09414+1.6958e-15i	0.043947-3.9274e-15i	0.29361+2.0237e-15i
150	0.29361	0.09414	0.29361	0.09414	330	0.29361+2.0237e-15i	0.09414+1.6958e-15i	0.043947-3.9274e-15i	0.29361+2.0237e-15i
160	0.29361	0.09414	0.29361	0.09414	340	0.29361+2.0237e-15i	0.09414+1.6958e-15i	0.043947-3.9274e-15i	0.29361+2.0237e-15i
170	0.29361	0.09414	0.29361	0.09414	350	0.29361+2.0237e-15i	0.09414+1.6958e-15i	0.043947-3.9274e-15i	0.29361+2.0237e-15i

Table 5-6 Antenna Spacing 0.5 λ, Angular Spread 5 degrees, Laplacian Model

Angular Spread 5, Antenna Spacing 0.5xWavelength

Angle of Arrival/Departure	1	0.96425	0.87044	0.74834	180	1	0.96425+3.6983e-16i	0.87044+6.8307e-16i	0.74834+1.2131e-15i
0	1	0.96425	0.87044	0.74834	180	1	0.96425+3.6983e-16i	0.87044+6.8307e-16i	0.74834+1.2131e-15i
10	0.82604-0.49943i	0.82604+0.49943i	0.40474+0.7745i	-0.04953+0.75251i	190	0.82604+0.49943i	0.82604-0.49943i	0.40474-0.7745i	-0.04953-0.75251i
20	0.46403+0.84985i	0.46403-0.84985i	-0.48015+0.74213i	-0.76882-0.06245i	200	0.46403+0.84985i	0.46403-0.84985i	-0.48015-0.74213i	-0.76882+0.06245i
30	0.0050506-0.97289i	0.0050506+0.97289i	-0.89968+0.0058631i	-0.0023102-0.79922i	210	0.0050506-0.97289i	0.0050506+0.97289i	-0.89968-0.0058631i	-0.0023102+0.79922i
40	-0.41834+0.8847i	-0.41834-0.8847i	-0.58072-0.71325i	0.81371-0.19212i	220	-0.41834+0.8847i	-0.41834-0.8847i	-0.58072+0.71325i	0.81371+0.19212i
50	-0.72492-0.66652i	-0.72492+0.66652i	0.52968+0.70126i	0.082283-0.93837i	230	-0.72492-0.66652i	-0.72492+0.66652i	0.52968-0.70126i	0.082283+0.93837i
60	-0.90011+0.41363i	-0.90011-0.41363i	0.62954-0.72965i	-0.26207+0.88458i	240	-0.90011+0.41363i	-0.90011-0.41363i	0.62954+0.72965i	-0.26207-0.88458i
70	-0.97548-0.19816i	-0.97548+0.19816i	0.90473-0.38189i	-0.97548+0.19816i	250	-0.97548-0.19816i	-0.97548+0.19816i	0.90473+0.38189i	-0.97548-0.19816i
80	-0.99679+0.059261i	-0.99679-0.059261i	0.98735-0.11734i	-0.97219+0.17323i	260	-0.99679+0.059261i	-0.99679-0.059261i	0.98735+0.11734i	-0.97219-0.17323i
90	-0.99958+0.011893i	-0.99958-0.011893i	0.99834-0.023645i	-0.99958+0.011893i	270	-0.99958+0.011893i	-0.99958-0.011893i	0.99834+0.023645i	-0.99958+0.011893i
100	-0.99679+0.059261i	-0.99679-0.059261i	0.98735-0.11734i	-0.97219+0.17323i	280	-0.99679+0.059261i	-0.99679-0.059261i	0.98735+0.11734i	-0.97219-0.17323i
110	-0.97548-0.19816i	-0.97548+0.19816i	0.90473-0.38189i	-0.97548+0.19816i	290	-0.97548-0.19816i	-0.97548+0.19816i	0.90473+0.38189i	-0.97548-0.19816i
120	-0.90011+0.41363i	-0.90011-0.41363i	0.62954-0.72965i	-0.26207+0.88458i	300	-0.90011+0.41363i	-0.90011-0.41363i	0.62954+0.72965i	-0.26207-0.88458i
130	-0.72492-0.66652i	-0.72492+0.66652i	0.52968+0.70126i	0.082283-0.93837i	310	-0.72492-0.66652i	-0.72492+0.66652i	0.52968-0.70126i	0.082283+0.93837i
140	-0.41834+0.8847i	-0.41834-0.8847i	-0.58072-0.71325i	0.81371-0.19212i	320	-0.41834+0.8847i	-0.41834-0.8847i	-0.58072+0.71325i	0.81371+0.19212i
150	0.0050506-0.97289i	0.0050506+0.97289i	-0.89968+0.0058631i	-0.0023102-0.79922i	330	0.0050506-0.97289i	0.0050506+0.97289i	-0.89968-0.0058631i	-0.0023102+0.79922i
160	0.46403+0.84985i	0.46403-0.84985i	-0.48015+0.74213i	-0.76882-0.06245i	340	0.46403+0.84985i	0.46403-0.84985i	-0.48015-0.74213i	-0.76882+0.06245i
170	0.82604-0.49943i	0.82604+0.49943i	0.40474+0.7745i	-0.04953+0.75251i	350	0.82604-0.49943i	0.82604+0.49943i	0.40474-0.7745i	-0.04953-0.75251i

Table 5-7 Antenna Spacing 4 λ, Angular Spread 5 degrees, Laplacian Model

Angular Spread 5, Antenna Spacing 4xWavelength										
Angle of Arrival/Departure	0	1	0.29329	0.094057	0.044131	180	1	0.29329+3.4466e-16i	0.094057-1.2264e-15i	0.044131-4.7768e-16i
	0.29329	1	0.29329	0.094057	0.044131		0.29329-3.4466e-16i	1	0.29329+3.4466e-16i	0.094057-1.2264e-15i
	0.094057	0.29329	1	0.094057	0.044131		0.094057+1.2264e-15i	0.29329-3.4466e-16i	1	0.29329+3.4466e-16i
	0.044131	0.094057	0.29329	1	0.044131		0.044131+4.7768e-16i	0.094057+1.2264e-15i	0.29329-3.4466e-16i	1
10	1	-0.099688-0.28261i	-0.074702+0.061389i	-0.099688-0.28261i	0.039141+0.023079i	190	1	-0.099688-0.28261i	-0.074702+0.061389i	-0.099688-0.28261i
		-0.074702+0.061389i	-0.099688+0.28261i	1	-0.099688-0.28261i			-0.074702+0.061389i	-0.099688-0.28261i	1
		0.039141-0.023079i	-0.074702-0.061389i	-0.099688+0.28261i	1		0.039141+0.023079i	-0.074702+0.061389i	-0.099688-0.28261i	1
20	1	-0.2203+0.23176i	-0.2203+0.23176i	-0.0072744-0.10492i	0.038978+0.030793i	200	1	-0.2203+0.23176i	-0.2203+0.23176i	-0.0072744+0.10492i
		-0.0072744+0.10492i	-0.2203-0.23176i	1	-0.2203+0.23176i			-0.0072744-0.10492i	-0.2203+0.23176i	1
		0.038978-0.030793i	0.3563+0.0096902i	0.12143+0.0035451i	0.057933+0.0013317i	210	1	0.038978+0.030793i	0.3563+0.0096902i	0.12143+0.0035451i
30	1	0.3563-0.0096902i	1	0.3563+0.0096902i	0.12143+0.0035451i	210	1	0.3563+0.0096902i	1	0.3563-0.0096902i
		0.12143-0.0035451i	0.3563-0.0096902i	1	0.3563+0.0096902i			0.12143+0.0035451i	0.3563+0.0096902i	1
		0.057933-0.0013317i	0.12143+0.0035451i	0.3563+0.0096902i	1		0.057933+0.0013317i	0.12143+0.0035451i	0.3563+0.0096902i	1
40	1	-0.36778+0.19243i	1	-0.36778-0.19243i	0.088691+0.12103i	220	1	-0.36778+0.19243i	1	-0.36778-0.19243i
		0.088691-0.12103i	-0.36778+0.19243i	1	-0.36778-0.19243i			0.088691+0.12103i	1	-0.36778-0.19243i
		-0.013992+0.071464i	0.088691-0.12103i	1	-0.36778-0.19243i			-0.013992+0.071464i	0.088691+0.12103i	1
50	1	0.45586-0.21529i	1	0.45586+0.21529i	0.12888+0.15323i	230	1	0.45586-0.21529i	1	0.45586+0.21529i
		0.12888+0.15323i	0.45586-0.21529i	1	0.45586+0.21529i			0.12888+0.15323i	0.45586+0.21529i	1
		0.029955-0.09555i	0.45586-0.21529i	1	0.45586+0.21529i			0.029955+0.09555i	0.45586-0.21529i	1
60	1	-0.61986+0.12583i	1	-0.61986-0.12583i	0.2737+0.10297i	240	1	-0.61986+0.12583i	1	-0.61986-0.12583i
		0.2737+0.10297i	-0.61986+0.12583i	1	-0.61986-0.12583i			0.2737-0.10297i	1	-0.61986-0.12583i
		-0.12944+0.085174i	0.2737+0.10297i	1	-0.61986-0.12583i			-0.12944+0.085174i	0.2737+0.10297i	1
70	1	0.031776-0.78946i	1	0.031776+0.78946i	0.031776-0.78946i	250	1	0.031776-0.78946i	1	0.031776+0.78946i
		0.031776+0.78946i	0.031776-0.78946i	1	0.031776+0.78946i			0.031776+0.78946i	1	0.031776-0.78946i
		-0.47785+0.10382i	0.031776+0.78946i	1	0.031776+0.78946i			-0.47785+0.10382i	0.031776+0.78946i	1
80	1	-0.83607+0.40081i	1	-0.83607-0.40081i	0.83607+0.40081i	260	1	-0.83607+0.40081i	1	-0.83607-0.40081i
		0.83607+0.40081i	-0.83607+0.40081i	1	0.83607+0.40081i			0.83607-0.40081i	1	-0.83607-0.40081i
		0.54711+0.57946i	0.83607+0.40081i	1	0.83607+0.40081i			0.54711-0.57946i	0.83607+0.40081i	1
90	1	0.97804+0.086342i	1	0.97804-0.086342i	0.97804+0.086342i	270	1	0.97804+0.086342i	1	0.97804-0.086342i
		0.93619+0.1455i	0.97804+0.086342i	1	0.97804-0.086342i			0.93619-0.1455i	0.97804+0.086342i	1
		0.89299+0.18437i	0.93619+0.1455i	1	0.97804-0.086342i			0.89299-0.18437i	0.93619+0.1455i	1
100	1	0.83607+0.40081i	1	0.83607-0.40081i	0.83607+0.40081i	280	1	0.83607+0.40081i	1	0.83607-0.40081i
		0.54711+0.57946i	0.83607+0.40081i	1	0.83607+0.40081i			0.54711-0.57946i	0.83607+0.40081i	1
		0.28778+0.60257i	0.54711+0.57946i	1	0.83607+0.40081i			0.28778-0.60257i	0.54711+0.57946i	1
110	1	0.031776-0.78946i	1	0.031776+0.78946i	0.031776-0.78946i	290	1	0.031776-0.78946i	1	0.031776+0.78946i
		0.031776+0.78946i	0.031776-0.78946i	1	0.031776+0.78946i			0.031776+0.78946i	1	0.031776-0.78946i
		-0.47785+0.10382i	0.031776+0.78946i	1	0.031776+0.78946i			-0.47785+0.10382i	0.031776+0.78946i	1
120	1	-0.61986+0.12583i	1	-0.61986-0.12583i	0.2737+0.10297i	300	1	-0.61986+0.12583i	1	-0.61986-0.12583i
		0.2737+0.10297i	-0.61986+0.12583i	1	-0.61986-0.12583i			0.2737-0.10297i	1	-0.61986-0.12583i
		-0.12944+0.085174i	0.2737+0.10297i	1	-0.61986-0.12583i			-0.12944+0.085174i	0.2737+0.10297i	1
130	1	0.45586-0.21529i	1	0.45586+0.21529i	0.12888+0.15323i	310	1	0.45586-0.21529i	1	0.45586+0.21529i
		0.12888+0.15323i	0.45586-0.21529i	1	0.45586+0.21529i			0.12888+0.15323i	0.45586+0.21529i	1
		0.029955-0.09555i	0.45586-0.21529i	1	0.45586+0.21529i			0.029955+0.09555i	0.45586-0.21529i	1
140	1	-0.36778+0.19243i	1	-0.36778-0.19243i	0.088691+0.12103i	320	1	-0.36778+0.19243i	1	-0.36778-0.19243i
		0.088691-0.12103i	-0.36778+0.19243i	1	-0.36778-0.19243i			0.088691+0.12103i	1	-0.36778-0.19243i
		-0.013992+0.071464i	0.088691-0.12103i	1	-0.36778-0.19243i			-0.013992+0.071464i	0.088691+0.12103i	1
150	1	0.3563-0.0096902i	1	0.3563+0.0096902i	0.12143+0.0035451i	330	1	0.3563-0.0096902i	1	0.3563+0.0096902i
		0.12143-0.0035451i	0.3563-0.0096902i	1	0.3563+0.0096902i			0.12143+0.0035451i	0.3563+0.0096902i	1
		0.057933-0.0013317i	0.12143+0.0035451i	0.3563+0.0096902i	1			0.057933+0.0013317i	0.12143+0.0035451i	0.3563+0.0096902i
160	1	-0.2203+0.23176i	1	-0.2203-0.23176i	0.038978+0.030793i	340	1	-0.2203+0.23176i	1	-0.2203-0.23176i
		-0.0072744+0.10492i	-0.2203+0.23176i	1	-0.2203-0.23176i			-0.0072744-0.10492i	-0.2203+0.23176i	1
		0.038978-0.030793i	-0.0072744+0.10492i	0.038978+0.030793i	1			0.038978-0.030793i	-0.0072744+0.10492i	0.038978+0.030793i
170	1	-0.099688+0.28261i	1	-0.099688-0.28261i	0.039141+0.023079i	350	1	-0.099688+0.28261i	1	-0.099688-0.28261i
		0.039141-0.023079i	-0.099688+0.28261i	1	-0.099688-0.28261i			0.039141+0.023079i	-0.099688+0.28261i	1
		-0.099688-0.28261i	0.039141-0.023079i	1	-0.099688-0.28261i			-0.099688+0.28261i	0.039141+0.023079i	1
		0.039141+0.023079i	-0.099688-0.28261i	1	-0.099688-0.28261i			0.039141+0.023079i	-0.099688+0.28261i	1

Table 5-8 Antenna Spacing 10 λ, Angular Spread 5 degrees, Laplacian Model

Angle of Arrival/Departure	Angular Spread 5, Antenna Spacing 10xWavelength				
0	1	0.062326	0.016355	0.0073024	180
	0.062326	0.062326	0.062326	0.062326	
	0.016355	0.016355	0.016355	0.016355	
	0.0073024	0.0073024	0.0073024	0.0073024	
10	-0.0049744+0.063941i	-0.0049744+0.063941i	-0.016623+0.0027812i	0.0019051+0.0073571i	190
	0.016623-0.0027812i	-0.0049744+0.063941i	1	-0.016623+0.0027812i	
	0.0019051-0.0073571i	-0.016623-0.0027812i	-0.0049744+0.063941i	1	
20	1	-0.061884+0.032678i	0.010079-0.015489i	-0.00059694+0.0082371i	200
	-0.061884+0.032678i	1	-0.061884+0.032678i	1	
	0.010079+0.015489i	-0.061884-0.032678i	0.010079-0.015489i	-0.00059694-0.0082371i	
	-0.00059694-0.0082371i	0.010079+0.015489i	-0.061884-0.032678i	1	
30	0.081314+0.0021124i	0.021679+0.00032722i	0.081314+0.0021124i	0.0097371+0.00013171i	210
	0.081314+0.0021124i	1	0.081314+0.0021124i	1	
	0.021679-0.00032722i	0.081314-0.0021124i	0.021679+0.00032722i	0.0097371+0.00013171i	
	0.0097371-0.00013171i	-0.093031+0.040736i	0.0175-0.021254i	-0.093031+0.040736i	
40	1	-0.093031-0.040736i	-0.093031+0.040736i	1	220
	0.0175+0.021254i	-0.093031-0.040736i	1	0.0175+0.021254i	
	-0.0027931-0.012093i	-0.093031+0.040736i	-0.093031-0.040736i	1	
50	1	-0.066323+0.12113i	-0.066323-0.12113i	1	230
	-0.066323+0.12113i	1	-0.066323-0.12113i	1	
	0.017474+0.0015759i	-0.066323-0.12113i	0.017474+0.0015759i	-0.066323+0.12113i	
	-0.066323-0.12113i	0.017474+0.0015759i	-0.066323+0.12113i	1	
60	1	-0.094927+0.18641i	-0.094927-0.18641i	1	240
	-0.094927+0.18641i	1	-0.094927-0.18641i	1	
	0.028584+0.002291i	-0.030551+0.05366i	0.028584+0.002291i	-0.030551+0.05366i	
	-0.030551+0.05366i	-0.094927+0.18641i	-0.030551-0.05366i	-0.094927-0.18641i	
70	1	-0.32602+0.17441i	-0.32602-0.17441i	1	250
	-0.32602+0.17441i	1	-0.32602-0.17441i	1	
	0.047468+0.11812i	-0.32602-0.17441i	0.047468+0.11812i	-0.32602+0.17441i	
	0.015763+0.051498i	-0.32602+0.17441i	0.015763+0.051498i	-0.32602-0.17441i	
80	1	-0.41023+0.60515i	-0.41023-0.60515i	1	260
	-0.41023+0.60515i	1	-0.41023-0.60515i	1	
	0.1467+0.18659i	-0.41023-0.60515i	0.1467+0.18659i	-0.41023+0.60515i	
	-0.1467-0.18659i	0.1467+0.18659i	-0.1467-0.18659i	0.1467+0.18659i	
90	1	-0.91432+0.1669i	-0.91432-0.1669i	1	270
	-0.91432+0.1669i	1	-0.91432-0.1669i	1	
	0.81721+0.229i	-0.91432-0.1669i	0.81721+0.229i	-0.91432+0.1669i	
	0.74314+0.25526i	-0.91432+0.1669i	0.74314+0.25526i	-0.91432-0.1669i	
100	1	-0.41023+0.60515i	-0.41023-0.60515i	1	280
	-0.41023+0.60515i	1	-0.41023-0.60515i	1	
	0.037843+0.4451i	-0.41023-0.60515i	0.037843+0.4451i	-0.41023+0.60515i	
	-0.037843-0.4451i	0.037843+0.4451i	-0.037843-0.4451i	0.037843+0.4451i	
110	1	-0.32602+0.17441i	-0.32602-0.17441i	1	290
	-0.32602+0.17441i	1	-0.32602-0.17441i	1	
	0.047468+0.11812i	-0.32602-0.17441i	0.047468+0.11812i	-0.32602+0.17441i	
	0.015763+0.051498i	-0.32602+0.17441i	0.015763+0.051498i	-0.32602-0.17441i	
120	1	-0.094927+0.18641i	-0.094927-0.18641i	1	300
	-0.094927+0.18641i	1	-0.094927-0.18641i	1	
	0.028584+0.002291i	-0.030551+0.05366i	0.028584+0.002291i	-0.030551+0.05366i	
	-0.030551+0.05366i	-0.094927+0.18641i	-0.030551-0.05366i	-0.094927-0.18641i	
130	1	-0.066323+0.12113i	-0.066323-0.12113i	1	310
	-0.066323+0.12113i	1	-0.066323-0.12113i	1	
	0.017474+0.0015759i	-0.066323-0.12113i	0.017474+0.0015759i	-0.066323+0.12113i	
	-0.066323-0.12113i	0.017474+0.0015759i	-0.066323+0.12113i	1	
140	1	-0.093031-0.040736i	-0.093031+0.040736i	1	320
	-0.093031-0.040736i	1	-0.093031+0.040736i	1	
	0.0175+0.021254i	-0.093031+0.040736i	0.0175+0.021254i	-0.093031-0.040736i	
	-0.0027931-0.012093i	-0.093031-0.040736i	-0.0027931-0.012093i	0.0175+0.021254i	
150	1	0.081314+0.0021124i	0.021679+0.00032722i	1	330
	0.081314+0.0021124i	1	0.081314+0.0021124i	1	
	0.021679-0.00032722i	0.081314-0.0021124i	0.021679+0.00032722i	0.021679+0.00032722i	
	0.0097371-0.00013171i	-0.093031+0.040736i	0.0097371+0.00013171i	-0.093031+0.040736i	
160	1	-0.061884+0.032678i	0.010079-0.015489i	-0.00059694+0.0082371i	340
	-0.061884+0.032678i	1	-0.061884+0.032678i	1	
	0.010079+0.015489i	-0.061884-0.032678i	0.010079-0.015489i	-0.00059694-0.0082371i	
	-0.00059694-0.0082371i	0.010079+0.015489i	-0.061884-0.032678i	1	
170	1	-0.0049744+0.063941i	-0.0049744-0.063941i	1	350
	-0.0049744+0.063941i	1	-0.0049744-0.063941i	1	
	0.016623-0.0027812i	-0.0049744-0.063941i	0.016623+0.0027812i	-0.0049744+0.063941i	
	0.0019051-0.0073571i	0.016623-0.0027812i	0.0019051+0.0073571i	0.016623+0.0027812i	

Table 5-10 Antenna Spacing 10 λ, Angular Spread 2 degrees, SCM Model

Angular Spread 2, Antenna Spacing 10xWavelength, SCM Model									
Angle of Arrival/Departure									
0	1	0.0067-0.0033i	-0.0003+0.0009i	0.0008+0.0017i	180	1	-0.2075+0.0049i	0.1401-0.0004i	-0.1430-0.0099i
		0.0067+0.0033i	0.0060-0.0026i	-0.0012+0.0000i			-0.2075-0.0049i	-0.2066+0.0097i	0.1683+0.0057i
		-0.0003-0.0009i	0.0060+0.0026i	0.0060-0.0014i			0.1401+0.0004i	-0.2066-0.0097i	-0.2124+0.0108i
		0.0008-0.0017i	-0.0012-0.0000i	0.0060+0.0014i			-0.1430+0.0099i	0.1683+0.0057i	-0.2124-0.0108i
10	1	-0.0034-0.0008i	-0.0009-0.0019i	-0.0003+0.0006i	190	1	0.0034-0.0489i	0.0034+0.0489i	-0.0131-0.0202i
		-0.0009+0.0019i	-0.0040+0.0021i	0.0024-0.0013i			-0.0131+0.0202i	-0.0374+0.0552i	-0.0304-0.0048i
		-0.0003-0.0006i	-0.0046-0.0025i	-0.0046+0.0025i			0.0300+0.0195i	-0.0304-0.0048i	-0.0020+0.0511i
20	1	0.0050-0.0050i	0.0001-0.0004i	-0.0038-0.0019i	200	1	0.0979+0.1250i	0.0979-0.1250i	-0.0461-0.0443i
		0.0001+0.0004i	0.0035+0.0071i	-0.0005+0.0002i			-0.0461+0.0443i	-0.0461+0.0443i	0.0238-0.0433i
		-0.0038+0.0019i	0.0034+0.0068i	0.0034+0.0068i			0.0238+0.0433i	0.0238+0.0433i	-0.0686-0.0519i
30	1	-0.0013-0.0112i	-0.0013+0.0112i	-0.0003+0.0001i	210	1	-0.4794+0.2222i	-0.4794-0.2222i	0.3094+0.2503i
		-0.0047+0.0009i	-0.0018-0.0106i	-0.0030-0.0018i			-0.4794-0.2222i	-0.4794-0.2222i	-0.2468-0.2281i
		-0.0003-0.0001i	-0.0003+0.0001i	-0.0003+0.0009i			0.3094-0.2503i	-0.4792-0.2245i	0.3171+0.2454i
40	1	0.0076-0.0068i	0.0076+0.0068i	0.0010-0.0028i	220	1	-0.5027-0.3071i	-0.5027+0.3071i	-0.4867-0.2147i
		-0.0034-0.0021i	0.0086-0.0082i	0.0078-0.0077i			-0.5027+0.3071i	0.3792-0.2696i	-0.2996+0.2482i
		0.0010+0.0028i	-0.0052+0.0002i	0.0078+0.0077i			0.3792+0.2696i	-0.4998+0.2976i	-0.5044+0.2930i
50	1	0.0113-0.0048i	0.0113+0.0048i	0.0014+0.0060i	230	1	-0.0228+0.0497i	-0.0228-0.0497i	0.0071-0.0130i
		0.0044-0.0053i	0.0076-0.0066i	0.0110+0.0041i			0.0071+0.0130i	-0.0063+0.0614i	0.0229-0.0241i
		-0.0048+0.0017i	0.0014-0.0060i	0.0076+0.0066i			0.0229+0.0241i	-0.0063-0.0614i	-0.0060+0.0011i
60	1	0.0231-0.0240i	0.0208+0.0223i	0.0055+0.0000i	240	1	-0.0727-0.0256i	-0.0727+0.0256i	0.0130+0.0643i
		-0.0035-0.0085i	0.0208-0.0223i	-0.0025+0.0130i			0.0370-0.0329i	-0.0060+0.0011i	0.0370+0.0329i
		0.0055-0.0000i	-0.0025-0.0130i	0.0178+0.0225i			-0.0280+0.0048i	-0.0654-0.0224i	-0.0628-0.0177i
70	1	-0.1512+0.0399i	-0.1512-0.0399i	0.0024-0.0007i	250	1	-0.3027+0.0121i	-0.3027-0.0121i	0.0398+0.0471i
		-0.0093+0.0241i	-0.1513-0.0366i	-0.0098-0.0244i			0.0856-0.0220i	0.0856+0.0220i	0.0846-0.0231i
		0.0024+0.0007i	-0.0098+0.0244i	-0.1507+0.0377i			0.0398-0.0471i	-0.3006-0.0098i	-0.3018-0.0111i
80	1	0.2782+0.4263i	0.2778+0.4276i	0.0840-0.1380i	260	1	0.4166+0.4326i	0.4166+0.4326i	0.1906+0.2141i
		0.0889+0.2620i	0.2778+0.4276i	0.0886-0.2592i			0.2399-0.2524i	0.4155+0.4323i	0.2407+0.2531i
		0.0840+0.1380i	0.0886+0.2592i	0.2773-0.4278i			0.1906-0.2141i	0.2407-0.2531i	0.4147+0.4323i
90	1	0.8500-0.2532i	0.8500-0.2532i	0.5763-0.2570i	270	1	0.7549+0.3215i	0.7549+0.3215i	0.4500+0.2509i
		0.6688+0.2801i	0.8497+0.2529i	0.6699-0.2798i			0.5287-0.3182i	0.7547+0.3213i	0.5288+0.3193i
		0.5763+0.2570i	0.6699+0.2798i	0.8498-0.2523i			0.4500-0.2509i	0.7549-0.3204i	0.7549+0.3204i
100	1	0.4373+0.3689i	0.4370+0.3704i	0.2980-0.2558i	280	1	0.3328-0.4564i	0.3328+0.4564i	0.1040+0.1396i
		0.3789+0.2032i	0.4370+0.3704i	0.3790-0.2032i			0.1142-0.2642i	0.3320-0.4567i	0.1136+0.2649i
		0.2980+0.2558i	0.3790+0.2032i	0.4374-0.3691i			0.1040-0.1396i	0.1136-0.2649i	0.3313+0.4568i
110	1	-0.2034+0.1698i	-0.2034-0.1698i	0.0279+0.0190i	290	1	-0.0825-0.0318i	-0.0825+0.0318i	-0.0025+0.0172i
		-0.0600-0.0438i	-0.2049+0.1704i	-0.0582+0.0453i			-0.0198-0.0312i	-0.0821+0.0334i	-0.0193+0.0274i
		0.0279-0.0190i	-0.0582-0.0453i	-0.2066-0.1713i			-0.0025-0.0172i	-0.0193-0.0274i	-0.0803+0.0311i
120	1	0.0856+0.0885i	0.0856+0.0885i	0.0035+0.0061i	300	1	-0.0525-0.0090i	-0.0525+0.0090i	0.0070+0.0182i
		0.0189+0.0408i	0.0827+0.0835i	0.0364-0.0411i			0.0070-0.0182i	-0.0539+0.0113i	-0.0109+0.0152i
		0.0035-0.0061i	0.0364+0.0411i	0.0913+0.0916i			-0.0010+0.0082i	0.0070+0.0182i	-0.0531+0.0097i
130	1	0.0085+0.0408i	0.0182+0.0541i	-0.0101-0.0403i	310	1	-0.0074-0.0218i	-0.0074+0.0218i	-0.0039-0.0004i
		0.0144-0.0236i	0.0182+0.0541i	0.0175+0.0092i			-0.0039+0.0004i	-0.0083+0.0176i	-0.0038-0.0007i
		-0.0101+0.0403i	0.0175-0.0092i	0.0208+0.0590i			-0.0027+0.0031i	-0.0038+0.0007i	-0.0067+0.0192i
140	1	0.0062+0.0287i	-0.0126-0.0145i	0.0234+0.0085i	320	1	0.0030-0.0165i	0.0030+0.0165i	-0.0025+0.0038i
		-0.0070-0.0014i	-0.0126+0.0145i	-0.0089-0.0024i			-0.0025-0.0038i	-0.0017-0.0041i	-0.0017+0.0041i
		0.0234-0.0085i	-0.0089+0.0024i	-0.0113-0.0361i			0.0020-0.0002i	0.0020+0.0164i	0.0002+0.0203i
150	1	-0.0439-0.0257i	-0.0439+0.0257i	0.0289+0.0148i	330	1	-0.0038+0.0150i	-0.0038-0.0150i	-0.0024-0.0002i
		-0.0183+0.0199i	-0.0363-0.0016i	0.0176-0.0158i			-0.0038+0.0150i	-0.0048+0.0146i	-0.0013+0.0015i
		0.0289-0.0148i	-0.0307-0.0163i	-0.0307+0.0163i			-0.0024-0.0002i	-0.0048+0.0146i	-0.0049+0.0156i
160	1	0.0069+0.0606i	0.0176+0.0158i	0.0037-0.0157i	340	1	-0.0027-0.0009i	0.0082+0.0076i	0.0000+0.0020i
		-0.0045-0.0139i	0.0069+0.0606i	-0.0394-0.0167i			0.0082-0.0076i	-0.0019-0.0013i	-0.0002+0.0011i
		0.0037+0.0157i	0.0140-0.0767i	0.0175+0.0659i			-0.0019+0.0013i	0.0069+0.0073i	0.0000+0.0020i
170	1	-0.2934+0.1433i	-0.2934+0.1433i	0.1944-0.0967i	350	1	-0.0002-0.0011i	-0.0002+0.0011i	0.0049+0.0048i
		-0.2934-0.1433i	-0.2945-0.1525i	-0.1919+0.0790i			-0.0002+0.0011i	-0.0045-0.0017i	-0.0003+0.0008i
		-0.1919-0.0790i	-0.2945+0.1525i	-0.1944+0.0967i			-0.0003-0.0008i	-0.0003-0.0012i	-0.0053+0.0001i

Appendix C FER vs. E_b/N_0 Curves for Forward Link Packet Formats

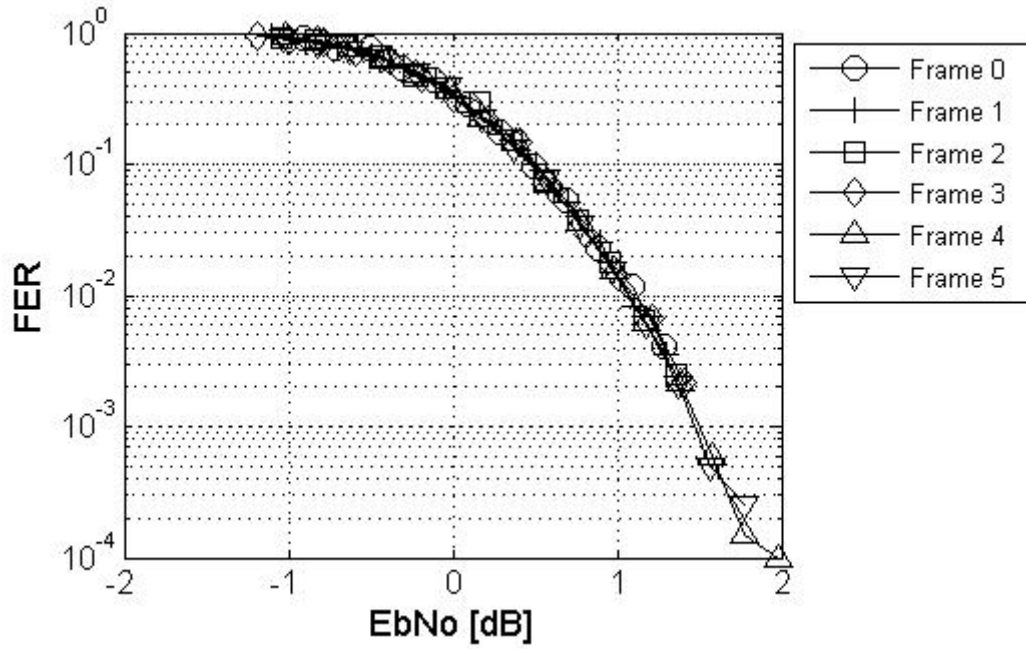


Figure 5-1 FL FER vs. E_b/N_0 for packet format 0

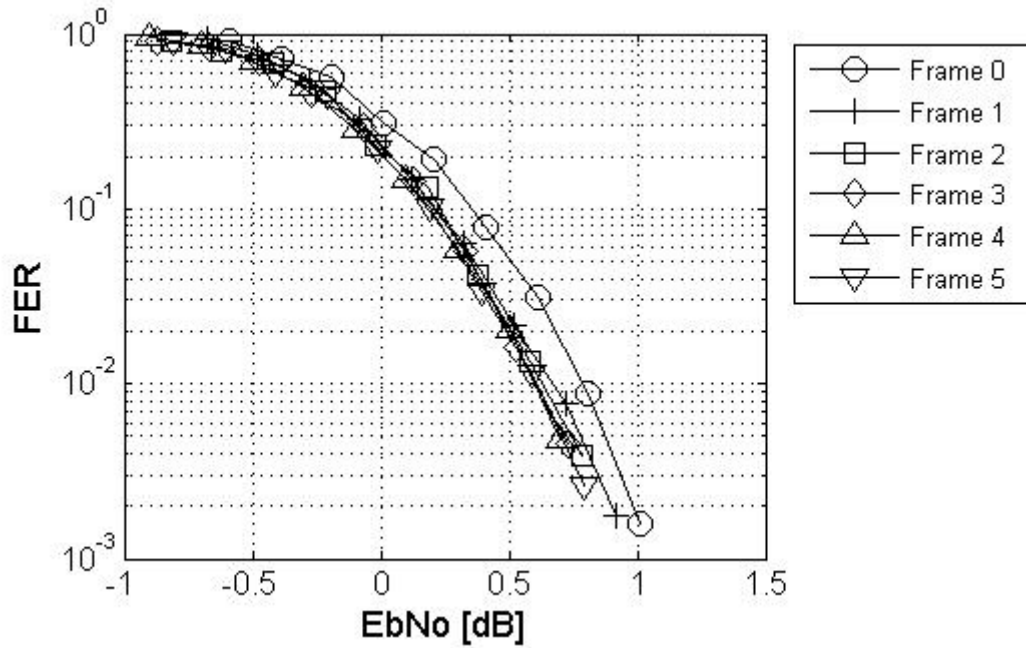


Figure 5-2 FL FER vs. E_b/N_0 for packet format 1

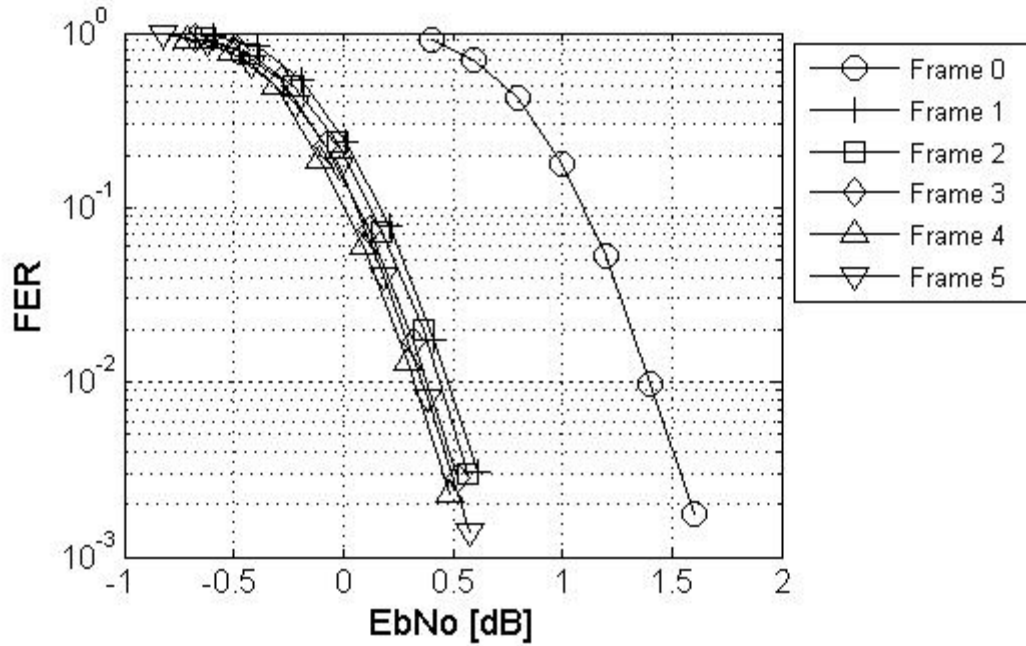


Figure 5-3 FL FER vs. E_b/N_0 for packet format 2

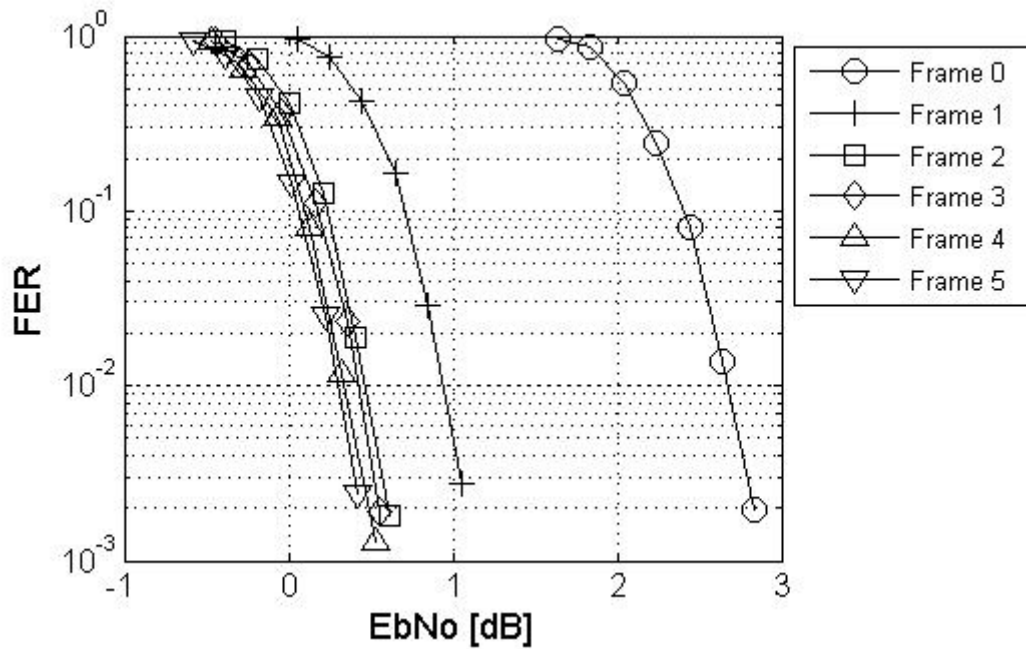


Figure 5-4 FL FER vs. E_b/N_0 for packet format 3

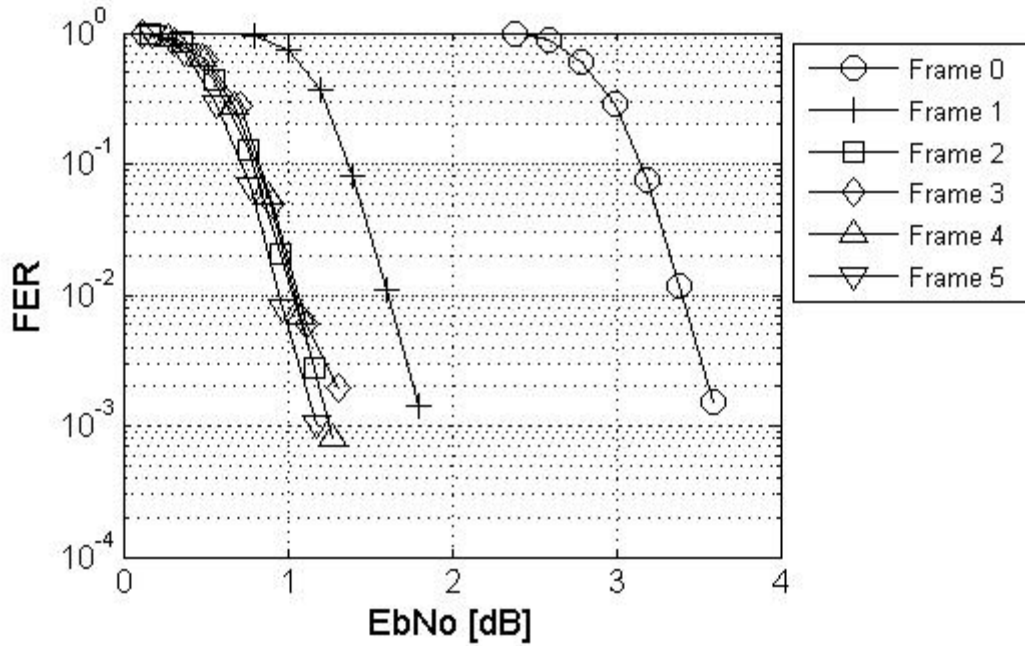


Figure 5-5 FL FER vs. E_b/N_0 for packet format 4

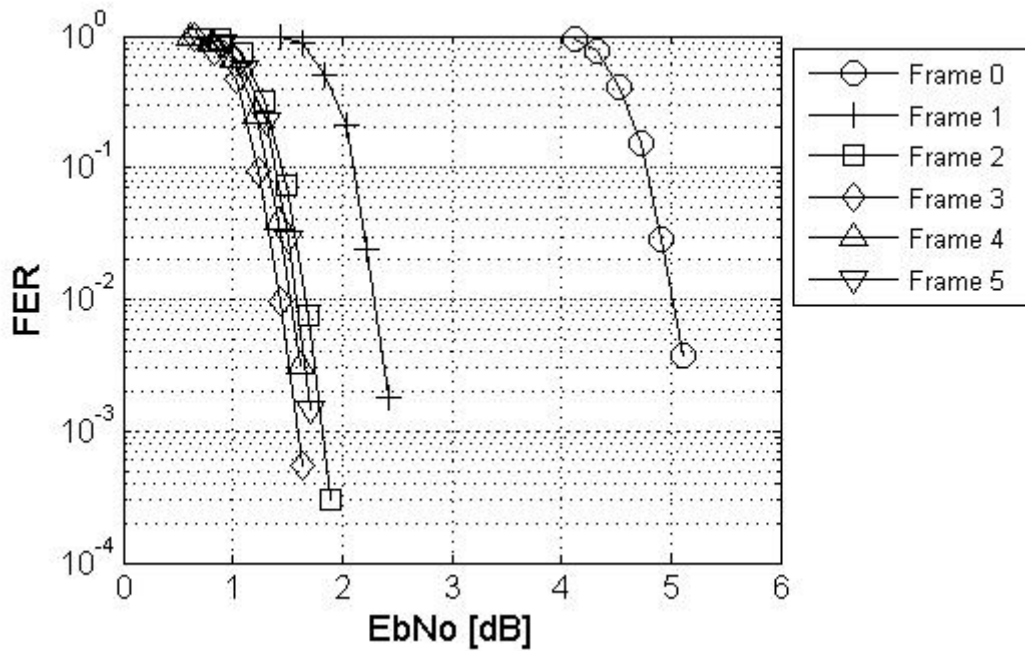


Figure 5-6 FL FER vs. E_b/N_0 for packet format 5

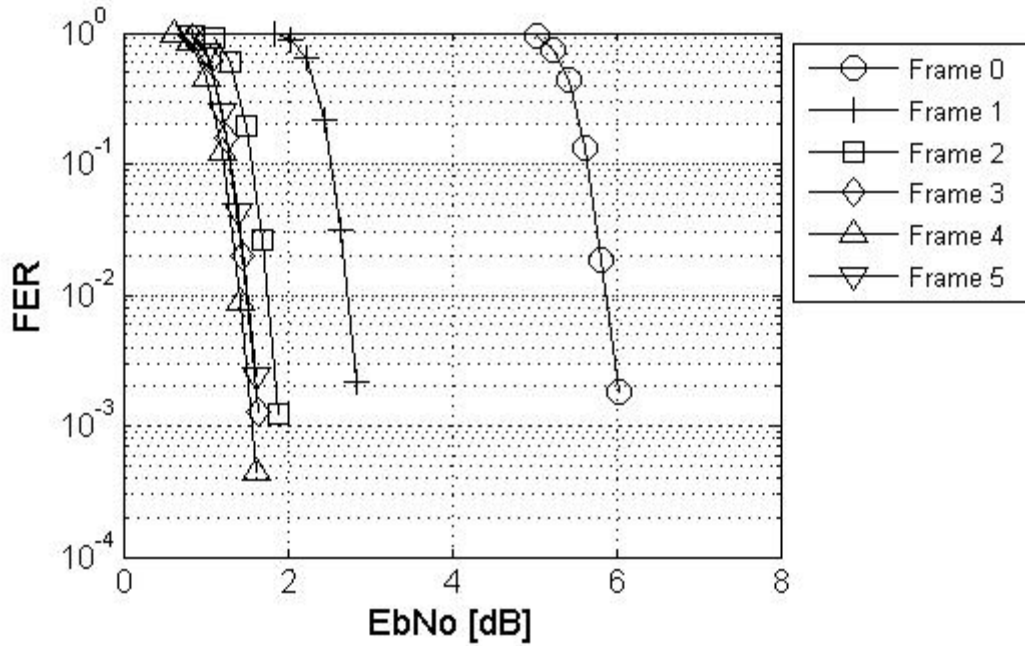


Figure 5-7 FL FER vs. E_b/N_0 for packet format 6

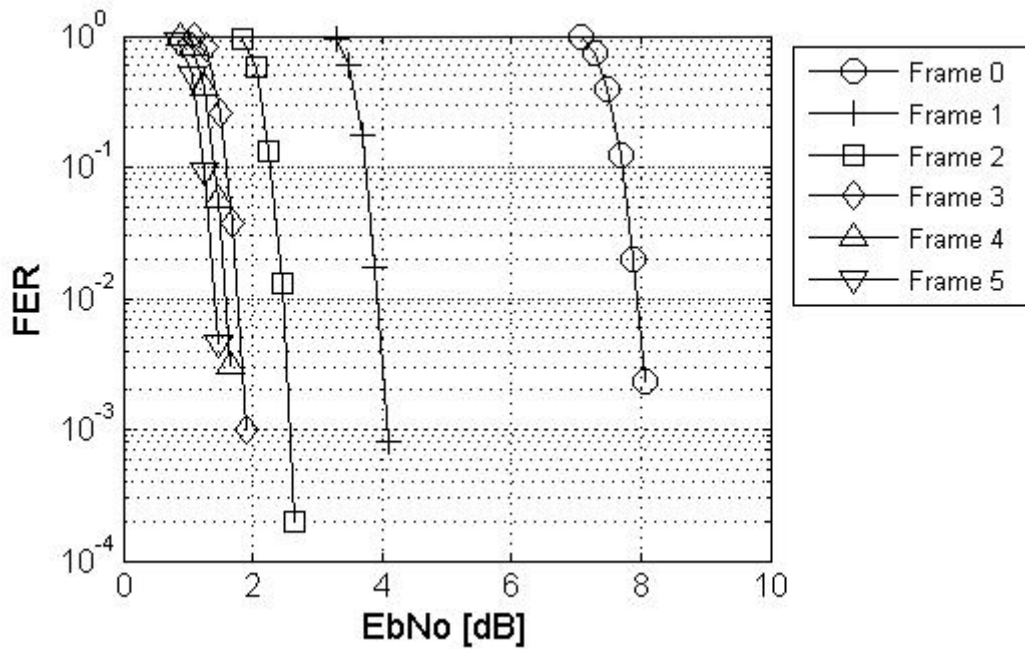


Figure 5-8 FL FER vs. E_b/N_0 for packet format 7

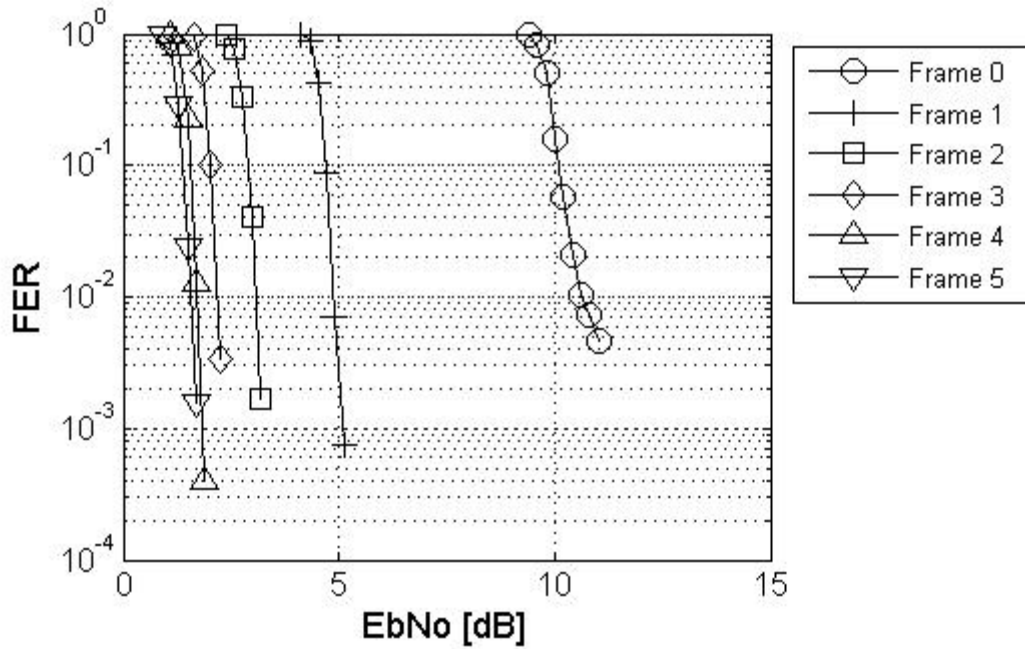


Figure 5-9 FL FER vs. E_b/N_0 for packet format 8

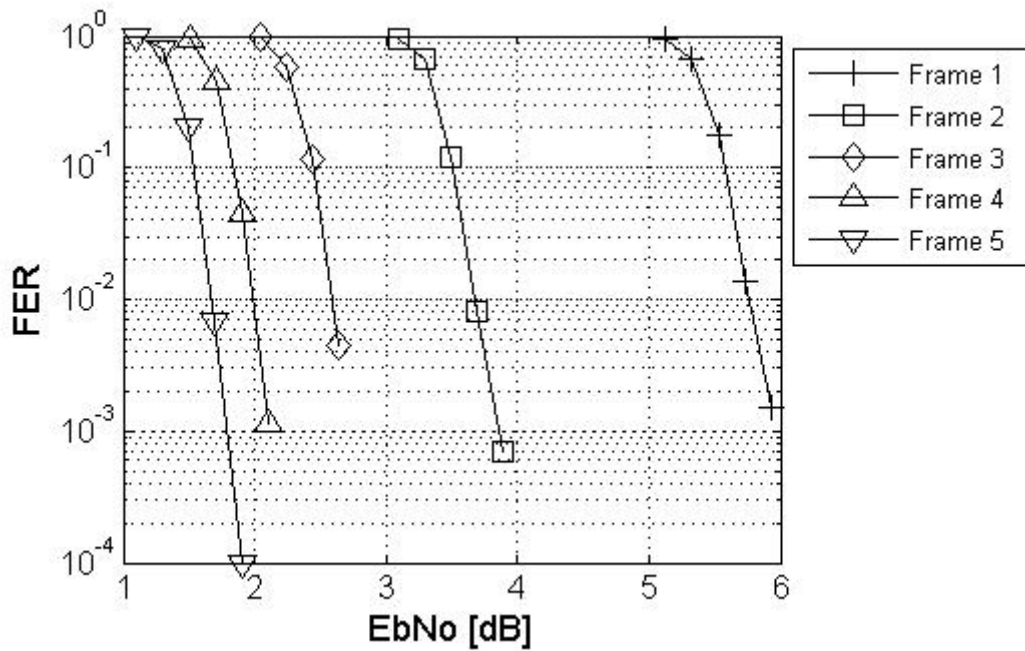


Figure 5-10 FL FER vs. E_b/N_0 for packet format 9

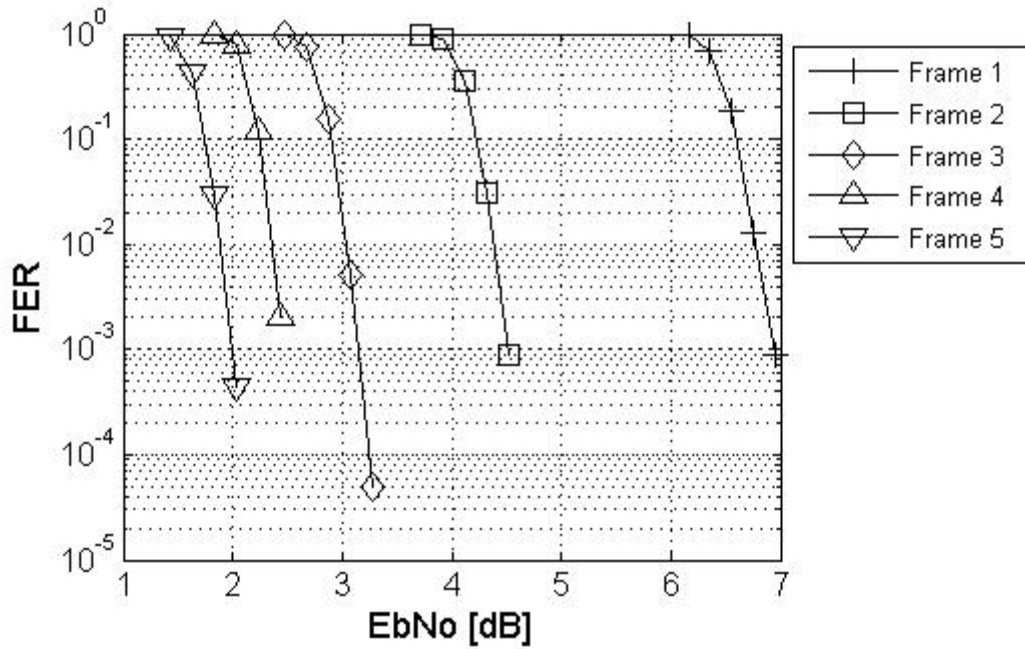


Figure 5-11 FL FER vs. E_b/N_0 for packet format 10

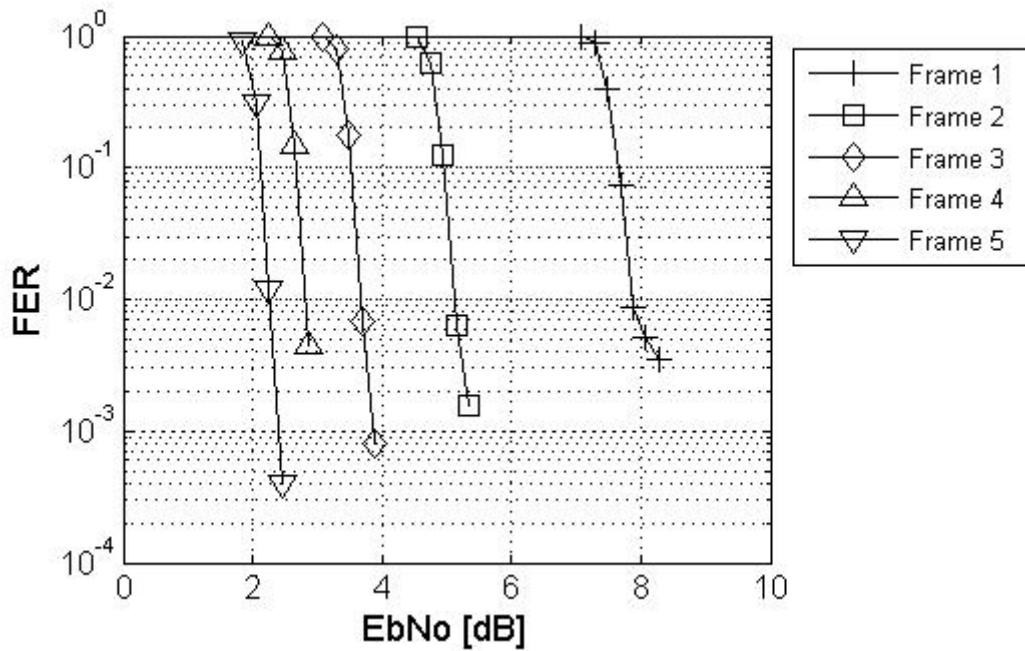


Figure 5-12 FL FER vs. E_b/N_0 for packet format 11

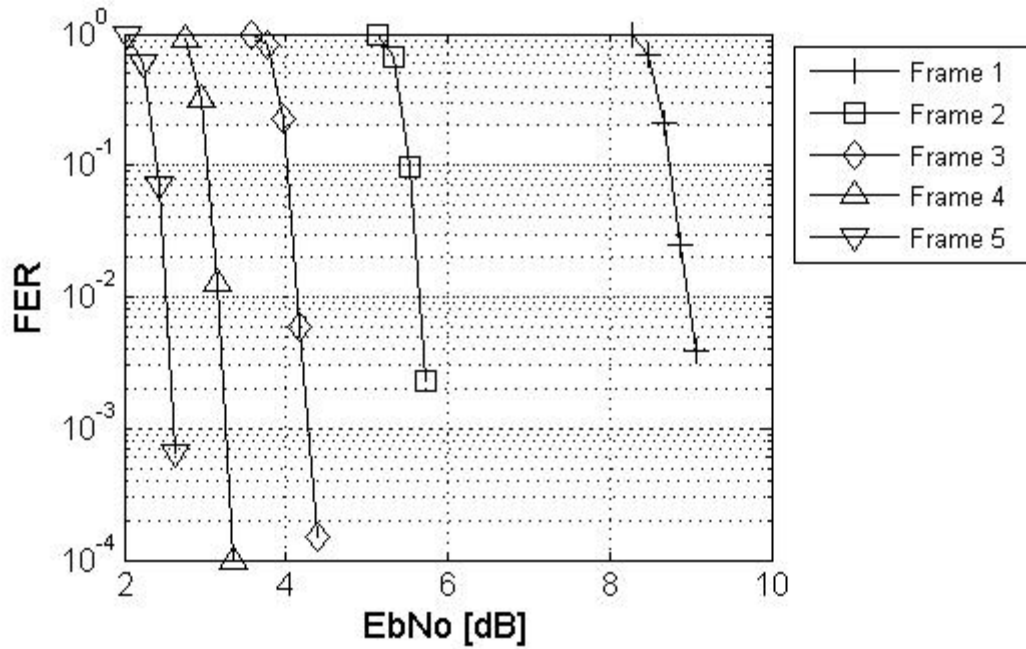


Figure 5-13 FL FER vs. E_b/N_0 for packet format 12

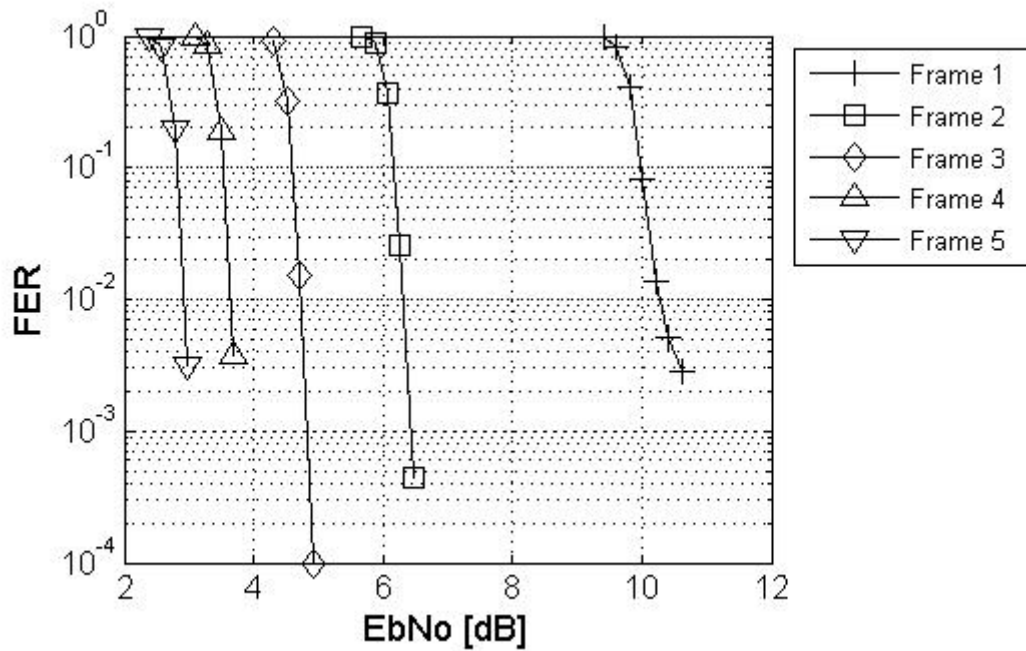


Figure 5-14 FL FER vs. E_b/N_0 for packet format 13

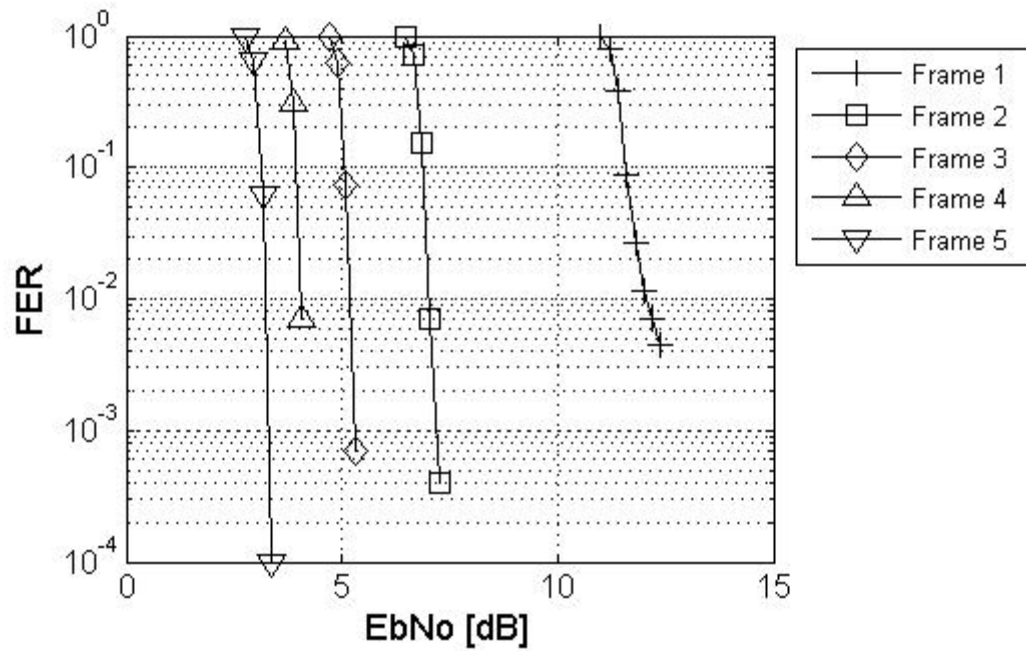


Figure 5-15 FL FER vs. E_b/N_0 for packet format 14

Appendix D FER vs. E_b/N_0 Curves for Reverse Link Packet Formats

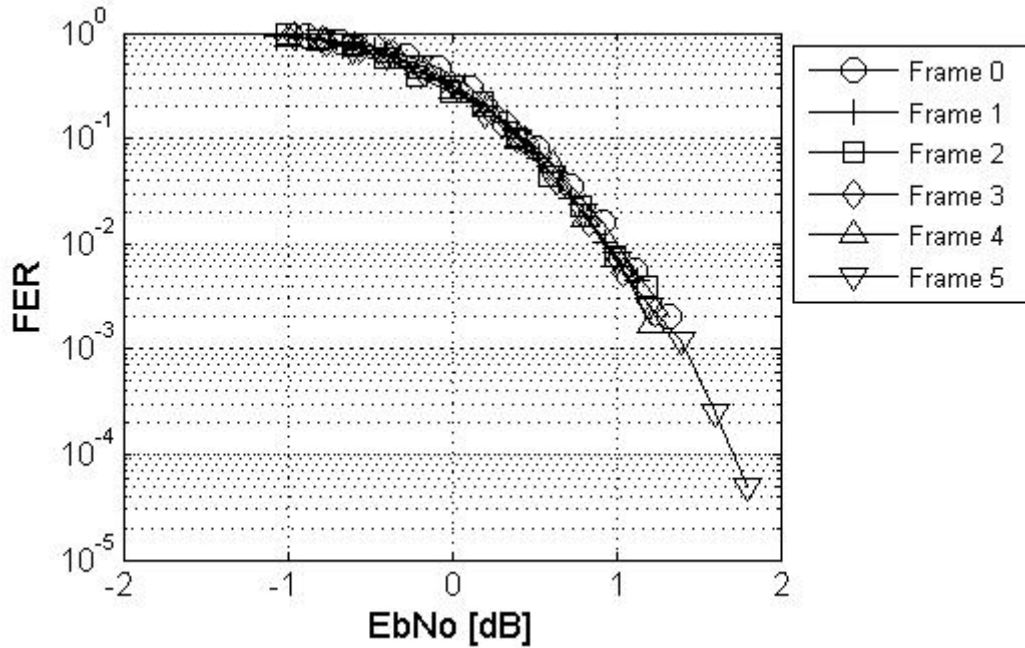


Figure 5-16 RL FER vs. E_b/N_0 for packet format 0

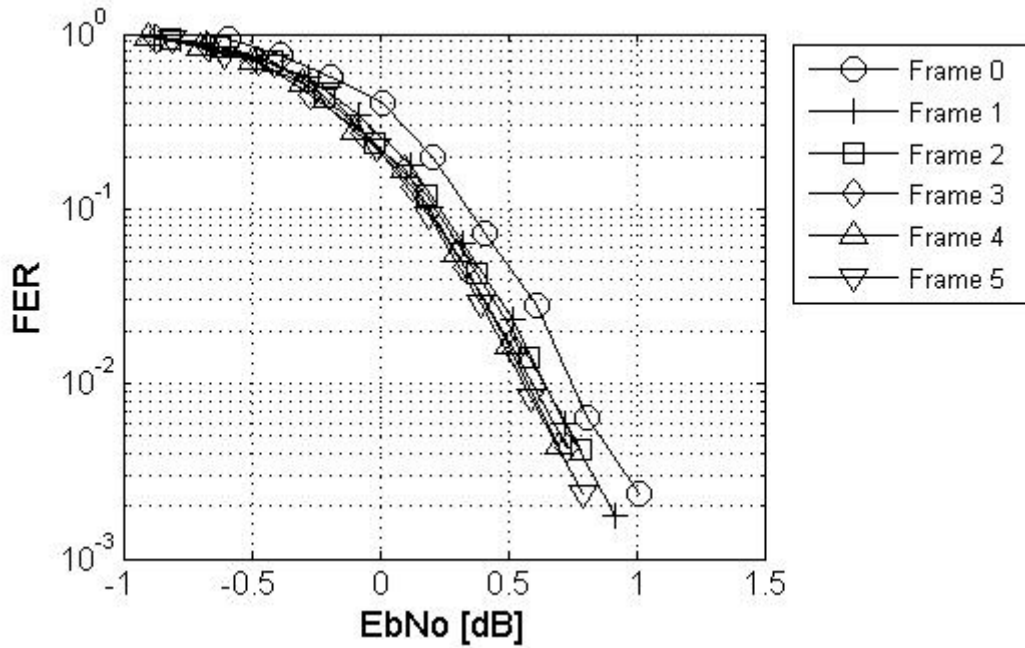


Figure 5-17 RL FER vs. E_b/N_0 for packet format 1

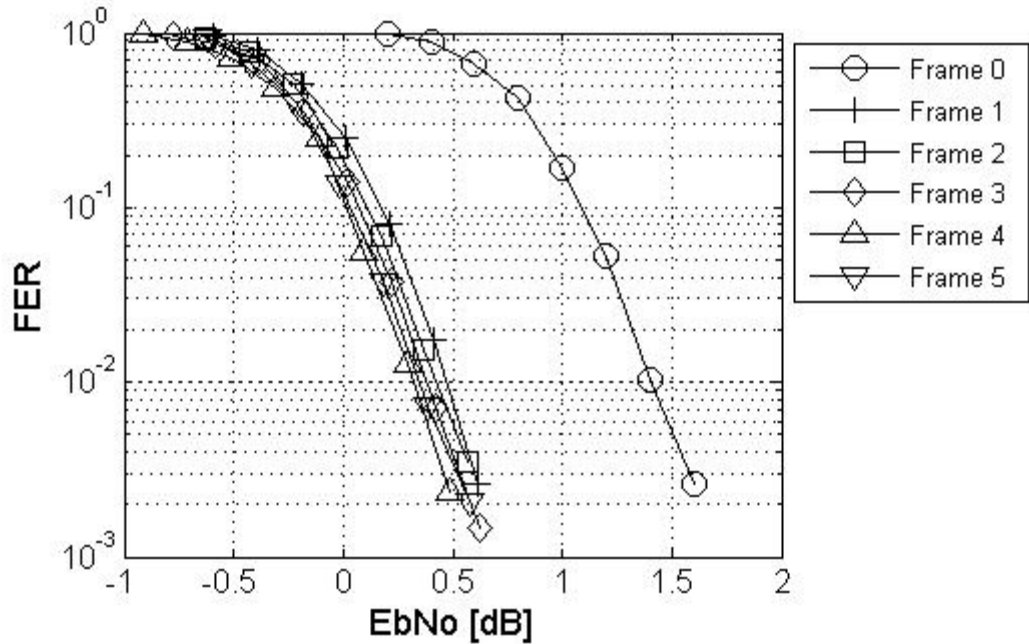


Figure 5-18 RL FER vs. E_b/N_0 for packet format 2

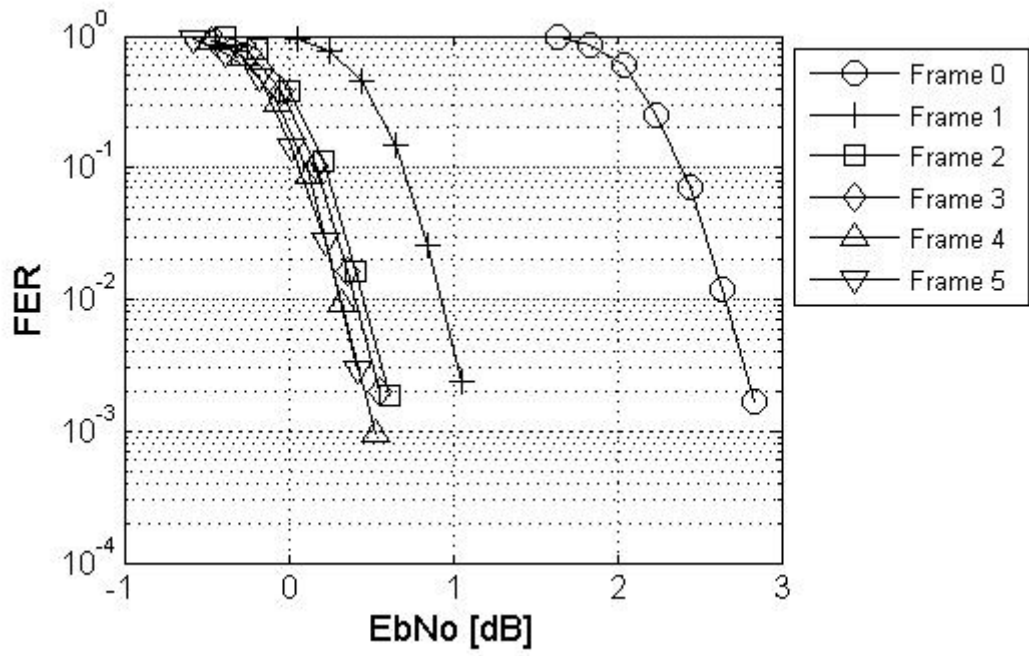


Figure 5-19 RL FER vs. E_b/N_0 for packet format 3

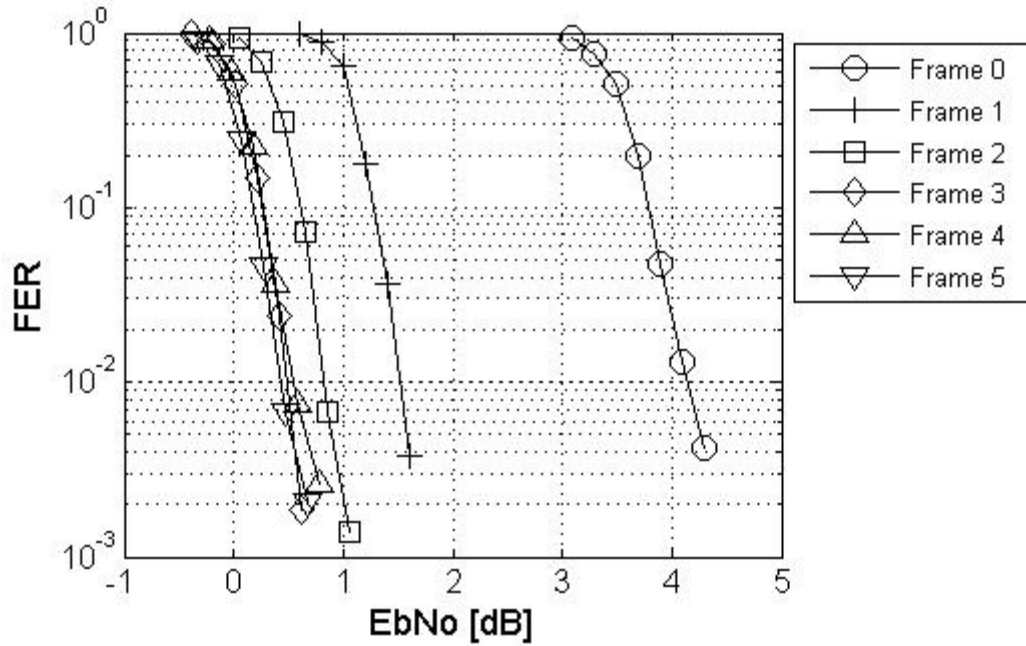


Figure 5-20 RL FER vs. E_b/N_0 for packet format 4

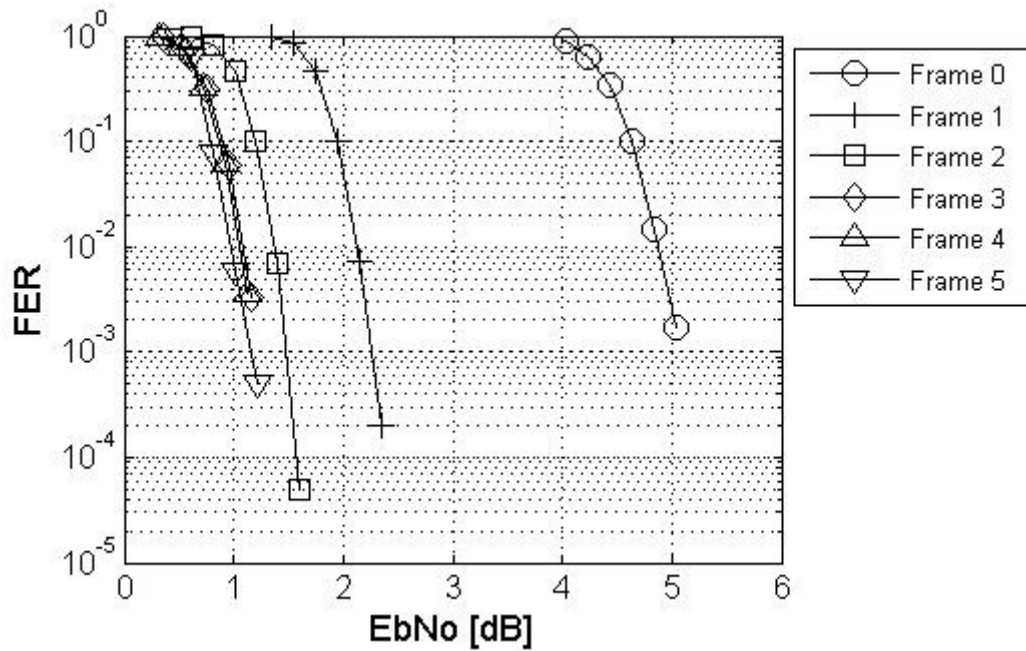


Figure 5-21 RL FER vs. E_b/N_0 for packet format 5

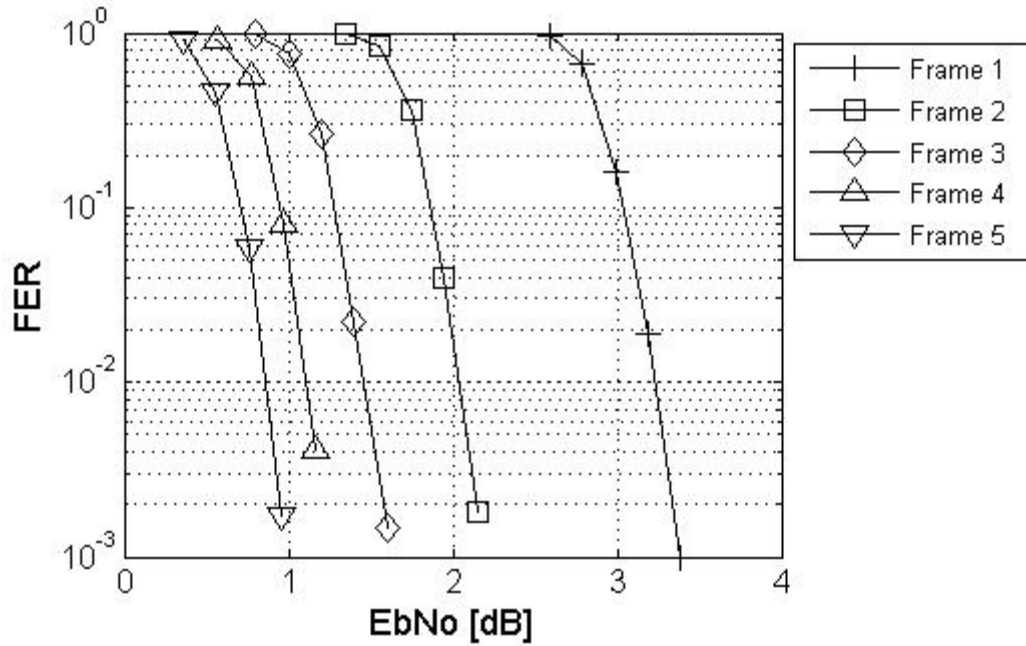


Figure 5-22 RL FER vs. E_b/N_0 for packet format 6

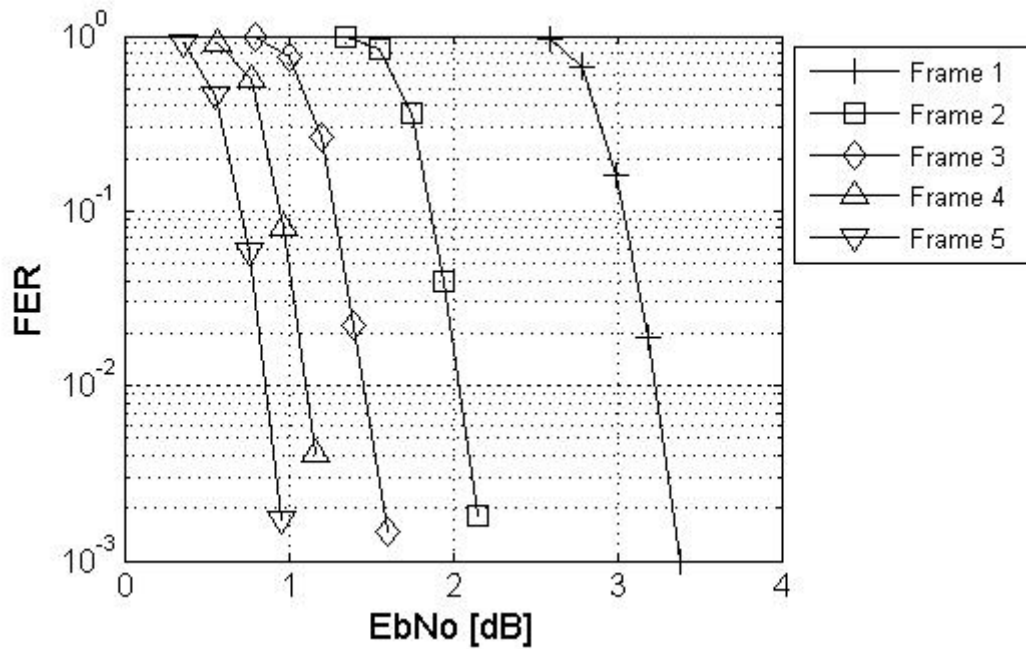


Figure 5-23 RL FER vs. E_b/N_0 for packet format 7

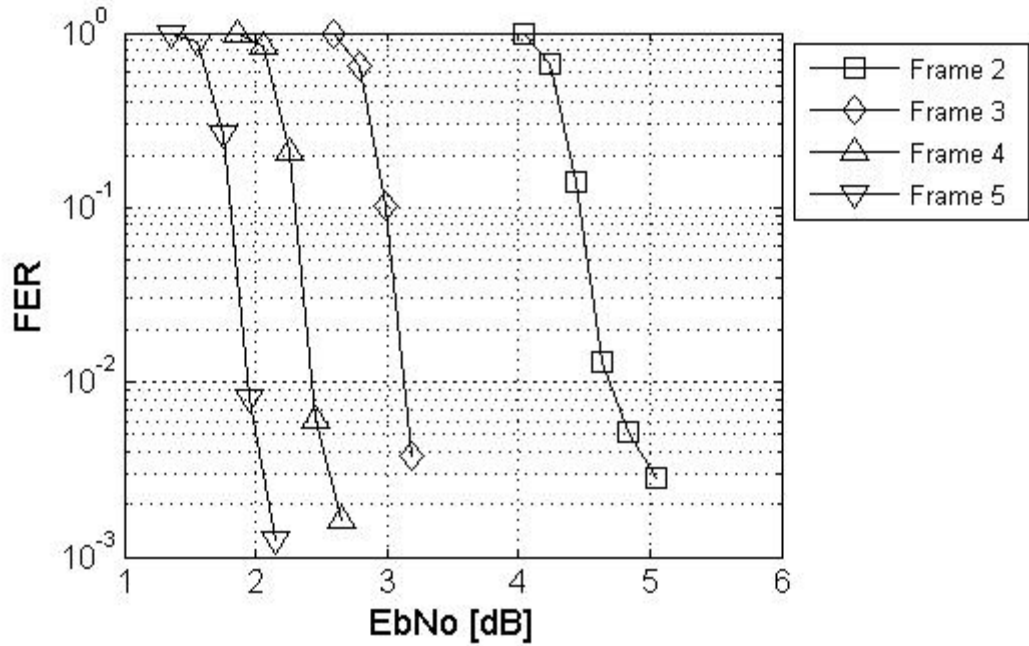


Figure 5-24 RL FER vs. E_b/N_0 for packet format 8

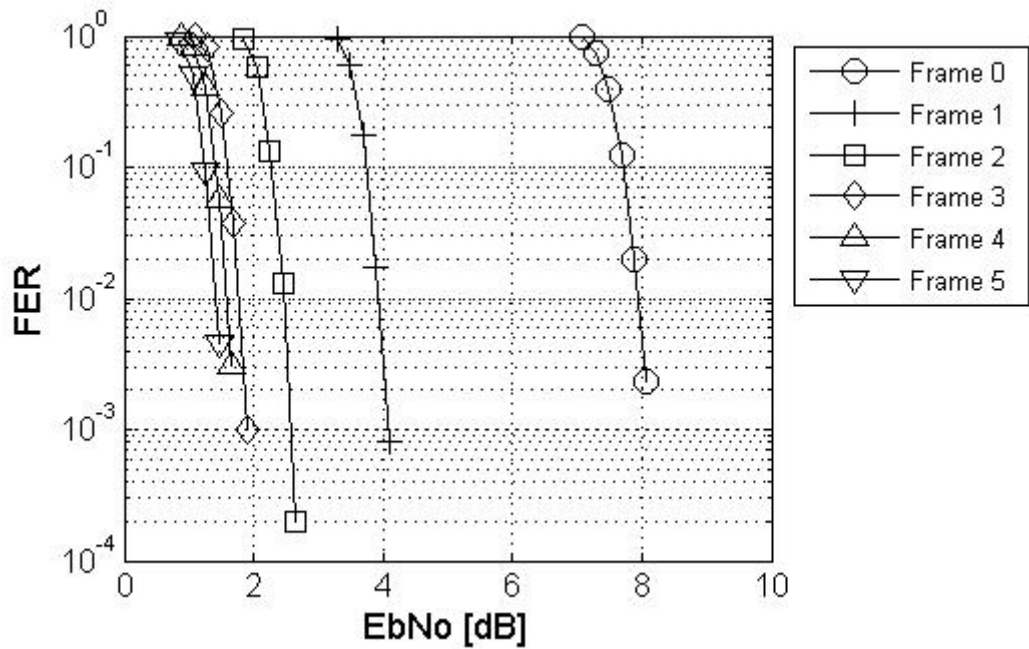


Figure 5-25 RL FER vs. E_b/N_0 for packet format 9

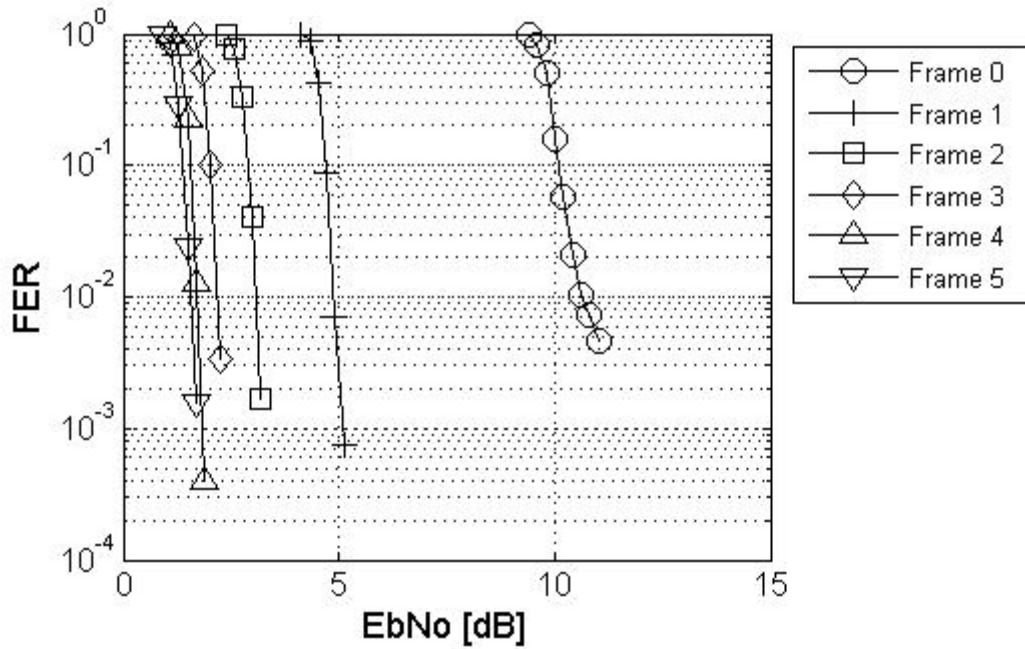


Figure 5-26 RL FER vs. E_b/N_0 for packet format 10

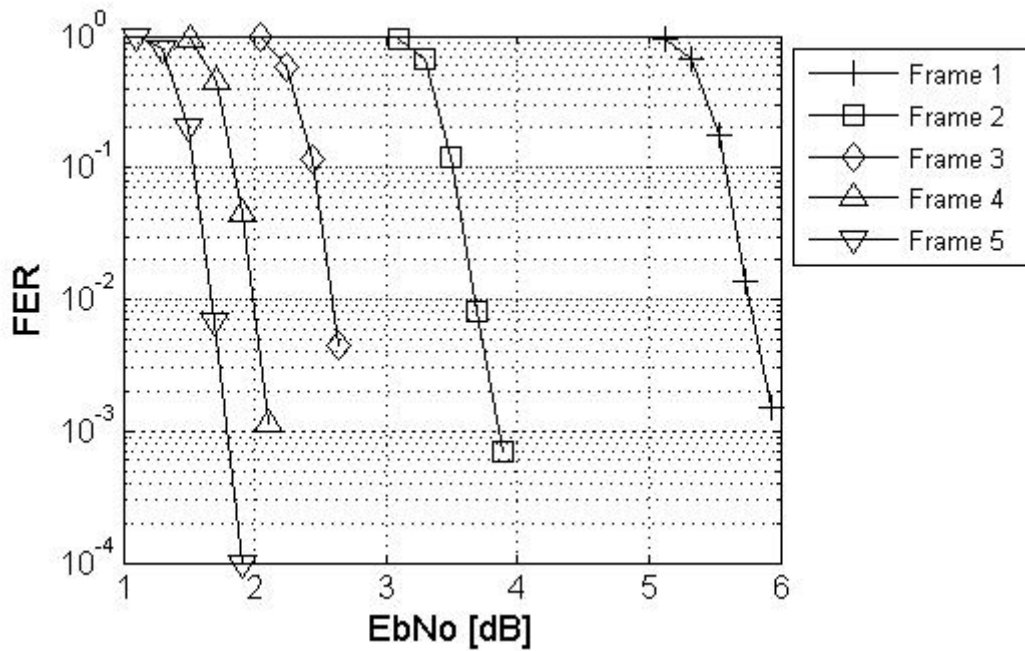


Figure 5-27 RL FER vs. E_b/N_0 for packet format 11

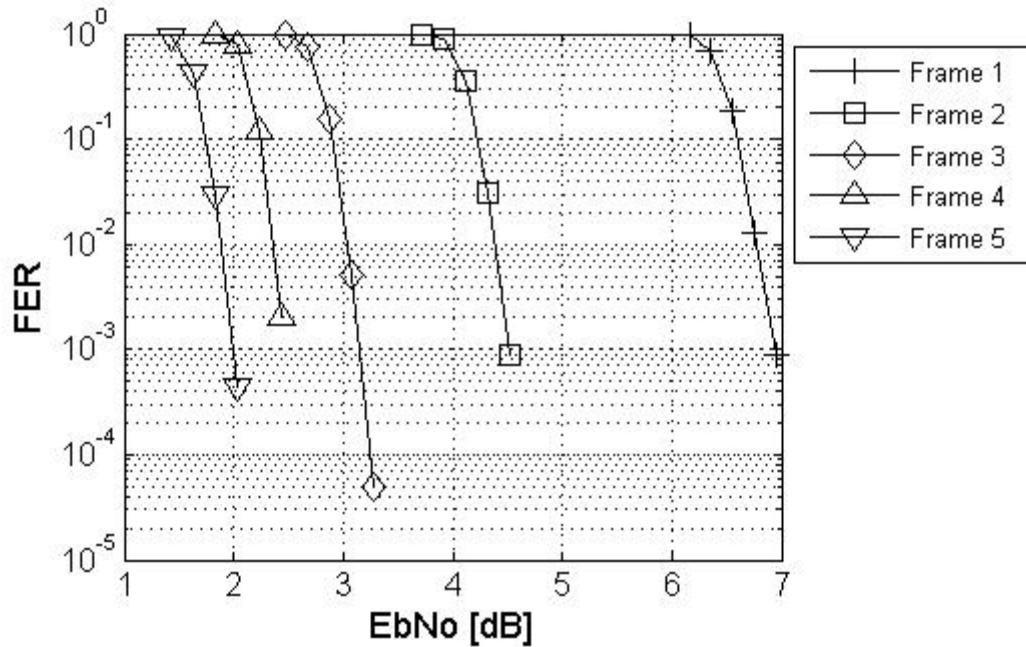


Figure 5-28 RL FER vs. E_b/N_0 for packet format 12

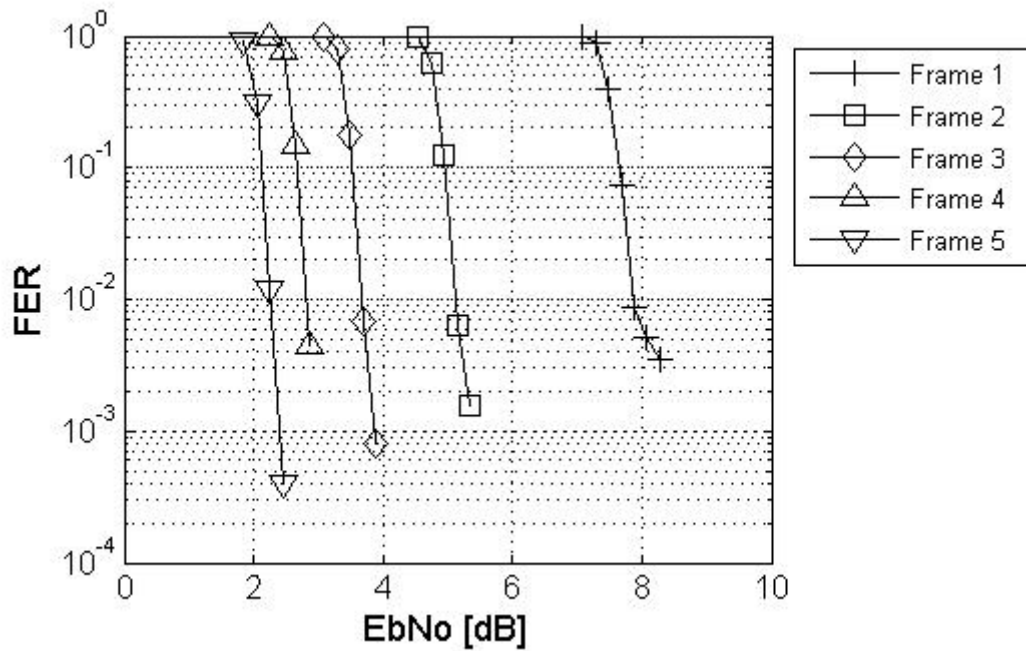


Figure 5-29 RL FER vs. E_b/N_0 for packet format 13

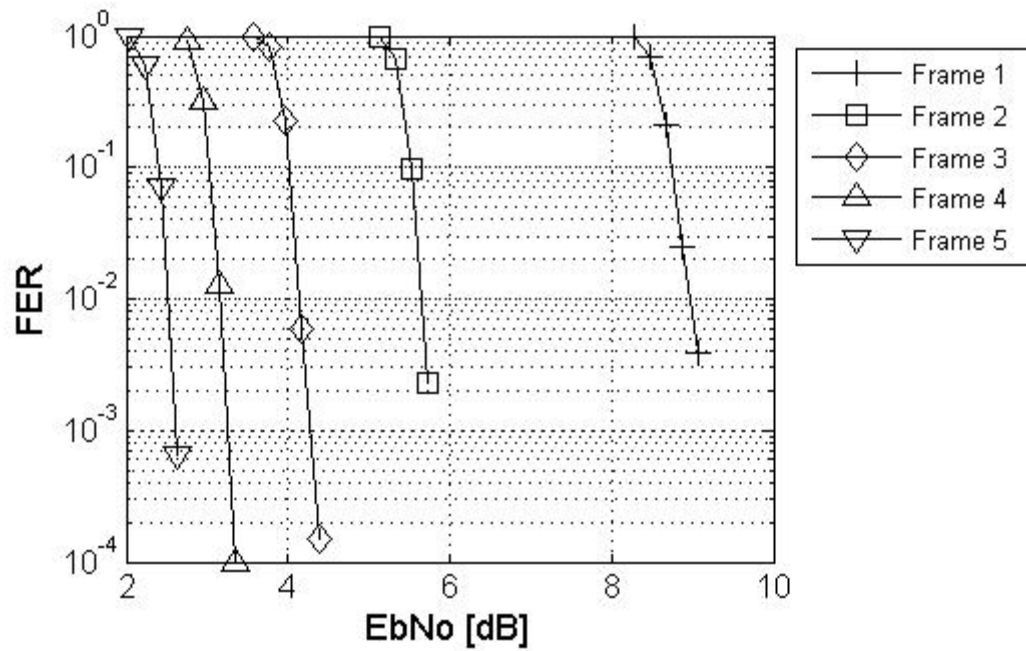


Figure 5-30 RL FER vs. E_b/N_0 for packet format 14

Appendix E Location Calibration Table

g.sc.id	l.ms.id	bs.loc.x	bs.loc.y	ms.loc.x	ms.loc.y	C/I	Path Loss	Chandiff
		(m)	(m)	(m)	(m)	(dB)	(dB)	(dB)
0	0	0	0	923.1855	-821.784	-8.35971	154.18	1.22076
0	1	0	0	1110.356	-66.758	8.76876	125.031	13.2174
0	2	0	0	362.1842	359.5489	4.77396	127.683	8.8168
0	3	0	0	129.4834	201.0195	0.767965	134.083	1.7633
0	4	0	0	319.7925	-92.287	7.45047	127.121	12.8739
0	5	0	0	1054.627	533.2838	-0.12349	126.29	0.656323
0	6	0	0	997.3494	-473.953	-2.78099	143.36	5.05722
0	7	0	0	922.0448	-449.127	1.96235	119.722	5.8613
0	8	0	0	367.9087	135.2231	15.1784	112.771	19.0204
0	9	0	0	641.6122	524.2848	8.35487	127.928	12.3431
1	0	0	0	-62.6639	518.8976	6.44211	118.776	8.96731
1	1	0	0	254.3962	447.7367	-1.65286	134.455	2.7543
1	2	0	0	-432.835	36.29939	-1.67037	141.616	2.9388
1	3	0	0	-786.331	350.0729	-0.60861	135.091	7.24162
1	4	0	0	-15.6605	108.6677	15.7723	101.039	18.8147
1	5	0	0	-916.291	781.3853	-3.11849	135.44	0.547633
1	6	0	0	-51.0684	280.9349	14.6912	103.792	19.0204
1	7	0	0	-668.559	587.4711	10.5346	133.341	19.1159
1	8	0	0	-746.416	125.9838	-2.58887	141.197	5.66178
1	9	0	0	-574.016	68.56649	-1.8725	133.283	2.49885
2	0	0	0	-555.214	-1092.14	-6.83238	150.806	4.62117
2	1	0	0	-124.703	-125.46	11.7518	124.741	17.6129
2	2	0	0	-76.5442	-499.441	9.22151	120.526	12.5985
2	3	0	0	-440.678	-646.422	7.2362	135.081	15.9262
2	4	0	0	231.2735	-490.612	2.19259	126.326	2.9388
2	5	0	0	-544.939	-991.515	8.35803	120.465	13.6179
2	6	0	0	-529.258	-912.051	-3.43493	144.18	4.29039
2	7	0	0	-873.75	-378.997	1.68117	123.629	6.95358
2	8	0	0	-701.09	-1032.67	-3.73433	134.746	0.398971
2	9	0	0	-319.491	-345.003	-1.48732	143.424	2.8273
3	0	2165.064	0	2813.238	198.6431	0.511935	120.491	3.42123
3	1	2165.064	0	3113.951	-19.502	-0.99228	134.948	5.12137
3	2	2165.064	0	2849.724	107.6759	3.08155	132.341	6.59297

g.sc.id	l.ms.id	bs.loc.x	bs.loc.y	ms.loc.x	ms.loc.y	C/I	Path Loss	Chandiff
3	3	2165.064	0	2430.914	459.1096	-4.92334	129.249	0
3	4	2165.064	0	3151.596	-341.482	-6.91609	153.366	3.07286
3	5	2165.064	0	2382.451	123.5847	11.2794	121.738	17.6329
3	6	2165.064	0	2755.978	-32.9127	8.45873	118.922	12.0404
3	7	2165.064	0	2891.392	-138.144	0.188327	145.548	12.4502
3	8	2165.064	0	2433.837	-352.504	2.28733	128.062	4.1138
3	9	2165.064	0	2852.353	294.3411	0.744479	131.789	4.28438
4	0	2165.064	0	1580.508	754.0377	0.70714	139.221	6.98976
4	1	2165.064	0	1683.133	86.92938	-0.69939	133.418	2.8129
4	2	2165.064	0	1920.734	890.1078	5.882	126.174	8.43115
4	3	2165.064	0	2071.205	948.422	1.38261	138.78	5.63941
4	4	2165.064	0	1846.079	274.9923	13.9143	101.721	19.1159
4	5	2165.064	0	1384.902	492.8636	-3.84991	136.126	1.36755
4	6	2165.064	0	1897.183	510.4331	13.7532	125.496	19.9902
4	7	2165.064	0	2126.786	354.3951	7.88163	118.431	13.2751
4	8	2165.064	0	1701.31	210.56	9.54946	118.574	14.1061
4	9	2165.064	0	2031.886	601.995	-2.76625	141.295	1.10516
5	0	2165.064	0	1366.635	-584.462	6.38504	118.527	11.113
5	1	2165.064	0	2030.457	-139.734	7.41256	121.499	8.95773
5	2	2165.064	0	1357.25	-251.724	7.2822	128.529	9.9918
5	3	2165.064	0	2335.386	-638.119	-0.36846	132.608	5.87377
5	4	2165.064	0	1994.359	-290.479	16.7299	114.225	20
5	5	2165.064	0	1878.936	-1143.72	-1.40757	140.605	4.86754
5	6	2165.064	0	1888.376	-879.947	1.18369	129.982	6.42977
5	7	2165.064	0	2570.726	-976.892	-2.61743	146.234	6.09922
5	8	2165.064	0	1630.826	-675.119	-0.50069	135.912	3.18694
5	9	2165.064	0	1530.563	-18.9858	-0.55367	131.104	1.1755
6	0	4330.127	0	5094.74	-720.449	-4.49159	147.234	1.24598
6	1	4330.127	0	5500.737	313.3131	1.76951	134.775	5.45832
6	2	4330.127	0	4900.546	-733.138	3.65355	123.815	8.47124
6	3	4330.127	0	4829.239	-826.475	-1.35598	140.344	1.9354
6	4	4330.127	0	5051.454	-128.66	3.12511	121.837	7.2657
6	5	4330.127	0	4923.893	-61.4923	13.0327	116.27	16.9657
6	6	4330.127	0	4482.365	35.87273	16.4219	110.562	19.5861
6	7	4330.127	0	4640.798	82.49157	7.54564	116.181	12.0085
6	8	4330.127	0	4631.296	119.1396	12.5626	119.37	18.5389
6	9	4330.127	0	4743.273	-101.487	15.1654	121.796	19.52
7	0	4330.127	0	4082.053	263.3563	3.1585	127.189	10.3323

g.sc.id	l.ms.id	bs.loc.x	bs.loc.y	ms.loc.x	ms.loc.y	C/I	Path Loss	Chandiff
7	1	4330.127	0	4476.015	727.1476	-3.05621	137.862	0.631701
7	2	4330.127	0	4523.355	450.0568	3.31426	125.056	4.1138
7	3	4330.127	0	4210.85	687.8458	1.41385	122.76	3.59851
7	4	4330.127	0	4183.234	363.777	5.75839	140.271	16.2062
7	5	4330.127	0	3753.109	51.99575	-3.18381	137.269	0.057367
7	6	4330.127	0	4529.848	1202.126	-0.79829	126.945	3.7307
7	7	4330.127	0	4271.968	103.8453	14.2151	126.279	19.9976
7	8	4330.127	0	4134.173	5.926098	0.604758	123.374	1.1755
7	9	4330.127	0	4392.764	450.006	10.6986	114.122	12.9307
8	0	4330.127	0	3431.87	-64.9339	-1.67123	142.069	4.58333
8	1	4330.127	0	4258.635	-49.6718	15.1451	86.9318	18.4694
8	2	4330.127	0	3887.333	-170.29	7.04395	126.048	12.3431
8	3	4330.127	0	4421.684	-158.886	-0.33939	119.386	0
8	4	4330.127	0	4230.507	-94.3659	12.7833	108.462	17.4302
8	5	4330.127	0	3703.769	-385.744	2.86566	134.541	7.05726
8	6	4330.127	0	3736.384	-746.191	9.56095	130.453	17.2672
8	7	4330.127	0	4054.884	-55.6294	5.45672	111.267	6.465
8	8	4330.127	0	3967.102	-30.6317	-1.61463	133.575	2.9388
8	9	4330.127	0	3429.084	-862.527	-5.09633	143.749	1.84402
9	0	3247.595	1875	3645.094	1405.343	0.789066	127.581	5.8776
9	1	3247.595	1875	4336.808	2149.508	-4.43369	151.395	11.8638
9	2	3247.595	1875	4019.379	1542.779	-2.01654	139.849	0.869649
9	3	3247.595	1875	3404.079	2093.873	2.69256	110.634	3.5268
9	4	3247.595	1875	3427.725	1848.156	12.5242	130.38	19.8433
9	5	3247.595	1875	3565.054	1866.12	15.5135	119.925	19.9902
9	6	3247.595	1875	4432.714	2114.643	1.36913	128.043	4.07428
9	7	3247.595	1875	3478.522	1841.445	13.1605	126.048	19.8433
9	8	3247.595	1875	4209.648	1570.112	0.754508	130.437	1.56328
9	9	3247.595	1875	3459.693	1798.212	10.0409	120.623	13.8329
10	0	3247.595	1875	3469.451	2290.191	-2.12451	139.391	1.1755
10	1	3247.595	1875	2964.365	2387.695	13.8667	111.011	19.9976
10	2	3247.595	1875	2968.016	2135.161	7.42242	123.513	10.5505
10	3	3247.595	1875	3481.187	2475.652	2.812	133.93	5.2902
10	4	3247.595	1875	2810.534	2891.634	0.887629	121.388	4.1138
10	5	3247.595	1875	2078.927	1875.896	-2.77499	136.778	3.44333
10	6	3247.595	1875	2549.238	2050.552	2.45722	131.677	5.89963
10	7	3247.595	1875	3379.656	2245.959	3.04665	123.721	5.8776
10	8	3247.595	1875	3250.777	2736.837	5.76885	128.42	9.31027

g.sc.id	l.ms.id	bs.loc.x	bs.loc.y	ms.loc.x	ms.loc.y	C/I	Path Loss	Chandiff
10	9	3247.595	1875	2866.963	2534.517	-3.2729	144.769	3.9865
11	0	3247.595	1875	3341.305	1711.631	-0.39675	113.021	0
11	1	3247.595	1875	2940.518	1844.576	2.33131	135.437	3.5268
11	2	3247.595	1875	3028.162	967.1231	-3.95644	141.492	0.17462
11	3	3247.595	1875	2659.492	1367.545	8.00134	120.702	14.3599
11	4	3247.595	1875	2623.098	1142.329	-9.88154	155.273	1.8273
11	5	3247.595	1875	3145.265	1780.967	15.9333	107.877	19.2922
11	6	3247.595	1875	3105.91	1325.244	12.9524	121.202	19.3731
11	7	3247.595	1875	3020.459	1592.114	8.89267	132.321	17.8299
11	8	3247.595	1875	3273.296	1723.775	10.3566	104.278	11.7546
11	9	3247.595	1875	2697.506	1621.712	-0.8454	136.121	2.45703
12	0	1082.532	1875	1608.488	2053.788	4.37308	134.137	7.38909
12	1	1082.532	1875	1484.761	1966.286	0.135327	117.242	1.28387
12	2	1082.532	1875	1923.943	2146.101	6.58502	122.245	7.73611
12	3	1082.532	1875	1632.569	1607.426	10.2836	123.231	14.1323
12	4	1082.532	1875	1620.075	2231.833	5.88775	119.823	7.41143
12	5	1082.532	1875	1297.07	1952.78	13.8149	112.098	19.0204
12	6	1082.532	1875	1606.352	2758.131	5.69041	129.264	11.249
12	7	1082.532	1875	1623.971	1205.545	-4.8745	132.207	0.055342
12	8	1082.532	1875	1932.491	1949.975	-11.9532	159.14	7.28931
12	9	1082.532	1875	1417.159	2364.95	-3.21064	131.844	0.744962
13	0	1082.532	1875	853.0143	2687.499	-4.16806	128.955	0.151931
13	1	1082.532	1875	960.3293	1926.381	10.3696	128.04	13.5183
13	2	1082.532	1875	915.5712	2276.232	12.8129	121.146	17.6385
13	3	1082.532	1875	492.0917	2336.593	14.7135	109.193	18.8147
13	4	1082.532	1875	295.3142	1878.422	-3.04926	146.934	4.78473
13	5	1082.532	1875	1285.964	2288.921	-0.3693	130.275	2.351
13	6	1082.532	1875	1442.19	2542.938	-1.49988	126.504	1.1755
13	7	1082.532	1875	646.264	2176.875	10.0932	125.401	13.0661
13	8	1082.532	1875	598.7756	2378.857	6.60387	113.87	10.7379
13	9	1082.532	1875	-20.3609	2406.516	2.90679	132.28	8.75519
14	0	1082.532	1875	803.1839	1081.412	-3.7792	141.16	0.119668
14	1	1082.532	1875	936.5059	1830.325	7.97177	111.409	9.9918
14	2	1082.532	1875	673.0974	1766.382	7.01068	121.316	8.8168
14	3	1082.532	1875	539.8342	1175.88	-0.00533	139.034	6.04226
14	4	1082.532	1875	917.9504	1367.278	1.64282	125.23	5.16211
14	5	1082.532	1875	976.7574	1754.148	16.3839	104.596	19.7037
14	6	1082.532	1875	1013.383	1301.784	14.7745	119.353	18.7045

g.sc.id	l.ms.id	bs.loc.x	bs.loc.y	ms.loc.x	ms.loc.y	C/I	Path Loss	Chandiff
14	7	1082.532	1875	943.8625	1844.306	6.17501	109.843	7.0536
14	8	1082.532	1875	1042.447	1765.284	16.5411	116.244	19.7551
14	9	1082.532	1875	803.0607	1858.959	1.34327	118.259	1.7633
15	0	2165.064	3750	3125.097	3861.472	9.07032	122.866	15.2545
15	1	2165.064	3750	2369.754	3864.882	12.603	128.407	17.9404
15	2	2165.064	3750	2209.864	3777.062	14.2352	106.561	17.0445
15	3	2165.064	3750	2636.921	4547.035	-1.91249	129.389	4.03781
15	4	2165.064	3750	2577.893	3679.14	9.65678	132.06	14.2689
15	5	2165.064	3750	2285.947	3847.739	10.2838	120.174	12.3431
15	6	2165.064	3750	2952.167	3334.269	0.062856	128.671	2.42629
15	7	2165.064	3750	3106.942	4356.078	-3.82458	146.701	0.322477
15	8	2165.064	3750	2684.069	3750.581	4.66899	119.134	10.634
15	9	2165.064	3750	2419.564	3832.233	15.3161	111.519	19.2065
16	0	2165.064	3750	2569.846	4476.295	-2.53069	134.315	0.5878
16	1	2165.064	3750	1860.692	3795.926	2.49462	119.398	5.2902
16	2	2165.064	3750	2263.961	4492.828	4.45853	132.061	11.0933
16	3	2165.064	3750	2057.172	4824.111	6.90633	133.294	12.6964
16	4	2165.064	3750	2439.299	4658.445	-4.32787	134.268	0.337372
16	5	2165.064	3750	2071.096	4076.812	11.3197	119.069	14.4399
16	6	2165.064	3750	2159.548	3788.017	15.8041	83.3422	18.8147
16	7	2165.064	3750	2276.033	4669.642	0.466889	129.645	4.41156
16	8	2165.064	3750	2403.462	4259.266	-0.47548	146.632	11.724
16	9	2165.064	3750	2154.996	3854.04	15.5523	99.3807	18.5894
17	0	2165.064	3750	1222.487	3544.272	-3.88191	135.319	1.76262
17	1	2165.064	3750	2119.324	3718.22	15.3634	111.139	18.4694
17	2	2165.064	3750	1952.457	3582.317	15.3017	114.027	18.8147
17	3	2165.064	3750	2043.535	3457.58	15.0907	114.632	19.88
17	4	2165.064	3750	2084.438	3391.746	7.85217	135.074	13.509
17	5	2165.064	3750	2502.44	2680.271	-4.23776	140.381	4.05082
17	6	2165.064	3750	2198.714	3612.49	8.38073	96.0009	9.4038
17	7	2165.064	3750	2549.385	2864.089	0.682236	136.446	2.22736
17	8	2165.064	3750	2056.211	3724.442	6.82352	94.701	7.6412
17	9	2165.064	3750	1109.183	3506.143	4.42409	131.748	7.6412
18	0	0	3750	303.3748	4214.174	-3.61049	144.361	1.7633
18	1	0	3750	128.2674	3857.199	10.2432	104.913	11.7546
18	2	0	3750	514.2349	3762.608	15.5082	115.219	19.9976
18	3	0	3750	529.4765	4298.697	-1.96903	135.853	0.106174
18	4	0	3750	455.2791	4285.7	1.52158	128.316	5.8776

g.sc.id	l.ms.id	bs.loc.x	bs.loc.y	ms.loc.x	ms.loc.y	C/I	Path Loss	Chandiff
18	5	0	3750	654.384	3902.431	-8.23791	154.579	5.6081
18	6	0	3750	117.6796	3627.861	7.21333	119.715	8.229
18	7	0	3750	713.4089	4116.545	4.09948	128.376	7.65155
18	8	0	3750	740.6094	3075.999	-1.23169	142.354	1.71351
18	9	0	3750	263.8398	3846.246	14.6897	116.062	19.0204
19	0	0	3750	-435.882	4579.006	-3.44868	139.833	3.16632
19	1	0	3750	139.073	4001.65	-0.82098	139.209	0.5878
19	2	0	3750	94.20352	4391.331	-0.19343	134.976	5.90207
19	3	0	3750	518.5811	4794.841	-2.59524	131.038	0.837775
19	4	0	3750	161.6448	4307.421	4.50026	134.518	8.229
19	5	0	3750	-510.48	3848.427	2.9051	115.526	6.465
19	6	0	3750	152.0415	4061.063	-0.83483	133.253	2.351
19	7	0	3750	-410.912	4187.514	5.88303	137.44	16.3993
19	8	0	3750	-500.93	4021.272	4.96316	119.588	12.5125
19	9	0	3750	-196.312	3758.613	1.36805	110.128	1.7633
20	0	0	3750	-135.214	3633.945	15.9569	111.377	19.1159
20	1	0	3750	-577.153	3646.199	-3.56361	132.715	4.48233
20	2	0	3750	-222.067	3577.693	12.7747	123.079	18.8147
20	3	0	3750	-570.181	3265.84	1.84364	137.509	5.69094
20	4	0	3750	-137.701	3730.678	4.14816	94.2428	4.702
20	5	0	3750	-101.17	3636.226	16.4656	115.522	19.6473
20	6	0	3750	-82.3875	3677.894	16.0425	103.389	19.1159
20	7	0	3750	-312.556	3259.652	0.599244	131.376	4.76819
20	8	0	3750	203.3534	2950.936	-0.42304	142.303	5.75281
20	9	0	3750	97.32849	3472.569	5.55217	124.775	6.465
21	0	-1082.53	1875	-218.731	1402.461	5.92572	129.503	12.0824
21	1	-1082.53	1875	-435.128	2212.301	9.98075	131.457	16.8682
21	2	-1082.53	1875	-769.886	1452.207	-0.67321	134.764	3.5268
21	3	-1082.53	1875	-857.104	1634.44	-0.35337	126.674	1.20035
21	4	-1082.53	1875	-882.332	1660.154	-3.09044	143.054	0.024711
21	5	-1082.53	1875	-482.556	1604.6	0.957888	112.871	2.03532
21	6	-1082.53	1875	-112.609	1117.585	-3.63999	132.304	0.939121
21	7	-1082.53	1875	-718.42	1327.271	-4.59403	142.895	2.20094
21	8	-1082.53	1875	-820.639	2254.224	-1.44718	126.666	2.9388
21	9	-1082.53	1875	-825.468	2272.91	1.67655	134.995	7.7816
22	0	-1082.53	1875	-1179.78	2900.513	1.00302	138.678	6.51111
22	1	-1082.53	1875	-1069.44	2547.043	11.0059	117.335	17.0445
22	2	-1082.53	1875	-1264.54	1886.708	1.31357	117.835	2.351

g.sc.id	l.ms.id	bs.loc.x	bs.loc.y	ms.loc.x	ms.loc.y	C/I	Path Loss	Chandiff
22	3	-1082.53	1875	-1410.82	2600.859	-2.57553	139.182	3.37625
22	4	-1082.53	1875	-1457.78	2090.701	1.66082	128.99	4.88553
22	5	-1082.53	1875	-1346.04	2395.884	6.76859	136.931	12.1813
22	6	-1082.53	1875	-692.056	2594.102	-1.66523	134.402	2.16137
22	7	-1082.53	1875	-1085.5	2157.395	13.5783	113.668	17.9404
22	8	-1082.53	1875	-1151.47	1923.137	15.3179	112.025	18.4694
22	9	-1082.53	1875	-1951.89	2098.506	5.13734	133.48	9.38862
23	0	-1082.53	1875	-871.548	1488.926	-0.30076	126.387	0.5878
23	1	-1082.53	1875	-1717.67	1382.765	8.04944	135.064	18.8147
23	2	-1082.53	1875	-2103.64	1363.533	6.24998	108.843	8.33588
23	3	-1082.53	1875	-823.833	1121.123	-4.64595	138.429	0.576652
23	4	-1082.53	1875	-1112.33	1341.108	0.576988	137.615	3.61592
23	5	-1082.53	1875	-1352.49	1780.677	9.28845	108.551	11.1673
23	6	-1082.53	1875	-740.011	1141.111	-3.69959	132.409	0.905869
23	7	-1082.53	1875	-1030.5	1444.733	11.1916	119.361	13.5183
23	8	-1082.53	1875	-1262.78	1556.691	12.3424	114.156	20
23	9	-1082.53	1875	-1107.19	1172.935	-0.04213	138.24	6.56192
24	0	-2165.06	3750	-1643.83	3808.059	13.5975	125.085	19.9118
24	1	-2165.06	3750	-1417.55	4200.24	-2.80645	131.364	0.266776
24	2	-2165.06	3750	-1960.3	3626.597	11.1008	132.023	17.0445
24	3	-2165.06	3750	-1220.37	4525.375	4.22238	127.487	6.98474
24	4	-2165.06	3750	-1621.22	3837.383	-0.02092	129.458	3.17214
24	5	-2165.06	3750	-1733.02	3867.088	8.61836	135.093	15.8777
24	6	-2165.06	3750	-1143.25	3167.888	2.05679	137.657	9.60706
24	7	-2165.06	3750	-1963.54	3576.775	7.52417	123.342	11.1673
24	8	-2165.06	3750	-1457.69	3066.986	-6.02056	147.912	0.662589
24	9	-2165.06	3750	-1820.7	3993.578	9.62001	122.005	14.694
25	0	-2165.06	3750	-2031.81	4583.674	3.14546	128.621	7.74705
25	1	-2165.06	3750	-2176.25	3823.466	15.8912	104.303	18.92
25	2	-2165.06	3750	-2254.65	3813.862	15.4489	86.1053	18.4694
25	3	-2165.06	3750	-2567.47	4782.684	-3.12421	138.752	1.31504
25	4	-2165.06	3750	-2751.67	3959.474	6.70011	128.936	9.11141
25	5	-2165.06	3750	-3010.79	4234.056	-0.07066	123.713	2.83006
25	6	-2165.06	3750	-2234.92	4883.176	-1.35176	135.904	1.12902
25	7	-2165.06	3750	-1686.77	4856.409	5.70882	132.407	10.4544
25	8	-2165.06	3750	-2168.9	4030.248	12.6041	106.787	17.3585
25	9	-2165.06	3750	-2673.6	3981.6	-4.26255	135.696	0.116652
26	0	-2165.06	3750	-2084.03	3594.952	0.727579	120.674	1.1755

g.sc.id	l.ms.id	bs.loc.x	bs.loc.y	ms.loc.x	ms.loc.y	C/I	Path Loss	Chandiff
26	1	-2165.06	3750	-2210.74	3490.732	15.456	106.402	19.0204
26	2	-2165.06	3750	-2175.83	3557.5	11.487	132.354	18.2147
26	3	-2165.06	3750	-2566.92	3081.733	1.04421	134.077	3.39779
26	4	-2165.06	3750	-2766.67	3560.506	3.87993	124.609	9.05172
26	5	-2165.06	3750	-2245.99	3663.719	15.1056	120.26	19.5861
26	6	-2165.06	3750	-2537.36	3731.615	0.344916	129.771	1.7633
26	7	-2165.06	3750	-2335.95	3149.59	10.3122	121.635	16.3311
26	8	-2165.06	3750	-2938.23	3673.298	0.638785	142.38	7.36045
26	9	-2165.06	3750	-1921.89	3287.607	-1.78449	134.16	1.1755
27	0	-3247.6	1875	-2383.98	2614.566	-2.06638	137.289	0.961186
27	1	-3247.6	1875	-2485.16	1427.452	-0.28737	139.574	6.35431
27	2	-3247.6	1875	-2912.49	2167.852	8.20544	109.653	11.1673
27	3	-3247.6	1875	-2698.08	1799.775	15.8025	112.261	19.8433
27	4	-3247.6	1875	-2539.34	1487.432	0.695484	141.441	5.00907
27	5	-3247.6	1875	-2303.42	1714.364	0.659034	128.377	3.55238
27	6	-3247.6	1875	-2313.83	2202.366	-4.12118	139.613	2.05108
27	7	-3247.6	1875	-2524.11	2246.139	2.91246	135.404	5.71075
27	8	-3247.6	1875	-2808.56	1823.055	10.2279	110.032	12.7769
27	9	-3247.6	1875	-3138.91	2022.887	3.0041	122.403	3.5268
28	0	-3247.6	1875	-4198.59	2282.96	2.66075	137.569	6.86464
28	1	-3247.6	1875	-3355	1963.428	12.9486	106.82	16.4003
28	2	-3247.6	1875	-3391.06	2456.019	-7.11607	152.752	2.93345
28	3	-3247.6	1875	-3463.86	3059.139	2.25454	138.449	10.0319
28	4	-3247.6	1875	-3085.45	2351.977	3.43438	120.323	6.465
28	5	-3247.6	1875	-3859.74	1983.802	4.08413	129.508	5.8776
28	6	-3247.6	1875	-3354.13	1943.497	15.0454	109.09	18.2147
28	7	-3247.6	1875	-3587.28	1994.346	-2.89824	125.968	0.803306
28	8	-3247.6	1875	-3294.05	2299.803	-6.18638	144.084	0.173612
28	9	-3247.6	1875	-2889.46	2683.087	7.49466	111.378	11.3804
29	0	-3247.6	1875	-2915.32	1207.995	-1.39754	130.087	2.351
29	1	-3247.6	1875	-3277.79	1758.334	16.4338	95.3264	19.449
29	2	-3247.6	1875	-3226.18	840.1864	-3.42345	130.366	0.073156
29	3	-3247.6	1875	-3217.24	1728.104	8.37465	115.787	10.58
29	4	-3247.6	1875	-3971.32	985.0019	-1.90314	142.166	5.06331
29	5	-3247.6	1875	-4260.15	1649.315	-2.87787	130.52	0.949585
29	6	-3247.6	1875	-3871.35	1809.415	-1.42153	128.135	0.593979
29	7	-3247.6	1875	-3404.9	1301.769	15.5561	116.602	19.449
29	8	-3247.6	1875	-3481.55	1281.577	5.78449	124.889	12.2185

g.sc.id	l.ms.id	bs.loc.x	bs.loc.y	ms.loc.x	ms.loc.y	C/I	Path Loss	Chandiff
29	9	-3247.6	1875	-3832.91	1428.11	-0.28173	144.509	7.90073
30	0	-2165.06	0	-1992.95	150.1377	3.31976	132.172	6.34121
30	1	-2165.06	0	-1745.24	214.3123	-0.23796	124.762	0.244926
30	2	-2165.06	0	-1118.16	-123.39	-0.987	141.839	3.5268
30	3	-2165.06	0	-977.753	-14.4578	0.385152	133.982	4.68906
30	4	-2165.06	0	-1963.42	182.5436	8.52057	115.045	10.58
30	5	-2165.06	0	-1771.45	-348.896	-2.61144	144.451	1.57445
30	6	-2165.06	0	-1637.76	-481.603	0.172244	136.646	5.9436
30	7	-2165.06	0	-1739.81	274.1414	12.5161	117.063	15.8691
30	8	-2165.06	0	-1801.26	433.2537	1.37179	136.934	5.8776
30	9	-2165.06	0	-1092.5	-508.269	8.50376	112.254	14.12
31	0	-2165.06	0	-2361.19	347.419	7.51364	122.69	10.1997
31	1	-2165.06	0	-2697.94	61.40768	3.03677	126.616	4.1138
31	2	-2165.06	0	-2081.29	1035.734	-1.70769	125.459	0.357179
31	3	-2165.06	0	-2638.06	259.9491	-4.2033	136.231	1.40234
31	4	-2165.06	0	-2269.44	48.95822	12.0794	114.541	14.694
31	5	-2165.06	0	-2235.07	204.5774	13.9108	105.441	18.6246
31	6	-2165.06	0	-2650.04	599.9189	10.1411	125.633	16.2293
31	7	-2165.06	0	-2383.74	539.2605	7.11477	128.997	14.014
31	8	-2165.06	0	-2485.1	221.9309	4.58174	123.721	10.8576
31	9	-2165.06	0	-2084.58	968.0261	-7.07497	152.077	2.5529
32	0	-2165.06	0	-2032.97	-271.09	1.80499	118.328	2.351
32	1	-2165.06	0	-2394.98	-454.126	12.2558	117.583	15.7469
32	2	-2165.06	0	-2620.71	-378.706	-3.54091	147.954	1.47094
32	3	-2165.06	0	-2512.43	-184.055	6.93241	128.391	13.2222
32	4	-2165.06	0	-3128.06	-105.302	-0.78019	125.22	2.65705
32	5	-2165.06	0	-2017.08	-767.83	1.05146	138.612	3.54231
32	6	-2165.06	0	-2626.29	-293.236	7.7413	108.017	13.7681
32	7	-2165.06	0	-2402.68	-377.555	6.44263	126.103	11.5862
32	8	-2165.06	0	-2957.54	-811.278	1.32562	137.305	7.37951
32	9	-2165.06	0	-2293.15	-106.101	15.7781	91.3341	19.0204
33	0	-4330.13	0	-3413.82	-771.091	-0.21789	133.009	3.43229
33	1	-4330.13	0	-3754.51	-302.524	8.34615	131.421	13.456
33	2	-4330.13	0	-3334.4	-376.486	3.98755	121.452	6.16958
33	3	-4330.13	0	-3843.97	-567.17	5.00235	121.016	6.465
33	4	-4330.13	0	-4292.75	0.787308	16.9856	91.1638	19.9976
33	5	-4330.13	0	-3623.01	-142.939	1.26842	128.644	5.80759
33	6	-4330.13	0	-3524.24	-30.225	-10.1777	156.548	3.33836

g.sc.id	l.ms.id	bs.loc.x	bs.loc.y	ms.loc.x	ms.loc.y	C/I	Path Loss	Chandiff
33	7	-4330.13	0	-3758.15	509.8115	-0.50404	137.92	7.65632
33	8	-4330.13	0	-4200.59	-22.4047	16.6369	96.5517	19.7551
33	9	-4330.13	0	-3354.35	-275.12	0.410734	141.424	3.93927
34	0	-4330.13	0	-5253.47	353.6781	3.30359	130.662	5.62655
34	1	-4330.13	0	-4175.04	679.259	1.10045	131.08	7.0235
34	2	-4330.13	0	-5075.78	412.5934	0.966779	140.838	6.36451
34	3	-4330.13	0	-4216.92	234.2934	-0.74032	129.707	2.351
34	4	-4330.13	0	-4491.77	1086.71	1.74864	132.737	7.35921
34	5	-4330.13	0	-5160.87	396.7665	-0.54043	142.23	4.31659
34	6	-4330.13	0	-4864.12	654.6192	9.44317	114.858	18.3377
34	7	-4330.13	0	-4732.27	643.7965	12.4197	121.617	19.4339
34	8	-4330.13	0	-4425.7	849.234	13.337	124.192	18.5894
34	9	-4330.13	0	-4490.77	123.7115	14.8132	104.455	18.8147
35	0	-4330.13	0	-4026.25	-610.488	-1.56983	131.76	0.918927
35	1	-4330.13	0	-4666.51	-153.536	3.55107	136.112	8.5941
35	2	-4330.13	0	-4248.88	-327.1	7.73988	115.338	9.4038
35	3	-4330.13	0	-4236.69	-874.259	1.15203	133.556	3.47278
35	4	-4330.13	0	-4287.74	-889.788	4.38738	133.855	10.4403
35	5	-4330.13	0	-4778.25	-404.348	13.2116	112.198	18.8149
35	6	-4330.13	0	-4630.21	-60.3906	2.22355	137.37	6.465
35	7	-4330.13	0	-4712.33	-263.02	-0.14647	130.913	0.349071
35	8	-4330.13	0	-4296.29	-157.116	9.01056	113.441	10.58
35	9	-4330.13	0	-4305.2	-495.223	-5.56434	149.162	2.70895
36	0	-3247.6	-1875	-2455.62	-1986.98	5.87234	124.591	7.39751
36	1	-3247.6	-1875	-3007.07	-1719.85	1.73439	126.749	3.59958
36	2	-3247.6	-1875	-2666.23	-1832.1	7.99954	135.081	16.0692
36	3	-3247.6	-1875	-2395.27	-2034.85	0.273427	132.739	3.10883
36	4	-3247.6	-1875	-3114.81	-1708.97	4.46595	117.51	5.2902
36	5	-3247.6	-1875	-2678.16	-1135.94	-4.1919	144.092	2.89926
36	6	-3247.6	-1875	-3048.17	-1928.86	12.7495	104.203	19.0921
36	7	-3247.6	-1875	-2400.9	-1746.5	10.5705	125.939	16.476
36	8	-3247.6	-1875	-3198.22	-1827.33	8.31967	111.355	9.4038
36	9	-3247.6	-1875	-3162.46	-1830.76	15.1929	83.6485	18.2147
37	0	-3247.6	-1875	-3919.38	-1185.69	1.3121	131.869	6.465
37	1	-3247.6	-1875	-4193.26	-1760.63	7.71897	130.273	14.2719
37	2	-3247.6	-1875	-3289.28	-1872.95	1.37348	86.7615	1.7633
37	3	-3247.6	-1875	-2956.92	-1100.88	-6.37728	153.628	13.3612
37	4	-3247.6	-1875	-3833.53	-964.391	3.0465	136.308	8.46342

g.sc.id	l.ms.id	bs.loc.x	bs.loc.y	ms.loc.x	ms.loc.y	C/I	Path Loss	Chandiff
37	5	-3247.6	-1875	-3655.25	-1269.24	4.81225	129.117	13.0384
37	6	-3247.6	-1875	-3213.36	-1738.97	8.33201	116.288	9.4038
37	7	-3247.6	-1875	-3488.47	-1853.67	1.71109	129.994	2.9388
37	8	-3247.6	-1875	-3664.66	-1634.66	11.2164	113.162	17.4448
37	9	-3247.6	-1875	-3817.53	-1070.62	-6.46312	150.419	1.92389
38	0	-3247.6	-1875	-3648.68	-2040.12	6.23412	127.163	9.67589
38	1	-3247.6	-1875	-3295.28	-1926.25	16.5524	90.8982	19.5861
38	2	-3247.6	-1875	-3351.34	-2772.14	-0.85184	144.364	7.63004
38	3	-3247.6	-1875	-2968.4	-2359.8	-2.19724	116.015	0
38	4	-3247.6	-1875	-3544.37	-3032.04	1.10888	132.495	8.06349
38	5	-3247.6	-1875	-3532.84	-2194.58	13.8602	123.108	19.6473
38	6	-3247.6	-1875	-2774.3	-2916.57	0.645658	124.4	4.75352
38	7	-3247.6	-1875	-2848.27	-2581.92	-1.49558	130.554	0.5878
38	8	-3247.6	-1875	-3063.92	-2545.75	-1.89746	141.523	0.541675
38	9	-3247.6	-1875	-2969.78	-2529.56	0.591988	125.638	3.19061
39	0	-1082.53	-1875	-649.947	-2179.82	12.0259	114.276	14.694
39	1	-1082.53	-1875	-354.797	-1827	12.0413	125.778	19.9608
39	2	-1082.53	-1875	-932.757	-2037.91	6.33652	105.673	7.6412
39	3	-1082.53	-1875	-873.199	-2065.7	8.25977	131.615	10.58
39	4	-1082.53	-1875	-540.776	-2155.5	6.03074	130.449	9.0012
39	5	-1082.53	-1875	-608.396	-2310.67	6.10216	127.686	12.1313
39	6	-1082.53	-1875	-810.189	-2011.53	6.31218	138.51	18.2147
39	7	-1082.53	-1875	-501.427	-2682.32	-0.82499	139.127	4.52606
39	8	-1082.53	-1875	-731.253	-2183.26	2.25287	127.703	5.45957
39	9	-1082.53	-1875	-406.599	-2817.49	-3.79859	146.199	3.70125
40	0	-1082.53	-1875	-1767.71	-1469.41	0.416446	132.32	2.44691
40	1	-1082.53	-1875	-1112.61	-1717.86	16.0873	95.4892	19.1159
40	2	-1082.53	-1875	-840.16	-1071.18	-2.93396	137.607	0.558806
40	3	-1082.53	-1875	-2233.5	-1438.17	-2.12397	124.903	4.53044
40	4	-1082.53	-1875	-1079.84	-1508.44	11.8122	117.952	17.6329
40	5	-1082.53	-1875	-1884.86	-1197.33	-1.72964	141.758	4.44624
40	6	-1082.53	-1875	-1446.39	-713.665	1.77587	126.109	6.33301
40	7	-1082.53	-1875	-1208.85	-1262.57	0.318323	130.434	4.68829
40	8	-1082.53	-1875	-2160.52	-1700.7	-1.61379	136.94	1.48291
40	9	-1082.53	-1875	-2025.04	-1756.24	6.62747	124.41	12.1926
41	0	-1082.53	-1875	-1793.29	-2725.36	-0.63858	135.375	2.69743
41	1	-1082.53	-1875	-1331.54	-2738.55	11.7686	125.006	16.9229
41	2	-1082.53	-1875	-1769.35	-2064.13	5.06613	121.366	8.8168

g.sc.id	l.ms.id	bs.loc.x	bs.loc.y	ms.loc.x	ms.loc.y	C/I	Path Loss	Chandiff
41	3	-1082.53	-1875	-997.591	-2654.67	2.66266	142.139	13.2766
41	4	-1082.53	-1875	-1301.4	-1921.45	6.21815	117.196	7.0536
41	5	-1082.53	-1875	-825.759	-2332.35	-1.2662	127.956	0.5878
41	6	-1082.53	-1875	-1213.77	-2899.49	1.00601	142.261	10.58
41	7	-1082.53	-1875	-1457.43	-2282.76	1.66055	136.313	7.75983
41	8	-1082.53	-1875	-1317.43	-2682.42	1.10259	130.81	4.36343
41	9	-1082.53	-1875	-1249.76	-2395.3	5.57877	137.603	10.6329
42	0	-2165.06	-3750	-954.574	-3949.18	4.15826	129.334	6.67148
42	1	-2165.06	-3750	-1976.89	-4019.07	-0.09599	123.407	2.9388
42	2	-2165.06	-3750	-1045.86	-3398.92	0.609571	137.897	4.77543
42	3	-2165.06	-3750	-1538.63	-3497.59	2.15867	118.022	4.99934
42	4	-2165.06	-3750	-1360.65	-3838.61	0.63141	133.169	3.55697
42	5	-2165.06	-3750	-1535.61	-4611.65	-0.21161	142.929	6.1698
42	6	-2165.06	-3750	-2026.26	-3965.3	1.24648	113.804	1.7633
42	7	-2165.06	-3750	-1624.34	-4393.45	-1.24614	136.349	5.22814
42	8	-2165.06	-3750	-1839.93	-3724.04	15.3025	118.378	19.9388
42	9	-2165.06	-3750	-1561.95	-3200.43	5.08212	123.664	10.58
43	0	-2165.06	-3750	-3350.6	-3478.43	2.50973	142.591	9.17134
43	1	-2165.06	-3750	-2635.09	-3394.78	15.4958	111.033	18.7045
43	2	-2165.06	-3750	-1854.02	-2854.22	-0.55379	127.413	4.75858
43	3	-2165.06	-3750	-3078.39	-3212.42	-0.9481	144.336	3.75038
43	4	-2165.06	-3750	-2619.36	-2925.66	-2.22777	141.954	5.05356
43	5	-2165.06	-3750	-2735.91	-2760.16	-4.9451	139.15	0
43	6	-2165.06	-3750	-2560.81	-3491.99	-4.49257	148.576	2.87645
43	7	-2165.06	-3750	-2212.88	-3020.61	3.54883	131.379	7.33057
43	8	-2165.06	-3750	-2869.01	-2827.19	-3.25513	129.349	1.44464
43	9	-2165.06	-3750	-2177.33	-3643.05	15.6714	104.066	18.7045
44	0	-2165.06	-3750	-2525.04	-4383.98	9.37717	107.363	13.2
44	1	-2165.06	-3750	-2483.93	-3946.48	14.8869	104.558	18.08
44	2	-2165.06	-3750	-2804.13	-4426.87	-0.30589	141.791	5.68091
44	3	-2165.06	-3750	-2259.85	-3753.09	0.77309	100.969	1.1755
44	4	-2165.06	-3750	-2154.38	-3894.87	12.6591	113.157	15.282
44	5	-2165.06	-3750	-2318.19	-3907.48	10.8217	125.559	14.1664
44	6	-2165.06	-3750	-2467.16	-4181.37	-4.98945	132.241	0.324708
44	7	-2165.06	-3750	-2548.08	-4932.62	-2.04282	137.316	1.78605
44	8	-2165.06	-3750	-2191.32	-3963.16	14.1645	113.319	18.7045
44	9	-2165.06	-3750	-2681.03	-4495.86	11.7222	122.151	19.6941
45	0	0	-3750	428.0281	-3513.5	2.25597	143.193	12.1901

g.sc.id	l.ms.id	bs.loc.x	bs.loc.y	ms.loc.x	ms.loc.y	C/I	Path Loss	Chandiff
45	1	0	-3750	142.6564	-3703.52	15.8731	104.505	19.2065
45	2	0	-3750	714.8465	-4252.62	1.74461	128.212	5.57195
45	3	0	-3750	589.3146	-3949.95	13.9908	126.593	19.1159
45	4	0	-3750	809.7475	-3570.79	4.64999	133.17	12.1253
45	5	0	-3750	206.9272	-3718.7	14.5139	110.72	19.8016
45	6	0	-3750	685.6309	-2976.71	-3.27927	144.57	0.027989
45	7	0	-3750	1108.208	-4004.79	0.920631	136.749	8.02119
45	8	0	-3750	369.5951	-3873.74	15.7554	107.547	19.1159
45	9	0	-3750	835.4426	-3923.83	0.539941	138.883	5.51756
46	0	0	-3750	-36.7851	-3233.45	2.06033	117.295	4.74787
46	1	0	-3750	-176.779	-3567.31	16.1801	108.604	19.52
46	2	0	-3750	-24.183	-3643.02	16.0518	114.596	19.2922
46	3	0	-3750	-3.20205	-3046.9	12.2484	112.153	17.6329
46	4	0	-3750	-795.051	-3308.81	-0.63486	132.642	2.14338
46	5	0	-3750	-247.24	-3137.15	6.5382	135.573	13.6023
46	6	0	-3750	-194.52	-3709.39	6.24033	104.778	7.0536
46	7	0	-3750	-220.642	-2904.85	-2.13122	138.181	2.41342
46	8	0	-3750	6.640478	-3451.3	13.6359	112.108	17.0445
46	9	0	-3750	81.08104	-3581.45	1.75933	111.303	2.351
47	0	0	-3750	-527.7	-4845.29	-7.32058	152.355	2.80786
47	1	0	-3750	179.0231	-4668.14	2.22107	136.321	8.75607
47	2	0	-3750	-498.51	-4232.54	2.32414	132.172	6.20667
47	3	0	-3750	-638.352	-4481.7	9.28019	134.724	19.2533
47	4	0	-3750	-292.567	-3833.71	7.00486	122.804	9.4038
47	5	0	-3750	-625.278	-4669.99	0.2141	133.41	2.0664
47	6	0	-3750	-443.176	-3772.34	-1.81516	134.456	1.7633
47	7	0	-3750	-1168.62	-3915.65	1.06734	116.349	4.47813
47	8	0	-3750	-306.157	-4367.19	11.1825	118.197	13.5194
47	9	0	-3750	-1008.4	-4004.24	5.74923	136.748	10.5365
48	0	1082.532	-1875	1381.115	-1379.94	-1.94801	127.576	0.5878
48	1	1082.532	-1875	1754.304	-2457.16	-2.82678	138.018	0.920667
48	2	1082.532	-1875	1802.558	-2762.59	-2.60327	141.573	0.666692
48	3	1082.532	-1875	1827.509	-2164.16	-1.03756	126.9	2.54331
48	4	1082.532	-1875	1147.516	-1777.57	1.89182	112.044	2.351
48	5	1082.532	-1875	1414.859	-2099.3	8.50834	129.77	15.282
48	6	1082.532	-1875	1730.011	-1773.51	7.30647	124.114	15.2505
48	7	1082.532	-1875	1170.157	-1739.27	1.07462	132.348	1.7633
48	8	1082.532	-1875	1661.285	-2169.47	3.30116	134.44	10.4554

g.sc.id	l.ms.id	bs.loc.x	bs.loc.y	ms.loc.x	ms.loc.y	C/I	Path Loss	Chandiff
48	9	1082.532	-1875	1618.704	-1979.61	9.74838	122.243	13.8457
49	0	1082.532	-1875	905.3655	-1413.56	6.35627	136.395	12.8489
49	1	1082.532	-1875	414.3523	-1161.46	-0.42531	137.739	4.08893
49	2	1082.532	-1875	1107.619	-1594.74	12.236	115.487	14.694
49	3	1082.532	-1875	-47.201	-1841.99	-2.70272	145.744	3.98544
49	4	1082.532	-1875	1309.678	-1409.15	-3.30358	133.839	0.187321
49	5	1082.532	-1875	1167.426	-1664.12	4.14808	93.52	4.702
49	6	1082.532	-1875	1363.692	-807.671	4.97276	132.439	8.8168
49	7	1082.532	-1875	1365.979	-1317.22	1.13857	108.445	1.7633
49	8	1082.532	-1875	1016.235	-1731.19	16.9232	92.3277	19.9388
49	9	1082.532	-1875	1069.808	-1771.37	15.6884	95.5937	18.7045
50	0	1082.532	-1875	875.7509	-3044.8	1.45156	117.789	2.74052
50	1	1082.532	-1875	755.076	-2099.61	14.724	111.167	18.3445
50	2	1082.532	-1875	913.5214	-1938.53	10.857	107.137	12.3431
50	3	1082.532	-1875	982.5634	-1957.7	15.9669	87.9174	19.0204
50	4	1082.532	-1875	-23.3392	-2016.14	-1.95781	134.561	2.28964
50	5	1082.532	-1875	214.1239	-2272.91	0.402437	132.063	1.32989
50	6	1082.532	-1875	1186.103	-2080.14	1.33721	106.429	1.7633
50	7	1082.532	-1875	1040.284	-1895.94	13.1126	96.5701	15.282
50	8	1082.532	-1875	389.1601	-2174.12	2.10926	128.961	3.89485
50	9	1082.532	-1875	1517.828	-2668.64	-2.1699	130.178	0.5878
51	0	2165.064	-3750	3102.937	-4097.57	7.88446	135.475	15.9179
51	1	2165.064	-3750	2386.898	-3939.21	4.93466	121.778	6.81975
51	2	2165.064	-3750	3212.811	-4234.99	-0.98794	129.668	3.20617
51	3	2165.064	-3750	2697.935	-2861.47	4.81191	138.498	15.9351
51	4	2165.064	-3750	2657.232	-3213.7	3.21906	133.702	6.54792
51	5	2165.064	-3750	2431.855	-3867.24	11.8077	121.02	18.5894
51	6	2165.064	-3750	2899.072	-3943.74	-4.927	145.564	0.209927
51	7	2165.064	-3750	2861.506	-4550.1	13.4486	110.535	19.7551
51	8	2165.064	-3750	2867.926	-2892.56	4.12969	129.087	8.79661
51	9	2165.064	-3750	2232.268	-3694.73	10.8581	105.565	12.3431
52	0	2165.064	-3750	1460.845	-3684.41	-3.76562	125.935	1.02318
52	1	2165.064	-3750	2132.731	-3063.45	9.17889	126.639	14.0721
52	2	2165.064	-3750	1365.471	-3395.86	1.73658	134.612	4.81637
52	3	2165.064	-3750	1832.062	-3473.26	12.9604	108.854	19.0204
52	4	2165.064	-3750	1400.743	-3100.06	-2.35741	144.424	0.131739
52	5	2165.064	-3750	2050.492	-3710.48	9.68436	110.238	11.1673
52	6	2165.064	-3750	1445.353	-3265.28	-1.46159	130.55	2.29794

g.sc.id	l.ms.id	bs.loc.x	bs.loc.y	ms.loc.x	ms.loc.y	C/I	Path Loss	Chandiff
52	7	2165.064	-3750	2244.209	-2644.09	-2.06706	146.526	7.2037
52	8	2165.064	-3750	1734.037	-3214.58	3.23231	135.732	7.40469
52	9	2165.064	-3750	2018.307	-2556.56	-2.57386	136.176	2.35194
53	0	2165.064	-3750	2413.001	-4410.43	-4.70944	144.689	0.713684
53	1	2165.064	-3750	2058.187	-4922.43	-0.67387	140.831	8.23268
53	2	2165.064	-3750	2116.957	-3907.3	15.4403	104.936	19.5861
53	3	2165.064	-3750	1308.596	-3888.32	-4.83105	145.017	0.26523
53	4	2165.064	-3750	2657.269	-4829.53	-1.88684	121.842	3.94924
53	5	2165.064	-3750	1586.435	-4046.81	4.5446	125.085	8.90518
53	6	2165.064	-3750	1736.919	-4860.47	1.21858	138.166	4.14762
53	7	2165.064	-3750	2182.03	-4767.88	5.44486	119.84	9.98723
53	8	2165.064	-3750	1853.401	-4268.36	11.6519	115.754	17.063
53	9	2165.064	-3750	1359.515	-4438.02	-1.83399	141.704	1.06294
54	0	3247.595	-1875	3841.354	-1398.43	-1.28295	126.809	0.659541
54	1	3247.595	-1875	3972.564	-2626.77	-4.67079	138.559	1.98597
54	2	3247.595	-1875	4205.84	-1120.37	-1.90759	137.073	0.324371
54	3	3247.595	-1875	4360.154	-2278.84	3.78395	124.176	5.55015
54	4	3247.595	-1875	3412.213	-1862.83	16.0718	122.028	19.9608
54	5	3247.595	-1875	3735.18	-1736.08	6.75015	130.354	11.6845
54	6	3247.595	-1875	3799.09	-1187.83	4.90421	121.758	8.04268
54	7	3247.595	-1875	3549.731	-2185.35	-2.52457	146.284	6.39439
54	8	3247.595	-1875	3663.105	-1756.96	10.7862	124.711	16.5282
54	9	3247.595	-1875	3910.4	-1586.22	3.95613	125.514	5.73797
55	0	3247.595	-1875	3273.242	-812.998	-5.34364	147.533	1.61015
55	1	3247.595	-1875	2312.462	-1223.42	1.0181	131.024	4.42804
55	2	3247.595	-1875	3191.983	-1431.65	7.88395	121.39	14.3755
55	3	3247.595	-1875	3156.073	-1632.27	14.7594	123.926	19.8016
55	4	3247.595	-1875	3199.669	-1870.05	3.04662	78.7964	3.5268
55	5	3247.595	-1875	3005.335	-902.139	-2.17296	138.425	3.28575
55	6	3247.595	-1875	3270.718	-1660.98	11.8302	120.526	14.1061
55	7	3247.595	-1875	3436.8	-1323.98	2.2239	121.197	6.465
55	8	3247.595	-1875	3108.55	-1198.24	1.23975	134.532	6.47527
55	9	3247.595	-1875	3358.347	-1350	6.57964	125.85	10.58
56	0	3247.595	-1875	2697.951	-2148.47	1.4069	123.153	4.80285
56	1	3247.595	-1875	3205.99	-2480.55	5.67943	131.846	10.4704
56	2	3247.595	-1875	2954.706	-2072.01	14.268	119.207	18.3445
56	3	3247.595	-1875	3176.999	-2199.92	8.42285	121.935	13.1704
56	4	3247.595	-1875	3080.936	-1969.49	13.819	124.751	17.6329

g.sc.id	l.ms.id	bs.loc.x	bs.loc.y	ms.loc.x	ms.loc.y	C/I	Path Loss	Chandiff
56	5	3247.595	-1875	3689.527	-2981.94	4.27154	129.795	9.25433
56	6	3247.595	-1875	3060.947	-2014.55	12.0668	114.833	16.7265
56	7	3247.595	-1875	3675.766	-2830.38	-2.22264	143.943	2.75386
56	8	3247.595	-1875	3492.249	-2908.17	-4.32119	141.002	0.635744
56	9	3247.595	-1875	2163.849	-2319.54	-2.43515	132.211	2.82137